Journal of chemical & engineering data

Article

pubs.acs.org/jced

The GERG-2008 Wide-Range Equation of State for Natural Gases and Other Mixtures: An Expansion of GERG-2004

O. Kunz† and W. Wagner*

Lehrstuhl für Thermodynamik, Ruhr-Universität Bochum, D-44780 Bochum, Germany

ABSTRACT: A new equation of state for the thermodynamic properties of natural gases, similar gases, and other mixtures, the GERG-2008 equation of state, is presented in this work. This equation is an expanded version of the GERG-2004 equation. GERG-2008 is explicit in the Helmholtz free energy as a function of density, temperature, and composition. The equation is based on 21 natural gas components: methane, nitrogen, carbon dioxide, ethane, propane, *n*-butane, isobutane, *n*-pentane, isopentane, *n*-hexane, *n*-heptane, *n*-octane, *n*-nonane, *n*-decane, hydrogen, oxygen, carbon monoxide, water, hydrogen sulfide, helium, and argon. Over the entire composition range, GERG-2008 covers the gas phase, liquid phase, supercritical region, and vapor−liquid equilibrium states for mixtures of these components. The normal range of validity of GERG-2008 includes temperatures from (90 to 450) K and pressures up to 35 MPa where the most accurate experimental data of the thermal and caloric properties are represented to within their accuracy. The extended validity range reaches from (60 to 700) K and up to 70 MPa. The given numerical information (including all of the sophisticated derivatives) enables the use of GERG-2008 for all of the various technical applications. Examples are processing, transportation through pipelines or by shipping, storage and liquefaction of natural gas, and processes to separate gas components. Comparisons with other equations of state, for example, AGA8-DC92 and Peng−Robinson equation (P-R), are also presented. GERG-2008 will be adopted as an ISO Standard (ISO 20765-2/3) for natural gases.

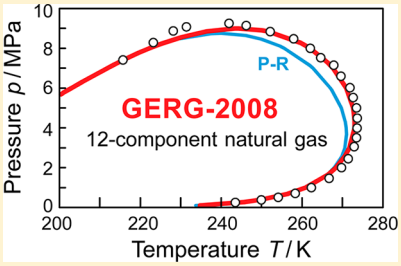

1. INTRODUCTION

The accurate knowledge of the thermodynamic properties of natural gases and other mixtures consisting of natural gas components is of indispensable importance for the basic engineering and performance of technical processes. The processing, transportation, storage, and liquefaction of natural gas are examples for technical applications where the thermodynamic properties of a variety of mixtures of natural gas components are required.

To meet pipeline-quality specifications or for commercial use as a fuel, natural gas in its raw form in general needs to be processed ahead of the feed into gas-pipeline systems or liquefaction facilities. This involves the separation of a number of components that are either undesirable (e.g., carbon dioxide, water, and hydrogen sulfide) or have more value on their own than when left in the natural gas (e.g., ethane, propane, butane, and heavier hydrocarbons and also helium).

The processed natural gas is transported in gaseous form through pipelines at pressures up to 12 MPa. Compressor stations placed periodically along the pipeline ensure that the natural gas remains pressurized. In addition, metering stations allow for monitoring and managing the natural gas in the pipes. Small differences in methods used to calculate flow rates in large scale metering can introduce large cost uncertainties. To match supply and demand, natural gas is injected at pressures up to 30 MPa into underground storage facilities, such as depleted gas reservoirs, aquifers, and salt caverns.

In situations where the economics of major gas-transmission pipelines are not viable (primarily across oceans), natural gas is cooled and condensed into liquid form, known as liquefied natural gas (LNG), thus making it transportable by specialized tanker ships. Modern and highly efficient liquefaction processes use mixtures of natural gas components as refrigerants in precooling, liquefaction, and subcooling cycles.

For the applications described above, the design of fractionation units, compressors, heat exchangers, and storage facilities requires property calculations over wide ranges of mixture compositions and operating conditions in the homogeneous gas, liquid, and supercritical regions and for vapor−liquid equilibrium (VLE) states. These data can be calculated in a very convenient way from equations of state.

The GERG-2004 wide-range equation of state for natural gases and other mixtures developed by Kunz et al.[1] is the only equation of state that is appropriate for nearly all of the technical applications described above and that satisfies the demands on the accuracy in the calculation of thermodynamic properties over the entire fluid region. Similar to other recent developments, the GERG-2004 equation of state is based on a multi-fluid approximation. The mixture model uses accurate equations of state in the form of fundamental equations for each mixture component along with functions developed for the binary mixtures of the components to take into account the residual mixture behavior. The GERG-2004 equation of state enables the calculation of thermal and caloric properties for natural gases and other mixtures consisting of 18 components: methane, nitrogen, carbon dioxide, ethane, propane, *n*-butane, isobutane, *n*-pentane,

Received: June 17, 2012
Accepted: August 2, 2012
Published: October 31, 2012

   dx.doi.org/10.1021/je300655b | *J. Chem. Eng. Data* 2012, 57, 3032−3091

isopentane, *n*-hexane, *n*-heptane, *n*-octane, hydrogen, oxygen, carbon monoxide, water, helium, and argon.

Aside from the 18 natural gas components covered by the GERG-2004 equation of state, natural gas may contain the heavier hydrocarbons *n*-nonane and *n*-decane. Even when only present in small amounts, these components significantly affect the phase behavior of a natural gas mixture. Moreover, hydrogen sulfide is present in many situations. It is contained in acid gases, which are mixtures that mainly consist of carbon dioxide and hydrogen sulfide with minor traces of hydrocarbons. Driven by the need to dispose of hydrogen sulfide produced with natural gas from sour-gas reservoirs, acid gases are nowadays injected into deep saline aquifers and depleted hydrocarbon reservoirs. The injection of acid gases occurs over a wide range of mixture compositions and operating conditions, frequently requiring the separation of one or more components from the mixture.

This work presents the GERG-2008 equation of state, eq 8, that is an expanded version of the GERG-2004 equation of state.[1] The development of this expanded equation was finished in 2008, and, therefore, this equation is called the GERG-2008 equation of state or GERG-2008 for short. In addition to the 18 components covered by GERG-2004, the expanded version GERG-2008 also includes the three additional components *n*-nonane, *n*-decane, and hydrogen sulfide, which add up to a total of 21 components (see Table 1). Thus, GERG-2008 covers all of the mixtures that can be formed by the 18 pure components GERG-2004 is based on and, in addition, also all mixtures that result from the combinations of the 18 components with the three additional components given above. This is the main difference between the two mixture models.

2. BACKGROUND

2.1. Examples of Equations of State Commonly Applied in the Natural Gas Industry. Many different types of equations of state are applied in the natural gas industry. The use of a certain equation depends on the fluid region where the calculation of the thermodynamic properties is required. For pipeline applications, which mainly deal with the gas-phase properties of natural gases, several equations of state of comparatively high accuracy exist. For certain applications, simplified equations were developed, for example, the SGERG equation of Jaeschke and Humphreys.[2] These equations use the mole fractions of specific natural gas components (e.g., nitrogen and carbon dioxide) in combination with physical properties, such as the relative density and the superior calorific value, as input variables instead of the complete molar composition analysis. In the liquid phase and for phase-equilibrium calculations, cubic equations of state (e.g., Peng and Robinson[3]), which show poor accuracy in the description of many thermodynamic properties (see Section 2.1.2), are commonly used. A more accurate description of, for example, the $p\rho T$ relation in the liquid phase, is achieved by equations with very limited ranges of validity for temperature, pressure, and composition (e.g., McCarty[4]). They are typically only applicable in the subcritical region. As a result of the use of individual equations for different fluid regions, there are inconsistencies in calculations when moving from one region to another and when more than one phase is involved, that is, for phase-equilibrium calculations.

Most of the standard natural gas applications, such as gas transmission and storage, are located in the "classical" natural gas region, that is, the gas phase, at temperatures from (250 to 350) K and pressures up to 30 MPa. Therefore, this region is of main interest for the calculation of thermodynamic properties. The internationally accepted standard for the calculation of thermodynamic properties in this region is, according to ISO 20765-1:2005,[5] the AGA8-DC92 equation of state of Starling and Savidge.[6]

Table 1. List of the 21 Main and Secondary Natural Gas Components and Their Equations of State[a] Used for the GERG-2008 Mixture Equation of State, eq 8

pure substance	reference of the used equation of state	range of validity: temperature, T/K	range of validity: pressure, p_{max}/MPa	no. terms
Main Components				
methane	Klimeck[22]	90 to 623	300	24
nitrogen	Klimeck[22]	63 to 700	300	24
carbon dioxide	Klimeck[22]	216[b] to 900	300	24
ethane	Klimeck[22]	90 to 623	300	24
Secondary Alkanes				
propane	Span and Wagner[23]	85 to 623	100	12
n-butane	Span and Wagner[23]	134 to 693	70	12
isobutane	Span and Wagner[23]	113 to 573	35	12
n-pentane	Span and Wagner[23]	143 to 573	70	12
isopentane	Lemmon and Span[24]	112 to 500	35	12
n-hexane	Span and Wagner[23]	177 to 548	100	12
n-heptane	Span and Wagner[23]	182 to 523	100	12
n-octane	Span and Wagner[23]	216 to 548	100	12
n-nonane	Lemmon and Span[24]	219 to 600	800	12
n-decane	Lemmon and Span[24]	243 to 675	800	12
Other Secondary Components				
hydrogen[c]	Kunz et al.[1]	14 to 700	300	14
oxygen	Span and Wagner[23]	54 to 303	100	12
carbon monoxide	Lemmon and Span[24]	68 to 400	100	12
water	Kunz et al.[1]	273 to 1273	100	16
hydrogen sulfide	Lemmon and Span[24]	187 to 760	170	12
helium[d]	Kunz et al.[1]	2.2 to 573	100	12
argon	Span and Wagner[23]	83 to 520	100	12

[a]The tabulated references correspond to the equations for the residual part of the Helmholtz free energy of the considered pure substances. For all components, the equations of Jaeschke and Schley[25] for the isobaric heat capacity in the ideal-gas state were used to derive the Helmholtz free energy of the ideal gas. [b]The equation can be extrapolated from the triple-point temperature down to 90 K.[1] [c]Represents equilibrium hydrogen. [d]Represents helium-4. The lower temperature limit of the equation of state is the lambda point at which helium I transitions to helium II.

2.1.1. The AGA8-DC92 Equation of State. The AGA8-DC92 equation of state[6] was originally designed as a thermal equation of state explicit in compression factor. This equation enables the calculation of thermodynamic properties of natural gases and similar mixtures consisting of up to 21 components. The range of validity is limited to the gas phase and covers temperatures from (143 to 673) K and pressures up to 280 MPa. Due to limited experimental data, a well-founded estimation of the uncertainty in the description of thermal properties (compression factor and density) of natural gases is only feasible in the temperature range 250 K $\leq T \leq$ 350 K at pressures up to 30 MPa. Detailed investigations concerning the uncertainty of the AGA8-DC92 equation in the description of thermal properties have been published by numerous authors (e.g., Jaeschke and Schley,[7] ISO 12213-2:2006,[8a] Lemmon et al.[8b]). Klimeck et al.[9] investigated the description of caloric properties, such as sound speed,

dx.doi.org/10.1021/je300655b | J. Chem. Eng. Data 2012, 57, 3032−3091

isobaric heat capacity, and enthalpy differences. The results of the investigations mentioned above can be summarized as follows:

- The uncertainty in the description of the $p\rho T$ relation of typical natural gases of pipeline quality amounts to 0.1 % in density. (In this work, the expression "pipeline quality" refers to the definition of the international standard ISO 20765-1:2005.[5] According to that, natural gases of pipeline quality are processed natural gases; i.e., impurities and heavier hydrocarbons and other components were removed from the raw natural gas.) This uncertainty is achieved for temperatures ranging from (290 to 350) K at pressures up to 30 MPa.
- For the calculation of caloric properties at temperatures above 270 K, the uncertainty in sound speed amounts to approximately 0.2 %. The uncertainty in isobaric heat capacity and isobaric enthalpy differences is about 1 %.

Nevertheless, the investigations revealed several shortcomings of the AGA8-DC92 equation of state, which is currently the internationally accepted standard for the gas phase:

- The development of AGA8-DC92 was based mainly on mixture data at temperatures above 270 K. Comparisons with the few available density data for natural gases in the temperature range from (250 to 270) K indicate a higher uncertainty in the prediction of thermal properties in this region. Moreover, at higher temperatures up to 290 K, the uncertainty in density of 0.1 % is restricted to pressures less than 12 MPa.
- For natural gases containing higher fractions of nitrogen, carbon dioxide, ethane, or heavier hydrocarbons, larger uncertainties have to be taken into account for the calculation of thermal properties from AGA8-DC92 in the lower temperature range.
- Significant deviations between calculated and measured caloric properties occur at temperatures below 270 K even for typical natural gases of pipeline quality. For example, sound speed deviations increase at higher pressures and reach a value of about −1 % at a pressure of 20 MPa.
- An increase of the uncertainty in caloric properties for natural gases containing higher fractions of heavier hydrocarbons such as propane and the butanes has to be taken into account even at higher temperatures. This shortcoming of the AGA8-DC92 equation[6] becomes even more evident for increasing pressures while the temperature decreases.

2.1.2. Cubic Equations of State. Due to their simple mathematical structure, the pressure explicit cubic equations of state, with their huge amount of existing modifications, are still commonly used in technical applications.

Klimeck et al.[9] (see Section 2.1.1) investigated the suitability of the cubic equation of state of Peng and Robinson[3] for use in technical applications that require high accuracy predictions of the properties of natural gases. They found serious deficiencies with respect to the representation of thermal properties in the liquid phase and the description of caloric properties. Many cubic equations of state have these weaknesses in common due to their simple structure:

- Major shortcomings already occur for the description of the $p\rho T$ relation of pure methane at temperatures and pressures typically encountered in standard applications related to the transmission and distribution of pipeline quality gases. For instance, density values calculated from the cubic equation of state of Peng and Robinson[3] deviate from the reference equation of state of Setzmann and Wagner[10] by up to 5 % at pressures below 30 MPa.
- Comparisons of calculated values for the sound speed show deviations of more than ± 10 % in the same temperature and pressure ranges. A similar insufficient behavior is observed for the calculation of properties in the liquid phase. Calculated saturated-liquid densities deviate from experimental data for natural gases and state-of-the-art measurements on pure substances by up to 15 %. This inaccurate description of saturated-liquid densities is observed for compressed liquid densities as well. (The poor quality of cubic equations of state in the description of liquid-phase densities is generally known. One method that has become quite popular for improving the density calculation from cubic equations of state is called "volume shifting."[11] However, the validity of this correction is restricted to a limited range of the liquid phase.)

These results demonstrate that the cubic equation of state of Peng and Robinson[3] is not suitable for an accurate description of thermal and caloric properties in the homogeneous region and for saturated-liquid densities. Nevertheless, for the calculation of vapor pressures and equilibrium-phase compositions of mixtures, and also for the evaluation of corresponding experimental data, the use of cubic equations of state is quite functional, as they yield relatively accurate results. For example, experimental data for the vapor pressure of many binary mixtures of natural gas components are reproduced by the cubic equation of state of Peng and Robinson[3] to within ± (3 to 5) % over wide ranges of temperature and composition, which is in most cases in agreement with the experimental uncertainty of the measurements.

2.2. Multi-Fluid Approximations and the GERG-2004 Equation of State. Recent equations of state for mixtures are based on multi-fluid approximations and are explicit in the Helmholtz free energy. The models use equations of state in the form of fundamental equations for each mixture component along with further correlation equations to take into account the residual mixture behavior. The models enable the accurate description of the thermodynamic properties of mixtures in the entire fluid region (i.e., in the homogeneous gas, liquid, and supercritical regions and for vapor−liquid equilibrium states) over wide ranges of temperature, pressure, and composition. For a pure component, the models default to the fundamental equation used for the respective substance. The basis for the development and evaluation of such empirical equations of state for mixtures are experimental data (see also Section 3).

The first models of this type were developed independently by Tillner-Roth[12] for the binary refrigerant mixture R-152a−R-134a and by Lemmon[13] for mixtures of polar and nonpolar substances, including natural gas components. Based on the structures of these models, further equations of state for the binary mixture water−ammonia (Tillner-Roth and Friend[14]), dry air and similar mixtures (Lemmon et al.[15]), mixtures of hydrocarbon refrigerants (Miyamoto and Watanabe[16]), and hydrofluorocarbon refrigerant mixtures (Lemmon and Jacobsen;[17] Tillner-Roth et al.[18]) have been reported since 1998. Detailed descriptions of the general structures of these models are given by Tillner-Roth[19] and Lemmon and Tillner-Roth.[20] Lemmon and Jacobsen[21] revised the model of Lemmon[13] for the mixture components relevant to this work.

Kunz et al.[1] developed the GERG-2004 wide-range equation of state for natural gases and other mixtures. Similar to the developments mentioned above, the GERG-2004 equation of state is based on a multi-fluid approximation. The equation covers 18 natural gas components: methane, nitrogen, carbon dioxide, ethane, propane, *n*-butane, isobutane, *n*-pentane, isopentane, *n*-hexane, *n*-heptane, *n*-octane, hydrogen, oxygen, carbon monoxide, water, helium, and argon. GERG-2004 is appropriate for various natural gas applications and satisfies the demands on the accuracy in the calculation of thermodynamic properties over the entire fluid region.

2.2.1. General Structure of Multi-Fluid Approximations. The mixture models mentioned above and the new model for natural gases, similar gases, and other mixtures presented here are fundamental equations explicit in the Helmholtz free energy a with the independent mixture variables density ρ, temperature T, and the vector of the molar composition $\overline{x}$. The function $a(\rho,T,\overline{x})$ is split into a part a^{o}, which represents the properties of ideal-gas mixtures at given values for ρ, T, and $\overline{x}$, and a part a^{r}, which takes into account the residual mixture behavior:

$$a(\rho, T, \overline{x}) = a^{o}(\rho, T, \overline{x}) + a^{r}(\rho, T, \overline{x}) \quad (1)$$

The use of the Helmholtz free energy in its dimensionless form $\alpha = a/(RT)$ results in the following equation (note that α^{o} does not depend on δ and τ of the mixture, but on ρ and T)

$$\alpha(\delta, \tau, \overline{x}) = \alpha^{o}(\rho, T, \overline{x}) + \alpha^{r}(\delta, \tau, \overline{x}) \quad (2)$$

where δ is the reduced mixture density and τ is the inverse reduced mixture temperature according to

$$\delta = \rho/\rho_{r} \quad \text{and} \quad \tau = T_{r}/T \quad (3)$$

with ρ_{r} and T_{r} being the composition-dependent reducing functions for the mixture density and temperature:

$$\rho_{r} = \rho_{r}(\overline{x}) \quad (4)$$

$$T_{r} = T_{r}(\overline{x}) \quad (5)$$

The dimensionless form of the Helmholtz free energy for the ideal-gas mixture α^{o} is given by

$$\alpha^{o}(\rho, T, \overline{x}) = \sum_{i=1}^{N} x_i[\alpha_{oi}^{o}(\rho, T) + \ln x_i] \quad (6)$$

where N is the number of components in the mixture, α_{oi}^{o} is the dimensionless form of the Helmholtz free energy in the ideal-gas state of component i (see eq 12), and the quantities x_i are the mole fractions of the mixture constituents. The term $x_i \ln x_i$ accounts for the entropy of mixing.

In a multi-fluid approximation, the residual part of the reduced Helmholtz free energy of the mixture α^{r} is given by:

$$\alpha^{r}(\delta, \tau, \overline{x}) = \sum_{i=1}^{N} x_i \alpha_{oi}^{r}(\delta, \tau) + \Delta\alpha^{r}(\delta, \tau, \overline{x}) \quad (7)$$

where α_{oi}^{r} is the residual part of the reduced Helmholtz free energy of component i (see eq 14), and $\Delta\alpha^{r}$ is the so-called departure function. The reduced residual Helmholtz free energy of each component depends on the reduced variables δ and τ of the mixture; the departure function additionally depends on the mixture composition $\overline{x}$.

This general structure is used by the models of, for example, Tillner-Roth,[12] Lemmon and Jacobsen,[21] and Kunz et al.,[1] which were developed to achieve an accurate description of the thermodynamic properties of nonideal mixtures.

According to eq 7, the residual part of the reduced Helmholtz free energy of the mixture α^{r} is composed of two different parts, namely:

- the linear combination of the residual parts of all considered mixture components, and
- the departure function.

In general, the contribution of the departure function to the reduced residual Helmholtz free energy of the mixture is less than the contribution of the equations for the pure components.

Summarized, the development of mixture models based on a multi-fluid approximation requires the following three elements:

- pure substance equations of state for all considered mixture components;
- composition-dependent reducing functions $\rho_{r}(\overline{x})$ and $T_{r}(\overline{x})$ for the mixture density and temperature;
- a departure function $\Delta\alpha^{r}$ depending on the reduced mixture density, the inverse reduced mixture temperature, and the mixture composition.

3. EXPERIMENTAL DATA

The GERG-2008 wide-range equation of state for natural gases, similar gases, and other mixtures is based on pure substance equations of state for each considered mixture component and correlation equations developed for binary mixtures consisting of these components (see Section 4). This allows for a suitable predictive description of multi-component mixtures over a wide range of compositions, which means it is able to predict the properties of a variety of natural gases and other multi-component mixtures. The basis for the development of such an empirical equation of state is experimental data for several thermodynamic properties. These data are used to determine the structures, coefficients, and parameters of the correlation equations and to evaluate the behavior of the equation of state in different fluid regions. The quality and the extent of the available data limit the achievable accuracy of the equation.

The database of experimental binary and multi-component mixture data used in this work builds up on the comprehensive database that has been used for the development of the GERG-2004 equation of state. This database has been continuously updated and expanded to mixtures containing the three additional components *n*-nonane, *n*-decane, and hydrogen sulfide. The updated and expanded database is also referred to in the following as the GERG-2008 database. Due to the extensive amount of data for a large number of different binary and multi-component mixtures, only basic remarks on the data sets are given in this subsection. Additional details on the data used to develop and evaluate the GERG-2004 equation of state are given by Kunz et al.[1] Details on the data used for the expansion of GERG-2004 are given in Section 3.1.

All collected data were assessed by means of comparisons to values calculated from different equations of state. The data classified as "reliable" form an experimental basis for the development (i.e., fitting and structure optimization) of the GERG-2008 equation of state. Other data were only used for comparisons. Many of the collected data do not meet present quality standards. However, for several binary mixtures these data represent the only available experimental information.

3.1. Properties and Mixtures Covered by the GERG-2008 Database. The updated and expanded database contains more than 125 000 experimental data for the thermal and caloric

dx.doi.org/10.1021/je300655b | J. Chem. Eng. Data 2012, 57, 3032−3091

properties of binary mixtures, natural gases, and other multi-component mixtures, which are described in about 650 different sources. The collected data cover the homogeneous gas, liquid, and supercritical regions as well as vapor−liquid equilibrium (VLE) states at temperatures ranging from (16 to 2500) K and pressures up to 2000 MPa. The most common types of thermodynamic properties are the following:

- $p\rho T$;
- isochoric heat capacity c_v;
- sound speed w;
- isobaric heat capacity c_p;
- enthalpy differences Δh;
- saturated-liquid density ρ';
- VLE data (mainly $pTxy$ data).

About 70 % of the available mixture data describe the $p\rho T$ relation. Nearly 21 % of the data are vapor−liquid equilibrium state points, and approximately 9 % account for caloric properties. About 95 000 data for thermal and caloric properties are available for a total of 135 binary mixtures consisting of the 21 natural gas components listed in Table 1. The number of binary data selected for the development of the GERG-2008 equation of state amounts to approximately 53 000. Thus, 56 % of all available binary mixture data were used for fitting the coefficients and parameters and for optimizing the structure of GERG-2008. All of the remaining data were used for comparisons. For multi-component mixtures, about 30 000 data for thermal and caloric properties are accessible. This enabled a comprehensive validation of this equation of state with data for natural gases, similar gases, and other binary and multi-component mixtures.

Aside from many ordinary natural gases, the present database also comprises data for the following types of multi-component mixtures:

- natural gases containing high fractions of methane, nitrogen, carbon dioxide, or ethane;
- natural gases containing substantial amounts of ethane, propane, and heavier alkanes;
- natural gases containing high fractions of hydrogen (natural gas−hydrogen mixtures);
- natural gases containing large amounts of coke-oven constituents;
- rich natural gases [Rich natural gases contain large amounts of ethane and heavier alkanes (e.g., $x_{C_2H_6}$ = 0.18, $x_{C_3H_8}$ = 0.08, $x_{n\text{-}C_4H_{10}}$ = 0.03, $x_{n\text{-}C_5H_{12}}$ = 0.005, $x_{n\text{-}C_6H_{14}}$ = 0.002) and comparatively low fractions of methane (down to x_{CH_4} = 0.50); the numbers correspond to mole fractions];
- LNG mixtures;
- ternary mixtures of light or heavier hydrocarbons, such as propane−*n*-butane−isobutane and *n*-pentane−*n*-hexane−*n*-heptane;
- air and other ternary and multi-component mixtures.

For multi-component mixtures, a huge amount of $p\rho T$ data were measured in the gas phase covering temperatures from (270 to 350) K at pressures up to 30 MPa. Most of these data were taken from the GERG databank given in GERG TM7,[26] which comprises a total of about 12 500 binary and 900 ternary data and about 16 000 data for more than 110 natural gases and other related multi-component mixtures. Many of these density data were measured using two methods of measurement, namely, the Burnett method and an optical interferometry method. The uncertainty of these measurements is claimed by the authors to be $\Delta\rho/\rho$ = (0.07 to 0.1) %, which agrees with the results of the investigations of Klimeck[22] and those carried out by Kunz et al.[1] Comparatively few $p\rho T$ data were measured at temperatures below 270 K. Nevertheless, they enable, along with the accurate and wide-ranging data for important binary mixtures, a well-founded estimation of the uncertainty in gas-phase densities at temperatures below 270 K. For instance, accurate and wide-ranging density and sound-speed data for the binary mixtures methane−nitrogen and methane−ethane cover large reduced temperature ranges, which include those relevant to natural gases. In standard natural gas applications, such as pipeline transport and natural gas storage, property calculations are required over the temperature range from (250 to 350) K. This range corresponds to reduced temperatures from T/T_r = 1.2 to T/T_r = 1.8, where T_r is an estimate for the reducing temperature of a typical natural gas.

For caloric properties, very accurate experimental data exist for sound speeds. Furthermore, some accurate measurements are available for enthalpy differences. Most of these caloric data cover the temperature range from (250 to 350) K at pressures up to (12 or 20) MPa.

3.1.1. Statements on the Accuracy of the Collected Experimental Data. Table 2 lists the total uncertainties of the most accurate experimental binary and multi-component mixture data (for selected thermodynamic properties) that were available at the time the equations of state GERG-2004 and GERG-2008 were developed. The tabulated values represent the lowest uncertainties achieved by the mixture model presented here. The corresponding experimental results are based on modern measurement techniques that fulfill present quality standards. For density measurements, very accurate results were obtained using a two-sinker or single-sinker densimeter (e.g., Glos et al.[27] and Chamorro et al.[28]). Highly accurate sound-speed data were measured by means of spherical-resonators (e.g., Costa Gomes and Trusler,[29] Estela-Uribe,[30] and Trusler[31]). Data that were measured with methods based on these particular techniques have uncertainties equal to or close to the lowest values listed in Table 2.

Table 2. Estimated Relative Experimental Uncertainties of the Most Accurate Binary and Multi-Component Mixture Data

data type	property	relative uncertainty
$p\rho T$ data (gas phase)	$\Delta\rho/\rho$	(0.03 to 0.1) %
isochoric heat capacity (gas and liquid phases)	$\Delta c_v/c_v$	(1 to 2) %
sound speed (gas phase)	$\Delta w/w$	(0.02 to 0.1) %
isobaric heat capacity (gas and liquid phases)	$\Delta c_p/c_p$	(1 to 2) %
enthalpy differences (gas phase)	$\Delta(\Delta h)/\Delta h$	(0.2 to 0.5) %
saturated-liquid density	$\Delta\rho'/\rho'$	(0.1 to 0.3) %
VLE data (vapor pressures)	$\Delta p_s/p_s$	(1 to 3) %

In contrast to the experimental uncertainties given for pure fluid properties, those estimated for the properties of mixtures are generally higher due to the significant contribution of the uncertainty in the mixture composition.

Most of the available VLE data are comprised of experimental values (simultaneously measured) for the temperature T, the pressure p, and the compositions $\overline{x}$ and $\overline{y}$ (also written as $\overline{x}'$ and $\overline{x}''$, respectively, where the superscripts $'$ and $''$ denote the saturated-liquid line and saturated-vapor line, respectively) of the two equilibrium phases. Since these data, which are referred to in

dx.doi.org/10.1021/je300655b | J. Chem. Eng. Data 2012, 57, 3032−3091

Table 3. Molar Compositions of Synthetic Natural-Gas-Like Mixtures Rich in Butanes and Pentanes[a] Used for the $p\rho T$ Measurements of McLinden[40] and Atilhan et al.[41]

	composition (100·mole fraction)								
mixture	CH_4	N_2	CO_2	C_2H_4	C_3H_8	n-C_4	i-C_4	n-C_5	i-C_5
SNG-1	89.990	1.699	1.707	3.150	1.583	0.790	0.781	0.150	0.150
SNG-2	89.982	1.697	1.701	3.009	1.506	0.753	0.752	0.300	0.300
SNG-3	89.975	1.713	1.699	2.855	1.427	0.722	0.709	0.450	0.450
SNG-4	90.001			4.565	2.243	1.151	1.140	0.450	0.450

[a]The mixtures were prepared gravimetrically by a commercial laboratory.

this work as $pTxy$ data, generally cover large composition ranges, they provide an essential amount of information on the mixture behavior for many of the considered binary systems.[1] This feature is important for fitting the parameters of the composition-dependent elements of a multi-fluid mixture model (e.g., the reducing functions) to experimental data. However, the quality of these data is relatively poor and in several cases not suitable for the development of an accurate equation of state. In contrast to the available data for the most accurate thermal and caloric properties of mixtures in the homogeneous region, which almost achieve the accuracy of the corresponding measurements for pure fluids, the experimental uncertainty in vapor pressure usually differs by one or two orders of magnitude. The total uncertainty in vapor pressure for binary and multi-component mixtures generally amounts to at least (1 to 3) %. For measured bubble- and dew-point compositions, dew-point temperatures, and saturated-vapor densities, similarly high experimental uncertainties occur. These weaknesses in the VLE data sets limit the achievable accuracy in the description of such properties by the developed mixture model GERG-2008; for additional details see Kunz et al.[1]

The most accurate VLE data are those measured by Haynes et al. (Hiza et al.,[32] Hiza and Haynes,[33] Haynes[34,35]) for saturated-liquid densities of binary and multi-component mixtures of liquefied natural gas (LNG) components. They cover the temperature range from (100 to 140) K. The uncertainty in density of these data is (0.1 to 0.2) %. Resulting from the chosen measuring technique, the measured pressures are considered as only approximate vapor pressures and cannot be used.

The most accurate caloric data are sound speeds and enthalpy differences as shown in Table 2. Usually, a substantial amount of these data were measured in the gas phase at temperatures ranging from (250 to 350) K and pressures up to 12 MPa. Comparatively few accurate caloric measurements exist for higher pressures. In contrast to the collected $p\rho T$ data, caloric data are only present for a limited number of binary and multi-component mixtures and cover, in general, limited composition ranges.

3.1.2. Accurate Measurements Improved the Data Basis over the Past 15 Years. The data situation has been significantly improved over the past 15 years since new data for several binary mixtures were measured as a part of the GERG project "Reference Equation of State for Thermal and Caloric Properties of Natural Gases" (see Klimeck[22]) and by numerous other independent authors. These include, for example, the very accurate measurements for gas-phase densities and sound speeds of the binary mixtures methane−nitrogen (Estela-Uribe,[30] Trusler,[31] Chamorro et al.[28]), methane−carbon dioxide (Estela-Uribe,[30] Glos et al.[27]), methane−ethane (Costa Gomes and Trusler[29]), and nitrogen−ethane (Trusler[31]). For vapor−liquid equilibrium states, comparatively accurate data were reported, for example, for methane−ethane and nitrogen−ethane (Raabe et al.[36]), methane−carbon dioxide and methane−propane (Webster and Kidnay[37]), propane−n-butane (VonNiederhausern and Giles[38]), and propane−isobutane (VonNiederhausern and Giles,[38] Lim et al.[39]).

For natural gases of pipeline quality, very accurate $p\rho T$ data in the gas phase, measured with a two-sinker densimeter, are available in the GERG databank mentioned above (Jaeschke et al.[26]). McLinden[40] recently reported very accurate gas-phase densities for four synthetic natural-gas-like mixtures. These mixtures contain comparatively high fractions of n-butane and isobutane as well as n-pentane and isopentane (see Table 3). The data were also measured using a two-sinker densimeter with a claimed total uncertainty in density of (0.0079 to 0.0086) % (standard uncertainty, coverage factor $k = 1$ corresponding to a confidence level of 68 %). Since in the field of equations of state, an experimental uncertainty based on a confidence level of 95 % ($k = 2$) is of interest, we take a density uncertainty of about 0.02 % for these data. The data cover the temperature range from (250 to 450) K at pressures up to 40 MPa. Density data of the same mixtures with exactly the same compositions in the same temperature range as used by McLinden[40] were measured by Atilhan et al.[41,42] with a single-sinker densimeter. These data cover pressures up to 150 MPa, and the authors give a total experimental uncertainty in density of 0.13 % ($k = 1$), that is, about 0.3 % for $k = 2$.

3.1.3. Experimental Data Used for the Expansion of GERG-2004. As mentioned before, the GERG-2008 equation of state presented here is an expanded version of GERG-2004. In addition to the 18 components covered by GERG-2004, the GERG-2008 equation of state also considers the three components n-nonane, n-decane, and hydrogen sulfide, which adds up to the 21 components listed in Table 1.

The three additional components result in 57 additional binary combinations (i.e., binary mixtures composed of the three new components and the 18 natural gas components covered by GERG-2004). With these 57 additional combinations one obtains a total of 210 binary systems covered by the expanded mixture model GERG-2008 (see also Figure 1).

In this subsection, references of articles and reports are given that contain experimental data for properties of these additional mixtures. The data used for the development (i.e., fitting the binary parameters) of the equations in GERG-2008 that refer to the additional mixtures are also outlined. It should be noted that the data collected for the expansion of GERG-2004 contribute to the total number of measurements (more than 125 000) contained in the GERG-2008 database described above.

For the expansion work, more than 16 000 experimental data points were collected and made available for 37 of the 57 additional binary mixtures. The measurements originate in more than 90 different sources. They cover temperatures from (182 to 613) K and pressures up to 140 MPa. For many of the 37 mixtures, data are available that cover wide composition ranges

Table 4. Information on the Experimental Data of Mixtures Containing the Additional Components *n*-Nonane, *n*-Decane, and Hydrogen Sulfide

		no. data		temperature range	pressure range	composition range
mixture	data types	total	selected	T/K	p/MPa	x/mole fraction
methane−*n*-nonane[43−45]	$p\rho T$, VLE[a]	438	404	223 to 423	1.01 to 32.3	0.0001 to 0.9671
methane−*n*-decane[46−56]	$p\rho T$, VLE	2454	1538	244 to 583	0.1 to 140	0.0425 to 0.9983
methane−hydrogen sulfide[57−62]	$p\rho T$, VLE	1419	1130	189 to 501	0.048 to 68.9	0.1 to 0.9993
nitrogen−*n*-nonane[44,63,64]	VLE	96	78	262 to 543	1.59 to 49.8	0.2341 to 0.9745
nitrogen−*n*-decane[49,63,65−68]	VLE	304	101	263 to 411	0.2 to 34.6	0.6 to 0.9915
nitrogen−hydrogen sulfide[69−71]	$p\rho T$, VLE	270	252	200 to 373	0.141 to 24.1	0.086 to 0.9996
carbon dioxide−*n*-nonane[72−74]	VLE	67	39	315 to 419	2.03 to 16.8	0.059 to 0.854
carbon dioxide−*n*-decane[67,74−88]	$p\rho T$, VLE	2393	1978	278 to 594	0.345 to 68.9	0.0054 to 0.9573
carbon dioxide−hydrogen sulfide[57,89−92]	$p\rho T$, VLE	1092	1023	225 to 501	0.103 to 60.6	0.033 to 0.991
ethane−*n*-decane[93−95]	$p\rho T$, VLE	1674	1534	278 to 511	0.276 to 68.9	0.005 to 0.983
ethane−hydrogen sulfide[90,96−101]	$p\rho T$, VLE	737	481	182 to 363	0.016 to 21.5	0.0259 to 0.9915
propane−*n*-nonane[74]	VLE	5	5	377 to 377	0.938 to 3.47	0.1457 to 0.7064
propane−*n*-decane[74,102,103]	$p\rho T$, VLE	1672	1609	210 to 511	0.033 to 68.9	0.013 to 0.981
propane−hydrogen sulfide[90,98,104−106]	$p\rho T$, VLE	597	253	182 to 368	0.013 to 13.3	0.014 to 0.985
n-butane−*n*-decane[107,108]	$p\rho T$, VLE	744	683	311 to 511	0.063 to 68.9	0.0249 to 0.9676
n-butane−hydrogen sulfide[98,109]	VLE	62	51	182 to 418	0.006 to 7.89	0.0099 to 0.993
isobutane−hydrogen sulfide[109,110]	$p\rho T$, VLE	161	144	278 to 398	0.207 to 8.89	0.0048 to 0.9988
n-pentane−*n*-nonane[111]	$p\rho T$	9	9	298 to 298	0.101 to 0.101	0.096 to 0.9075
n-pentane−*n*-decane[111,112]	$p\rho T$, VLE	28	26	298 to 334	0.048 to 0.146	0.0992 to 0.8969
n-pentane−hydrogen sulfide[113]	$p\rho T$, VLE	652	637	278 to 511	0.069 to 68.9	0.0062 to 0.966
isopentane−hydrogen sulfide[114]	VLE	35	32	323 to 413	0.31 to 8.38	0.009 to 0.993
n-hexane−*n*-nonane[111,115,116]	$p\rho T$	50	50	283 to 313	0.101 to 0.101	0.0748 to 0.9273
n-hexane−*n*-decane[111,115−120]	$p\rho T$, VLE, w[b]	115	115	283 to 313	0.003 to 100	0.021 to 0.9936
n-hexane−hydrogen sulfide[121]	VLE	25	25	323 to 423	0.43 to 7.55	0.023 to 0.914
n-heptane−*n*-nonane[111,115]	$p\rho T$	18	18	298 to 298	0.101 to 0.101	0.1004 to 0.8952
n-heptane−*n*-decane[111,115,117]	$p\rho T$	27	26	293 to 298	0.101 to 0.101	0.097 to 0.9015
n-heptane−hydrogen sulfide[122,123]	$p\rho T$, VLE	159	153	293 to 478	0.16 to 9.55	0.0177 to 0.997
n-octane−*n*-nonane[111,115]	$p\rho T$	18	0	298 to 298	0.101 to 0.101	0.0975 to 0.8908
n-octane−*n*-decane[111,115,117,124]	$p\rho T$, VLE	54	54	293 to 392	0.02 to 0.101	0.011 to 0.992
n-nonane−*n*-decane[111,115]	$p\rho T$	18	0	298 to 298	0.101 to 0.101	0.0983 to 0.8949
n-nonane−hydrogen sulfide[125]	VLE	15	14	311 to 478	0.137 to 2.76	0.0419 to 0.2088
n-decane−hydrogen[67,126,127]	VLE	50	44	323 to 583	1.93 to 25.5	0.0251 to 0.5013
n-decane−carbon monoxide[128,129]	VLE	29	18	311 to 378	1.27 to 10.2	0.0222 to 0.1599
n-decane−water[130]	VLE	22	18	573 to 613	1.3 to 9.27	0.0067 to 0.6684
n-decane−hydrogen sulfide[131]	$p\rho T$, VLE	552	548	278 to 444	0.138 to 68.9	0.075 to 0.994
carbon monoxide−hydrogen sulfide[132]	VLE	50	49	203 to 293	0.158 to 23.7	0.828 to 0.9996
water−hydrogen sulfide[133−136]	$p\rho T$, VLE	186	100	303 to 589	0.345 to 34.5	0.0029 to 0.1586

[a]Vapor−liquid equilibrium (vapor pressures and compositions of the vapor and liquid phases). [b]Sound speed.

or even the entire (mole fraction) range from 0 to 1. With about 76 % (≈12 500 data points), the majority of the collected data describes the $p\rho T$ relation in the homogeneous gas, liquid, and supercritical regions followed by VLE properties with roughly 23 % (≈3800 data points). Only a few data are sound-speed measurements. For some mixtures (e.g., *n*-pentane−*n*-nonane, *n*-heptane−*n*-nonane, *n*-nonane−*n*-decane), very few $p\rho T$ data are available as liquid densities measured at (around) 298 K and 0.1 MPa, covering the entire composition range, but representing the only available experimental information. Most of the 16 000 collected data points (more than 13 000 data points) were used for fitting the binary parameters of the expanded model. Table 4 gives an overview of the experimental data used for the expansion of GERG-2004.

About 86 % of the collected data (≈14 000 data points) account for the following 11 binary mixtures, for which more than 500 data points per mixture are available: methane−*n*-decane, ethane−*n*-decane, propane−*n*-decane, *n*-butane−*n*-decane, carbon dioxide−*n*-decane, methane−hydrogen sulfide, ethane−hydrogen sulfide, propane−hydrogen sulfide, *n*-pentane−hydrogen sulfide, *n*-decane−hydrogen sulfide, and carbon dioxide−hydrogen sulfide. The remaining 14 % (≈2300 data points) are spread over the other 26 binary mixtures. This shows that the data situation is rather unsatisfactory for the majority of mixtures. Particularly for mixtures with *n*-nonane, only few measurements are available.

In comparison to the binary mixtures consisting of the main natural-gas components, the quality of the experimental data used for the expansion work is poor. Moreover, no high-accuracy measurements, for example, density and sound-speed measurements with an uncertainty of less than 0.1 %, are available. For numerous measurements in the homogeneous region, the uncertainty in density is estimated to be roughly (0.5 to 2) % (e.g., density data of Reamer et al., refs 52, 95, and 131, for pressures up to 69 MPa). For many of the VLE data collected for the 37 binary mixtures mentioned above, the total uncertainty in vapor pressure is within the range usually observed for this data type, which is at least (1 to 3) %. Several VLE measurements are

dx.doi.org/10.1021/je300655b | J. Chem. Eng. Data 2012, 57, 3032−3091

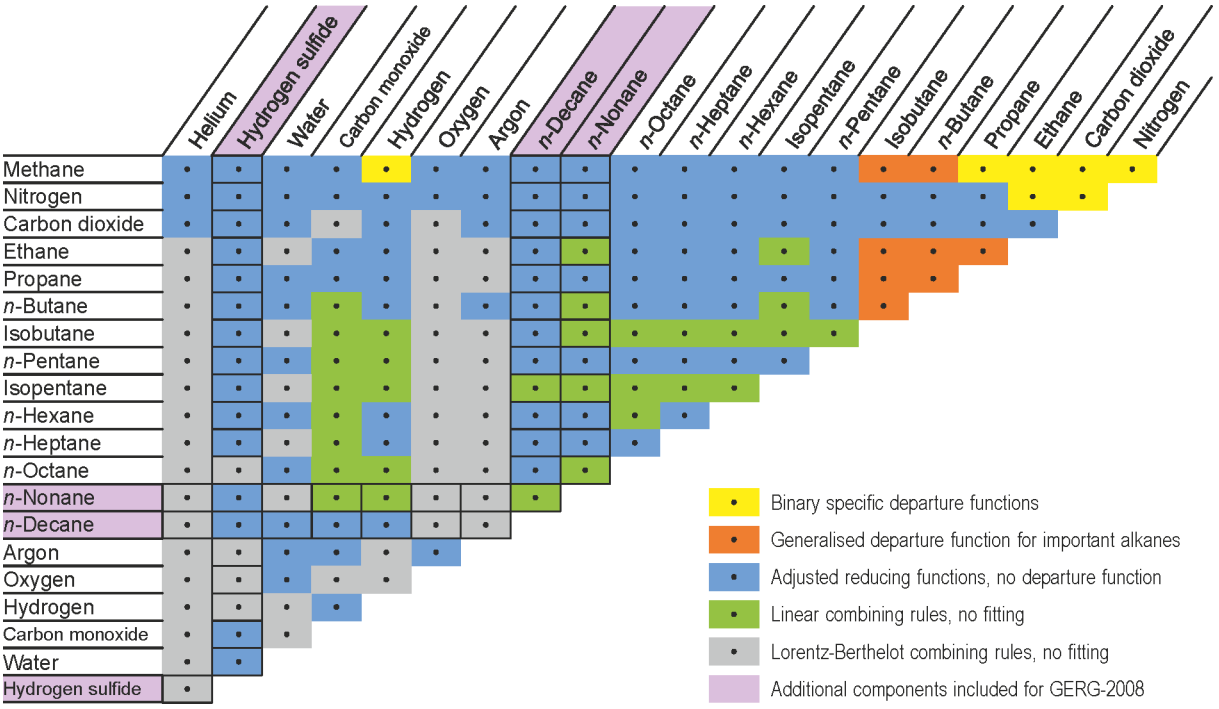

Figure 1. Overview of the 210 binary combinations that result from the 21 natural gas components considered for the development of the GERG-2008 equation of state, eq 8. The fields corresponding to the additional 57 binary mixtures, which are formed by the combinations of the three additional components *n*-nonane, *n*-decane, and hydrogen sulfide with the "old" 18 components of GERG-2004, are framed. The diagram illustrates the different types of functions used for the description of the binary mixtures. The fields marked in yellow and orange show which of the two types of departure functions were used to fit the function to experimental data; in these cases, the parameters of the reducing functions were also fitted. The blue fields refer to binary mixtures where only the parameters of the reducing functions were fitted to experimental data. The green and gray fields indicate with which combining rule the reducing functions (without any fitting) were used. The additional components included for GERG-2008 are marked in lilac.

associated with even higher uncertainties. The lack of very accurate measurements has complicated the development of the expanded model.

3.2. Recommendations for Further Improving the Data Basis. The development of the GERG-2008 equation of state revealed several weaknesses in the data sets, especially for mixtures containing secondary components. For example, only relatively few data exist for binary mixtures consisting of the secondary natural gas components listed in Table 1. The same is true for binary mixtures containing one of the main natural gas components and a secondary component.[1] Especially for the binary mixtures of methane with the hydrocarbons *n*-butane, isobutane, *n*-pentane, isopentane, and *n*-hexane, accurate gas phase densities should be measured over large temperature, pressure, and composition ranges. In this way, the representation of rich natural gases and similarly special mixtures by equations of state could be further improved (see also Section 6.3). For the $p\rho T$ relation of many binary mixtures consisting of heavier hydrocarbons, the available data only cover the liquid phase at limited temperatures or pressures (e.g., at atmospheric pressure). For some binary mixtures, the development of GERG-2008 is only based on either $p\rho T$ or VLE data. For many mixtures containing oxygen, argon, and helium, no suitable data are available.

For many binary mixtures of important natural gas components, no wide-ranging data exist for liquid-phase densities. For several mixtures, however, accurate saturated-liquid densities and compressed-liquid densities located near the saturation boundary (at low pressures) were measured. Most of these data cover temperatures from (100 to 140) K, enabling the development of an equation of state that allows for the accurate description of liquid-phase densities over the temperature range that is important for custody transfer of LNG and natural-gas liquefaction processes. Liquid-phase densities of comparatively high quality and measured over wide ranges of pressure ($p \leq 40$ MPa) exist for the binary mixtures methane−nitrogen, methane−ethane, and some other mixtures, such as binary mixtures consisting of the heavier hydrocarbons *n*-pentane, *n*-hexane, and *n*-heptane. In contrast to the data sets for gas-phase densities, many of the liquid-phase densities were measured for a limited number of compositions, or at only one constant temperature (e.g., 298.15 K) or pressure (e.g., 0.1 MPa).

Compared to the huge amount of available experimental $p\rho T$ and VLE data, measurements of caloric properties are scarce. For example, data for caloric properties of binary mixtures of methane with *n*-butane, isobutane, and heavier hydrocarbons (and other secondary components) are scarce or not available. Nevertheless, the available caloric data provide a suitable basis for the development of an accurate and wide-ranging equation of state for natural gases, since most of these data were measured for binary mixtures consisting of the main natural-gas components, which already cover about 97 % of the composition of typical natural gas mixtures.

Within the framework of the GERG project mentioned above, accurate data were measured for sound speeds of methane−nitrogen and nitrogen−ethane, which eliminated some of the weaknesses in these data sets. However, additional measurements are still worthwhile to improve the present data situation for caloric properties:

dx.doi.org/10.1021/je300655b | J. Chem. Eng. Data 2012, 57, 3032−3091

- For the binary mixtures methane−propane and methane−carbon dioxide, additional sound-speed data should be measured at pressures above 10 MPa.
- Since the heavier alkanes have a significant influence on the sound speed of multi-component mixtures at lower temperatures, accurate sound-speed data at supercritical temperatures should be measured for the binary mixtures methane−*n*-butane, methane−isobutane, methane−*n*-pentane, methane−isopentane, and methane−*n*-hexane.
- For mixtures of important natural gas components, such as nitrogen−carbon dioxide and carbon dioxide−propane, only few data are available for caloric properties.
- Moreover, for most of the binary mixtures that consist of secondary natural gas components, including mixtures with the three additional components considered for the expansion of GERG-2004, no (accurate) caloric data are available.

Due to the lack of (very) accurate experimental data for binary mixtures that contain one of the three new components *n*-nonane, *n*-decane, and hydrogen sulfide, it is highly recommended to perform accurate measurements for various properties for these mixtures over wide ranges of temperature, pressure, and composition. On the one hand, this recommendation refers to the binary combinations of the main natural gas components with the three new components. On the other hand, it also refers to mixtures of secondary components with the three new components and especially to mixtures containing *n*-nonane.

4. THE GERG-2008 EQUATION OF STATE FOR NATURAL GASES AND OTHER MIXTURES

The GERG-2008 equation of state is an expansion of the GERG-2004 equation of state.[1] In addition to the 18 components covered by GERG-2004, the GERG-2008 equation of state also considers the three components *n*-nonane, *n*-decane, and hydrogen sulfide. These additional components add up to the 21 components listed in Table 1. Thus, the GERG-2008 equation of state is valid for all of the mixtures that are covered by GERG-2004, and, in addition, it also covers all mixtures consisting of the 18 components of GERG-2004 and the three additional components in any arbitrary combination or concentration.

As shown in this section, the calculation of the thermodynamic properties of multi-component mixtures from GERG-2008 is based on equations developed for binary mixtures. In this sense, GERG-2004 covers 153 binary mixtures (formed from the 18 pure components). The three additional components mentioned above result in 57 additional binary mixtures. The 57 additional mixtures add up to a total of 210 binary mixtures (formed from the 21 pure components) covered by the expanded model GERG-2008. The numerical information given for the 153 binary mixtures of GERG-2004 remain almost entirely unchanged. The numerical values that characterize the 57 additional binary mixtures had to be added. Figure 1 shows how the 57 additional binary mixtures are formed.

For the mixtures of the 18 components covered by GERG-2004, the GERG-2008 equation of state yields virtually the same results as GERG-2004. Both equations are determined by the same mathematical formalism; only the maximum value for N in the corresponding summations is different.

If one is only interested in the application of GERG-2008 and not in the details of its development, sufficient information is given in Section 4.1.

4.1. Numerical Description of GERG-2008.

The GERG-2008 equation of state for natural gases and other mixtures of natural gas components is based on a multi-fluid approximation explicit in the reduced Helmholtz free energy

$$\alpha(\delta, \tau, \overline{x}) = \alpha^{o}(\rho, T, \overline{x}) + \alpha^{r}(\delta, \tau, \overline{x}) \tag{8}$$

where the α^{o} part represents the properties of the ideal-gas mixture at a given mixture density ρ, temperature T, and molar composition $\overline{x}$ according to

$$\alpha^{o}(\rho, T, \overline{x}) = \sum_{i=1}^{N} x_i[\alpha_{oi}^{o}(\rho, T) + \ln x_i] \tag{9}$$

The residual part α^{r} of the reduced Helmholtz free energy of the mixture is given by

$$\alpha^{r}(\delta, \tau, \overline{x}) = \sum_{i=1}^{N} x_i\alpha_{oi}^{r}(\delta, \tau) + \sum_{i=1}^{N-1}\sum_{j=i+1}^{N} x_i x_j F_{ij}\alpha_{ij}^{r}(\delta, \tau) \tag{10}$$

where δ is the reduced mixture density and τ is the inverse reduced mixture temperature according to

$$\delta = \frac{\rho}{\rho_r(\overline{x})} \quad \text{and} \quad \tau = \frac{T_r(\overline{x})}{T} \tag{11}$$

and $N = 21$ is the total number of components in the mixture. Since the mixture model is not limited to the currently considered 21 components, the summation variable N is continuously used in this work to denote the maximum number of components.

Equation 10 takes into account the residual behavior of the mixture at the reduced mixture variables δ and τ. The first sum in this equation is the linear contribution of the reduced residual Helmholtz free energy of the pure substance equations of state multiplied by the mole fractions x_i. The double summation in eq 10 is the departure function $\Delta\alpha^{r}(\delta,\tau,\overline{x})$ (see also eqs 7 and 44), which is the summation over all binary specific and generalized departure functions $\Delta\alpha_{ij}^{r}(\delta,\tau,\overline{x})$ developed for the respective binary mixtures (see eq 45).

In eq 9, the dimensionless form of the Helmholtz free energy in the ideal-gas state of component i is given by

$$\begin{aligned}\alpha_{oi}^{o}(\rho, T) = \ln\left(\frac{\rho}{\rho_{c,i}}\right) + \frac{R^*}{R}\Bigg[n_{oi,1}^{o} + n_{oi,2}^{o}\frac{T_{c,i}}{T} + n_{oi,3}^{o}\ln\left(\frac{T_{c,i}}{T}\right) \\ + \sum_{k=4,6} n_{oi,k}^{o}\ln\left(\left|\sinh\left(\vartheta_{oi,k}^{o}\frac{T_{c,i}}{T}\right)\right|\right) \\ - \sum_{k=5,7} n_{oi,k}^{o}\ln\left(\cosh\left(\vartheta_{oi,k}^{o}\frac{T_{c,i}}{T}\right)\right)\Bigg]\end{aligned} \tag{12}$$

where $\rho_{c,i}$ and $T_{c,i}$ are the critical parameters of the pure components (see Table A5 of Appendix A) and

$$R = 8.314472\ \mathrm{J\cdot mol^{-1}\cdot K^{-1}} \tag{13}$$

is the molar gas constant. This value corresponds to the internationally accepted standard for R at the time when the equations GERG-2004 and GERG-2008 were developed.[138] The equations for α_{oi}^{o} result from the integration of the c_p^{o} equations of Jaeschke and Schley[25] who used a different molar gas constant than the one used in the developed mixture model. The ratio R^*/R with $R^* = 8.314510\ \mathrm{J\cdot mol^{-1}\cdot K^{-1}}$, used in ref 25, takes into

dx.doi.org/10.1021/je300655b | J. Chem. Eng. Data 2012, 57, 3032−3091

account this difference and therefore leads to the exact solution of the original c_p^o equations. The values of the coefficients $n_{oi,k}^o$ and the parameters $\vartheta_{oi,k}^o$ of eq 12 for all of the considered 21 components are listed in Table A1 of Appendix A.

In eq 10, the residual part of the reduced Helmholtz free energy of component i (i.e., the residual part of the respective pure substance equations of state listed in Table 1) is given by

$$\alpha_{oi}^r(\delta, \tau) = \sum_{k=1}^{K_{Pol,i}} n_{oi,k}\delta^{d_{oi,k}}\tau^{t_{oi,k}} + \sum_{k=K_{Pol,i}+1}^{K_{Pol,i}+K_{Exp,i}} n_{oi,k}\delta^{d_{oi,k}}\tau^{t_{oi,k}}e^{-\delta^{c_{oi,k}}} \quad (14)$$

The respective values for the coefficients $n_{oi,k}$ and the exponents $d_{oi,k}$, $t_{oi,k}$, and $c_{oi,k}$ for all considered components are given in Tables A2 to A4, and the critical parameters are listed in Table A5. For the simultaneously optimized equations of state of Span and Wagner,[23] the old molar gas constant was substituted with the recent one without any other conversion. This change can be neglected with regard to the accuracy of the equations of state. The mathematical structure of eq 14 is identical for all components in GERG-2008.

The function $\alpha_{ij}^r(\delta,\tau)$ of eq 10, which is the part of the departure function $\Delta\alpha_{ij}^r(\delta,\tau,\overline{x})$ that depends only on the reduced mixture variables δ and τ (see eq 45), is given by

$$\alpha_{ij}^r(\delta, \tau) = \sum_{k=1}^{K_{Pol,ij}} n_{ij,k}\delta^{d_{ij,k}}\tau^{t_{ij,k}} + \sum_{k=K_{Pol,ij}+1}^{K_{Pol,ij}+K_{Exp,ij}} n_{ij,k}\delta^{d_{ij,k}}\tau^{t_{ij,k}} \cdot \exp[-\eta_{ij,k}(\delta - \varepsilon_{ij,k})^2 - \beta_{ij,k}(\delta - \gamma_{ij,k})] \quad (15)$$

where $\alpha_{ij}^r(\delta,\tau)$ was developed for either a specific binary mixture (a binary specific departure function with binary specific coefficients and parameters) or a certain group of binary mixtures (generalized departure function with a uniform structure for the group of binary mixtures considered). For a binary specific departure function, the adjustable factor F_{ij} in eq 10 is set to unity. The factor F_{ij} is fitted to binary specific data for each mixture in the group of generalized binary mixtures (see also Section 4.4.3). F_{ij} equals zero for those binary mixtures where departure functions were not developed. The nonzero F_{ij} parameters are listed in Table A6. The values for the coefficients $n_{ij,k}$ and the exponents $d_{ij,k}$, $t_{ij,k}$, $\eta_{ij,k}$, $\varepsilon_{ij,k}$, $\beta_{ij,k}$, and $\gamma_{ij,k}$ for all binary specific and generalized departure functions considered in the GERG-2008 equation of state are given in Table A7.

The reduced mixture variables δ and τ are calculated from eq 11 by means of the composition-dependent reducing functions for the mixture density

$$\frac{1}{\rho_r(\overline{x})} = \sum_{i=1}^{N} x_i^2\frac{1}{\rho_{c,i}} + \sum_{i=1}^{N-1}\sum_{j=i+1}^{N} 2x_ix_j\beta_{v,ij}\gamma_{v,ij}\cdot\frac{x_i + x_j}{\beta_{v,ij}^2x_i + x_j}\cdot \frac{1}{8}\left(\frac{1}{\rho_{c,i}^{1/3}} + \frac{1}{\rho_{c,j}^{1/3}}\right)^3 \quad (16)$$

and the mixture temperature

$$T_r(\overline{x}) = \sum_{i=1}^{N} x_i^2T_{c,i} + \sum_{i=1}^{N-1}\sum_{j=i+1}^{N} 2x_ix_j\beta_{T,ij}\gamma_{T,ij}\cdot \frac{x_i + x_j}{\beta_{T,ij}^2x_i + x_j}(T_{c,i}\cdot T_{c,j})^{0.5} \quad (17)$$

The binary parameters $\beta_{v,ij}$ and $\gamma_{v,ij}$ in eq 16 and $\beta_{T,ij}$ and $\gamma_{T,ij}$ in eq 17 are fitted to data for binary mixtures. The values of the binary parameters for all binary mixtures are listed in Table A8. The critical parameters $\rho_{c,i}$ and $T_{c,i}$ of the pure components are given in Table A5.

4.2. Property Calculations. All thermodynamic properties of a mixture (or pure substance) can be obtained by combining various derivatives of eq 8. The thermodynamic properties in the homogeneous gas, liquid, and supercritical regions of a mixture are related only to derivatives with respect to density and temperature. In addition, more complex derivatives with respect to the mixture composition, namely, the mole numbers n_i and mole fractions x_i, have to be taken into account for phase-equilibrium calculations (see Section 4.2.1).

For example, in the homogeneous gas, liquid, and supercritical regions, the pressure p, the enthalpy h, and the entropy s can be determined from the following equations:

$$\frac{p(\delta, \tau, \overline{x})}{\rho RT} = 1 + \delta\alpha_\delta^r \quad (18)$$

$$\frac{h(\delta, \tau, \overline{x})}{RT} = 1 + \tau(\alpha_\tau^o + \alpha_\tau^r) + \delta\alpha_\delta^r \quad (19)$$

$$\frac{s(\delta, \tau, \overline{x})}{R} = \tau(\alpha_\tau^o + \alpha_\tau^r) - \alpha^o - \alpha^r \quad (20)$$

with α^o and α^r according to eqs 9 and 10 and the abbreviations

$$\alpha_\delta^r = \left(\frac{\partial\alpha^r}{\partial\delta}\right)_{\tau,\overline{x}}, \qquad \alpha_\tau^r = \left(\frac{\partial\alpha^r}{\partial\tau}\right)_{\delta,\overline{x}}, \qquad \text{and} \qquad \alpha_\tau^o = \left(\frac{\partial\alpha^o}{\partial\tau}\right)_{\delta,\overline{x}} \quad (21)$$

for the derivatives of α^o and α^r with respect to the reduced mixture variables δ and τ see Table B5 of Appendix B. It should be noted that a stability investigation by means of, for example, the tangent-plane-distance method (e.g., Michelsen[139]), has to be performed to ensure that the mixture is homogeneous. A comprehensive list of common thermodynamic properties and their relations to the reduced Helmholtz free energy α, eq 8, is given in Table B1. Additionally, relations for derivatives of pressure, density, total volume, and temperature are summarized in Table B2. The relations between α and the chemical potential μ_i, the fugacity coefficient φ_i, and the fugacity f_i of component i, which are required for VLE calculations, are presented in Table B3. The calculation of these properties requires the determination of composition derivatives of α^o and α^r. Table B4 lists the first partial derivatives of α^o, α^r, and α_δ^r with respect to the mole numbers n_i. The second derivatives with respect to n_i and further relations required for advanced phase-equilibrium algorithms are given by Kunz et al.[1]

A complete list of all fundamental derivatives of eqs 9 and 10 with respect to δ, τ, and x_i, which are required for standard and advanced property calculations (see Tables B1 to B4), is presented in Table B5. The respective derivatives of α_{oi}^o, α_{oi}^r, and α_{ij}^r (see eqs 12, 14, and 15) are explicitly listed in Tables B6 to B8.

Aside from the basic derivatives of α^o with respect to δ and τ and of α^r with respect to δ, τ, and x_i (see Table B5), derivatives of the composition-dependent reducing functions for the mixture density and temperature (eqs 16 and 17) with respect to x_i have to be taken into account for the determination of the first and second derivatives of α^r with respect to the mole numbers n_i. These mole fraction derivatives of the reducing functions are explicitly listed in Table B9.

dx.doi.org/10.1021/je300655b | J. Chem. Eng. Data 2012, 57, 3032−3091

The formalism where the properties and their derivatives are calculated by combining partial derivatives of the Helmholtz free energy of the mixture ensures a consistent set of relations as shown in the tables of Appendix B and leads to an efficient computer code. As shown by Kunz et al.,[1] tests for the verification of the calculated fugacity coefficients and their partial derivatives are straightforward.

The calculation of phase-equilibrium properties of mixtures represents a considerable complex mathematical problem. This happens because of the large set of equations resulting from the large number of phase-equilibrium conditions, the large number of variables to be solved for, and the complex derivatives with respect to mixture composition. Furthermore, the number of equilibrium phases is usually not known in advance. Aside from the ordinary vapor−liquid equilibrium, further phase equilibria, such as liquid−liquid, vapor−liquid−liquid, and other multiphase equilibria, may occur when dealing with mixtures. To verify that the solution for an equilibrium mixture is stable, the thermodynamic state function involved in the calculation, for example, the total (or molar) Gibbs free energy G (or g) of the overall system for a pT flash calculation, has to be at its global minimum. In this context, for instance, the total Gibbs free energy is just the energy of a state point, and the overall Gibbs free energy would be the total energy of all the states (phases) in a system. Thus, to ascertain that the derived minimum is the global minimum, a stability analysis has to be performed as well.

4.2.1. Calculation of Vapor−Liquid Equilibrium Properties. Thermodynamic equilibrium between two or more coexisting phases exists when neither the net flux of heat, momentum, nor material is exchanged across the phase boundary. Consequently, temperature, pressure, and the chemical potentials μ_i of all components i have to be equal in all phases. For the common two-phase vapor−liquid equilibrium of a nonreacting mixture consisting of N components, the following phase-equilibrium conditions must be satisfied:

- Equality of temperature

$$T' = T'' = T \tag{22}$$

- Equality of pressure

$$p' = p'' = p_s \tag{23}$$

- Equality of chemical potentials

$$\mu_i' = \mu_i'' \qquad i = 1, 2, ..., N \tag{24}$$

where $'$ denotes the liquid phase and $''$ denotes the vapor phase.

For the calculation of phase equilibria, the fugacity f_i and the fugacity coefficient φ_i of component i are often used instead of the chemical potential. Equation 24 can then be replaced with one of the following equations:

$$f_i' = f_i'' \qquad i = 1, 2, ..., N \tag{25}$$

$$\varphi_i'/\varphi_i'' = x_i''/x_i' \qquad i = 1, 2, ..., N \tag{26}$$

The ratio of x_i'' over x_i' is defined as the K-factor of component i:

$$K_i = x_i''/x_i' \tag{27}$$

The fugacity f_i and fugacity coefficient φ_i of component i are related to eq 8 by

$$f_i = x_i \rho RT \exp\left(\frac{\partial n\alpha^r}{\partial n_i}\right)_{T,V,n_j} \tag{28}$$

and

$$\ln \varphi_i = \left(\frac{\partial n\alpha^r}{\partial n_i}\right)_{T,V,n_j} - \ln Z \tag{29}$$

for the derivatives of $n\alpha^r$ with respect to n_i see Table B4. The property Z is the compression factor with $Z = p/(RT\rho)$.

Aside from the equality of temperature, pressure, and chemical potentials, further equations, which result from the material balances between the molar amounts of the components in the overall system and the coexisting phases, have to be satisfied as secondary conditions according to

$$x_i = (1 - \beta)x_i' + \beta x_i'' \qquad i = 1, 2, ..., N \tag{30}$$

where the overall vapor fraction is

$$\beta = \frac{n''}{n} = \frac{n''}{n' + n''} \tag{31}$$

with

$$\sum_{i=1}^{N} x_i = 1, \qquad \sum_{i=1}^{N} x_i' = 1, \qquad \text{and} \qquad \sum_{i=1}^{N} x_i'' = 1 \tag{32}$$

Substituting eq 27 into the material balance equations, eq 30, yields

$$x_i' = \frac{x_i}{1 - \beta + \beta K_i} \quad \text{and} \quad x_i'' = \frac{K_i x_i}{1 - \beta + \beta K_i} \tag{33}$$

Thus, the phase mole fractions $\overline{x}'$ and $\overline{x}''$ can be calculated from the K-factors, the overall vapor fraction β, and the overall composition $\overline{x}$.

The phase equilibrium and secondary conditions form a nonlinear set of equations, which has to be solved by iteration. Over the past several decades, many of procedures, which are suitable for solving the phase equilibrium and secondary conditions based on equations of state for mixtures, have been reported. A survey of such procedures is given by Heidemann.[140] Computational aspects of a number of iterative procedures to solve two-phase and multiphase equilibrium conditions are presented by Michelsen and Mollerup.[141]

To enable the development of robust and efficient algorithms, all of the derivatives needed for such applications of the mixture model, even the second derivatives of α^r with respect to composition, were analytically determined. The derivatives are formulated in a general manner that enables the use of the derived formulations for any multi-fluid approximation based on a similar structure as the new mixture model presented here; for additional details see Kunz et al.[1]

4.2.2. Property Calculation Software. Along with the new mixture model, a comprehensive and user-friendly software package was developed. The software enables the calculation of many thermodynamic properties in the homogeneous gas, liquid, and supercritical regions and allows carrying out extensive VLE calculations at arbitrary mixture conditions where the prior knowledge of the number of phases (one or two) is not required. This includes pT flash, ph flash, ps flash, Tv flash, uv flash, phase envelope, dew-point, and bubble-point calculations without any user-provided initial estimates. The algorithms are based on modern numerical procedures developed by Michelsen (e.g., refs 139 and 142 to 144) and use various partial derivatives to solve the set of equations of equilibrium and secondary conditions for the unknown variables, to perform second-order Gibbs free

energy minimization, and to verify the (phase) stability of the solution by means of minimizing the tangent plane distance. Due to the increased complexity of the mixture model, a systematic and modular approach, where all required derivatives (including the complex composition derivatives) were analytically determined, was used to avoid inefficient and incorrect computer codes. Details on the available property calculation software are given on the web page http://www.thermo.rub.de/de/prof-w-wagner/software/gerg-2004-gerg-2008.html.

4.3. Ranges of Validity and Estimates of Uncertainty. The equation of state GERG-2008 covers wide ranges of temperature, pressure, and composition and is valid in the gas phase, liquid phase, supercritical region, and for vapor−liquid equilibrium (VLE) states. The model achieves high accuracy in the calculation of thermodynamic properties for a broad variety of natural gases and other multi-component and binary mixtures consisting of the 21 components listed in Table 1. The entire range of validity is divided into three parts: normal range of validity, extended range of validity, and extrapolation to temperatures and pressures beyond the extended range of validity. The estimated uncertainties given for the different ranges of validity, as described below, are based on the representation of experimental data for various thermodynamic properties of binary and multi-component mixtures by the GERG-2008 equation of state.

Due to the huge amount of experimental data for the different binary and multi-component mixtures and the varying real mixture behavior, which strongly depends on temperature, pressure, and composition, it is not practical to discuss each of the different binary and multi-component systems separately at this point. Therefore, only the most important statements on the ranges of validity and estimated uncertainties of the GERG-2008 equation of state are given in this section. The given statements are focused on the use of the equation in standard and advanced technical applications with natural gases and similar mixtures. In general, there are no restrictions on the composition range of binary and multi-component mixtures. Since the estimated uncertainty of the GERG-2008 equation of state is based on the experimental data used for the development and evaluation of the equation, the uncertainty is mostly unknown for the composition ranges not covered by experimental data. The data situation allows for a well-founded uncertainty estimation only for selected properties and parts of the fluid surface.

Comparisons of the GERG-2008 equation of state with selected experimental data and values calculated from other equations of state are the subject of Section 5.

4.3.1. Normal Range of Validity. The normal range of validity of the GERG-2008 equation of state, eq 8, covers the temperature and pressure ranges

$$90\ \mathrm{K} \leq T \leq 450\ \mathrm{K}$$

$$p \leq 35\ \mathrm{MPa}$$

This range corresponds to the use of the equation in both standard and advanced technical applications with natural gases and similar mixtures, for example, pipeline transport, natural gas storage, and improved processes with liquefied natural gas.

The uncertainty of GERG-2008, eq 8, in gas-phase density is 0.1 % over the temperature range from (250 to 450) K at pressures up to 35 MPa. This uncertainty estimate is valid for various types of natural gases (almost every natural gas mixture included in the GERG TM7 databank; see Section 3), including natural gases rich in nitrogen, rich in carbon dioxide, rich in ethane, or rich in hydrogen (natural gas−hydrogen mixtures), natural gases containing relatively high fractions or considerable amounts of propane and heavier hydrocarbons, carbon monoxide, or oxygen, and many other mixtures (e.g., coke-oven gases) consisting of the 21 natural gas components listed in Table 1.

The great majority of experimental densities for various rich natural gases, which contain comparatively large amounts of carbon dioxide (up to $x_{CO_2} = 0.20$), ethane (up to $x_{C_2H_6} = 0.18$), propane (up to $x_{C_3H_8} = 0.14$), *n*-butane (up to $x_{n\text{-}C_4H_{10}} = 0.06$), *n*-pentane ($x_{n\text{-}C_5H_{12}} = 0.005$), and *n*-hexane ($x_{n\text{-}C_6H_{14}} = 0.002$), are reproduced by GERG-2008 to within ± (0.1 to 0.3) % over the range covered by experimental data, namely, for temperatures from (280 to 350) K and pressures up to 30 MPa. For rich natural gases with carbon dioxide mole fractions of 0.14 and more, systematic deviations exceeding 0.3 % are observed at some states (see also Section 5.2.1.6).

The uncertainty in gas-phase sound speeds of common natural gases and similar mixtures is less than 0.1 % for temperatures ranging from (270 to 450) K at pressures up to 20 MPa and for temperatures from (250 to 270) K at pressures up to 12 MPa. At higher pressures, the data situation generally does not allow for a well-founded uncertainty estimation for multi-component (and also binary) mixtures. Therefore, an increased uncertainty of (0.2 to 0.3) % is assumed at higher pressures. The uncertainty in sound speed for some important binary mixtures, such as methane−nitrogen and methane−ethane, amounts to (0.05 to 0.1) % over wide temperature, pressure, and composition ranges, for example, down to temperatures of 220 K and at pressures up to 30 MPa for the methane−nitrogen system. Furthermore, GERG-2008 represents accurate data for isobaric enthalpy differences of binary and multi-component mixtures to within their experimental uncertainty, which is (0.2 to 0.5) %.

For binary and multi-component mixtures, measured isobaric and isochoric heat capacities in the homogeneous gas, liquid, and supercritical regions are accurately described by GERG-2008 to within ± (1 to 2) %, which is in agreement with the experimental uncertainty of the available data. Experimental liquid-phase isobaric enthalpy differences are represented to within ± (0.5 to 1) %.

In the liquid phase at pressures up to 40 MPa, the uncertainty of the equation in density amounts to approximately (0.1 to 0.5) % for many binary and multi-component mixtures, for example, LNG-like mixtures and mixtures of light or heavier hydrocarbons. This is in agreement with the experimental uncertainty. A similar uncertainty is estimated for saturated-liquid densities of different binary and multi-component LNG-like mixtures over the temperature range from (100 to 140) K, which is of considerable importance for processes with liquefied natural gas. In this temperature range, comparisons with experimental liquid-phase and saturated-liquid densities show that the uncertainty is in the range of (0.1 to 0.3) % for many mixtures.

The *pTxy* relation of binary and multi-component mixtures and the dew points of natural gases and hydrocarbon mixtures are accurately described as well. The most accurate vapor-pressure data for binary and ternary mixtures consisting of the natural gas main components (see Table 1) or the hydrocarbons propane, *n*-butane, and isobutane are reproduced by the equation to within their experimental uncertainty, which is approximately (1 to 3) % (see also Table 2). Other mixtures may have higher uncertainties of up to 5 % (or more) and are described with reasonable accuracy. This is mostly due to restrictions resulting from limited or poor data. Accurate experimental

vapor-phase compositions are described to within $x_i = \pm$ (0.005 to 0.01) mole fraction, which is well within the uncertainty of the measurements. In this context, it should be noted that the phase behavior of many mixtures is considerably sensitive to errors in the mixture composition. Limited or poor data require a very careful assessment of their representation by equations of state.

4.3.2. Extended Range of Validity and the Calculation of Properties beyond This Range. The extended range of validity covers the temperature and pressure ranges

$$60\ \mathrm{K} \leq T \leq 700\ \mathrm{K}$$

$$p \leq 70\ \mathrm{MPa}$$

The uncertainty of the equation in gas-phase density at temperatures and pressures outside the normal range of validity is roughly estimated to be (0.2 to 0.5) %. For certain mixtures, the extended range of validity covers temperatures of $T > 700$ K and pressures of $p > 70$ MPa. For example, the equation accurately describes gas-phase density data for air to within ± (0.1 to 0.2) % at temperatures up to 900 K and pressures up to 90 MPa. The data measured outside the normal range of validity generally do not allow for well-founded estimates of uncertainty in other thermodynamic properties.

When larger uncertainties are acceptable, tests have shown that the equation can be reasonably used outside the extended range of validity. For example, density data (frequently of questionable and low accuracy outside the extended range of validity) for certain binary mixtures are described to within ± (0.5 to 1) % at pressures up to 100 MPa and more.

4.3.3. Some General Statements on the Uncertainty in Calculated Properties for Binary Mixtures. The new mixture model basically allows for the calculation of thermodynamic properties of a total of 210 binary mixtures of arbitrary composition. These binary systems strongly differ in their real mixture behavior and in the quality and extent of the available experimental data. Therefore, it is not possible to give individual statements on the uncertainty in the description of thermodynamic properties for each binary mixture at this point. To provide at least some general statements on the uncertainty of the GERG-2008 equation of state in the description of the different binary mixtures, the classifications according to Table 5 (see also Figure 1) are made. The quality of the calculation of thermodynamic properties generally depends on the type of correlation equation developed for a binary mixture. The highest quality is achieved for binary mixtures for which a departure function (binary specific or generalized) was developed, followed by the binary mixtures where only the parameters of the reducing functions were adjusted. Aside from the type of correlation equation, the description of thermodynamic properties varies for the different fluid regions.

Table 5. List of the Binary Mixtures for Which Binary Specific or Generalized Departure Functions Were Developed

binary mixture	type of departure function	no. terms
methane−nitrogen	binary specific	9
methane−carbon dioxide	binary specific	6
methane−ethane	binary specific	12
methane−propane	binary specific	9
methane−*n*-butane	generalized	10
methane−isobutane	generalized	10
methane−hydrogen	binary specific	4
nitrogen−carbon dioxide	binary specific	6
nitrogen−ethane	binary specific	6
ethane−propane	generalized	10
ethane−*n*-butane	generalized	10
ethane−isobutane	generalized	10
propane−*n*-butane	generalized	10
propane−isobutane	generalized	10
n-butane−isobutane	generalized	10

Table 6 summarizes the estimated uncertainties in selected thermodynamic properties for those mixtures where a binary specific or generalized departure function was developed or only adjusted reducing functions were used. The given general statements result from conservative estimations. For many individual mixtures, properties, or compositions, the (total) uncertainty is often near the lower value of the uncertainty range given in Table 6. This applies, for example, to the uncertainties in liquid-phase density and vapor pressure of binary mixtures composed of very similar hydrocarbons, such as ethane−propane, propane−*n*-butane, propane−isobutane, or *n*-butane−isobutane, where a generalized departure function is used. Here, the uncertainty often extends over the entire uncertainty range given in Table 6 for mixtures for which a binary specific departure function was developed. The same is valid for other binary mixtures composed of similar (or similarly behaving) components with only adjusted reducing functions (or even without any fitting), such as methane−argon, nitrogen−oxygen, nitrogen−argon, carbon dioxide−ethane, *n*-heptane−*n*-octane, oxygen−argon, and so forth. Liquid phase densities for mixtures consisting of heavier hydrocarbons, such as *n*-pentane−*n*-hexane, *n*-pentane−*n*-heptane, or *n*-hexane−*n*-heptane, are reproduced within ± (0.2 to 0.5) %.

The uncertainty statements listed in Table 6 may be exceeded for mixtures that show relatively strong real mixture behavior. The difference between the critical temperatures of the pure components of a binary mixture can be used as a simplified indication of the extent of the real mixture behavior. When the critical temperatures differ by more than 150 K, increased uncertainties may exist. This is especially true for the uncertainty in vapor pressure.

It is very difficult to give a general statement on the accuracy achieved for binary mixtures for which only the reducing functions with different combining rules (no fitting) were used. For binary mixtures composed of similarly behaving components, for example, similar hydrocarbons, nearly the same uncertainties may be expected as for mixtures where the parameters of the reducing functions were adjusted. Because data are not available in most of these cases, the uncertainty is basically considered to be unknown.

As mentioned before, the development of the GERG-2008 equation of state and the estimates of uncertainty are based on experimental data. At least for the properties in the homogeneous region, the measurements often do not cover the entire composition range. Therefore, the uncertainty also depends on the composition. One exception of considerable importance for natural gases is the binary mixture methane−nitrogen. Here, the uncertainty statements given in Table 6 are approximately valid for all compositions.

4.3.4. The Pure Substance Equations of State. As mentioned before, the new mixture model uses pure substance equations of

dx.doi.org/10.1021/je300655b | J. Chem. Eng. Data 2012, 57, 3032−3091

Table 6. Estimates of Uncertainty of GERG-2008, eq 8, in the Description of Selected Thermal and Caloric Properties for Different Binary Mixtures[a]

	adjusted reducing functions		
mixture region	and a binary specific departure function	and a generalized departure function	only adjusted reducing functions (no departure function)
gas phase, $p \le 30$ MPa; $1.2 \le T/T_r \le 1.4$	$\Delta\rho/\rho$ = 0.1 %	$\Delta\rho/\rho$ = (0.1 to 0.2) %	$\Delta\rho/\rho$ = (0.5 to 1) %
gas phase, $p \le 30$ MPa; $1.4 \le T/T_r \le 2.0$	$\Delta\rho/\rho$ = 0.1 %	$\Delta\rho/\rho$ = 0.1 %	$\Delta\rho/\rho$ = (0.3 to 0.5) %
gas phase, $p \le 20$ MPa; $1.2 \le T/T_r \le 1.4$	$\Delta w/w$ = 0.1 %	$\Delta w/w$ = 0.5 %	$\Delta w/w$ = 1 %
gas phase, $p \le 20$ MPa; $1.4 \le T/T_r \le 2.0$	$\Delta w/w$ = 0.1 %	$\Delta w/w$ = 0.3 %	$\Delta w/w$ = 0.5 %
phase equilibrium, 100 K $\le T \le$ 140 K	$\Delta\rho'/\rho'$ = (0.1 to 0.2) %	$\Delta\rho'/\rho'$ = (0.2 to 0.5) %	$\Delta\rho'/\rho'$ = (0.5 to 1) %
phase equilibrium	$\Delta p_s/p_s$ = (1 to 3) %	$\Delta p_s/p_s$ = (1 to 5) %	$\Delta p_s/p_s$ = 5 %
liquid phase, $p \le 40$ MPa; $T/T_r \le 0.7$	$\Delta\rho/\rho$ = (0.1 to 0.3) %	$\Delta\rho/\rho$ = (0.2 to 0.5) %	$\Delta\rho/\rho$ = (0.5 to 1) %

[a]The relative uncertainty in isobaric and isochoric heat capacity is estimated to be (1 to 2) % for the homogeneous gas, liquid, and supercritical regions and does not depend on the type of correlation equation developed for a binary mixture.

state for each component in the mixture along with further correlation equations developed for binary mixtures to describe the real behavior of multi-component mixtures. Considering the use of the mixture model in technical applications, its structure had to be kept as simple as possible. In practice, this enables sound programming and computing-time saving algorithms. At the same time, accurate experimental data for the thermodynamic properties of natural gases and other mixtures have to be represented by the mixture model to within the uncertainty of the measurements. To meet these conflicting requirements, accurate technical equations of state with only 12 to 24 terms and a less complex structure than used for high accuracy equations of state (e.g., Setzmann and Wagner,[10] Span and Wagner,[145] and Wagner and Pruß[146]) make up the pure substance basis of the new mixture model. Note that all types of equations of state can be used in the mixture model presented here. However, due to the lack of highly accurate experimental data in the critical region of mixtures, highly accurate pure substance equations of state are not relevant for mixture calculations. The equations for the 21 components considered in this work were developed in preceding studies (Klimeck,[22] Span and Wagner,[147,23] Lemmon and Span,[24] Kunz et al.[1]) and are empirical descriptions of the Helmholtz free energy. A list of the 21 components and their equations of state is presented in Table 1. Details on the development of these equations of state and their uncertainties in several thermodynamic properties are given in the corresponding references.

4.4. Theoretical Background. *4.4.1. Reducing Functions for Density and Temperature.* The reducing functions are used to determine the reduced variables for the mixture density and temperature according to eq 11. The mathematical structures used for the reducing functions of the models reported in the literature differ. Tillner-Roth[12] used a quadratic structure to model binary mixtures. Lemmon and Jacobsen[21] used reducing functions based on a linear structure to describe multi-component mixtures. Both mathematical forms use adjustable mole fraction exponents to realize asymmetric shapes of the functions.

The use of noninteger exponents for composition variables (i.e., the mole fractions of the mixture components) of mixing rules is generally problematic (see Mathias et al.[148]). To avoid infinite slopes of the reducing functions for $x_i \to 0$ (i.e., small mole fractions of one component in a binary mixture, and of one or several components in a multi-component mixture such as natural gas), reducing functions that contain such exponents should not be used in formulations for mixtures. The use of noninteger exponents would lead to, for example, infinite fugacities in phase-equilibrium calculations and physically wrong derivatives of these with respect to temperature, pressure, and composition.

In recent models reported for binary and ternary mixtures, no asymmetric behavior of the reducing functions is considered by the authors (e.g., Lemmon et al.,[15] Miyamoto and Watanabe,[16] Lemmon and Jacobsen[17]). Such a feature is not necessarily needed for systems with small mixing effects. However, the use of an asymmetric expression significantly improves the accuracy of the mixture model in the description of the thermodynamic properties, especially for well-measured mixtures.

Therefore, Klimeck[22] introduced a new class of reducing functions containing an asymmetric expression proposed by Tillner-Roth[19] that overcomes the dilemma mentioned above. The adjustable parameters of the new reducing functions, which are also used for the mixture model presented in this work, are not restricted to certain ranges of value (e.g., they can be negative or positive). The reducing functions for the mixture density and temperature can be written as

$$\frac{1}{\rho_r(\bar{x})} = \sum_{i=1}^{N}\sum_{j=1}^{N} x_i x_j \beta_{v,ij}\gamma_{v,ij} \cdot \frac{x_i + x_j}{\beta_{v,ij}^2 x_i + x_j} \cdot \frac{1}{8}\left(\frac{1}{\rho_{c,i}^{1/3}} + \frac{1}{\rho_{c,j}^{1/3}}\right)^3 \tag{34}$$

and

$$T_r(\bar{x}) = \sum_{i=1}^{N}\sum_{j=1}^{N} x_i x_j \beta_{T,ij}\gamma_{T,ij} \cdot \frac{x_i + x_j}{\beta_{T,ij}^2 x_i + x_j} \cdot (T_{c,i} \cdot T_{c,j})^{0.5} \tag{35}$$

These functions are based on quadratic mixing rules, and with that they are reasonably connected to physically well-founded mixing rules. The two adjustable binary parameters β and γ ($\beta_{v,ij}$ and $\gamma_{v,ij}$ in eq 34, and $\beta_{T,ij}$ and $\gamma_{T,ij}$ in eq 35) allow for arbitrary symmetric and asymmetric shapes of the reducing functions.[1] The numerator $x_i + x_j$ in these reducing functions only affects multi-component mixtures and ensures that terms with identical indices smoothly connect to the product $x_i x_i$ for which $\beta_{v,ii} = \beta_{T,ii} = 1$.

The reducing functions according to eqs 34 and 35 ensure physically reasonable shapes of the functions for any value of their parameters. Equations 16 and 17, which enable computing-time saving algorithms, are the simplified formulations of

dx.doi.org/10.1021/je300655b | J. Chem. Eng. Data 2012, 57, 3032−3091

eqs 34 and 35 and result from obeying the following relations:

$$\gamma_{v,ij} = \gamma_{v,ji}, \quad \gamma_{T,ij} = \gamma_{T,ji} \quad \text{and} \quad \beta_{v,ij} = 1/\beta_{v,ji}, \quad \beta_{T,ij} = 1/\beta_{T,ji} \tag{36}$$

When all binary parameters of eqs 34 and 35 are set to unity, the reducing functions with adjustable parameters turn into quadratic mixing rules using the combining rules of Lorentz and Berthelot for the critical parameters of the pure components:

$$\frac{1}{\rho_{c,ij}} = \frac{1}{8}\left(\frac{1}{\rho_{c,i}^{1/3}} + \frac{1}{\rho_{c,j}^{1/3}}\right)^3 \tag{37}$$

$$T_{c,ij} = (T_{c,i} \cdot T_{c,j})^{0.5} \tag{38}$$

Therefore, the mixture model can easily be extended to components for which poor or even no experimental information is available for fitting the binary parameters of the reducing functions. Moreover, other combining rules can be used instead of eqs 37 and 38 to achieve different shapes of the reducing functions.

In the GERG-2008 equation of state, the arithmetic mean of the critical parameters of the pure components is used for some binary mixtures for which only poor data are available (see Section 4.3.3). For example, detailed investigations showed that the linear combining rules are generally more suitable for the description of the thermodynamic properties of binary hydrocarbon mixtures than those of Lorentz and Berthelot. For such binary systems, the arithmetic mean is applied by calculating the values for the parameters $\gamma_{v,ij}$ and $\gamma_{T,ij}$ from the following conversions:

$$\gamma_{v,ij} = 4\frac{[(1/\rho_{c,i}) + (1/\rho_{c,j})]}{[(1/\rho_{c,i}^{1/3}) + (1/\rho_{c,j}^{1/3})]^3} \quad \text{and} \quad \gamma_{T,ij} = \frac{1}{2}\frac{(T_{c,i} + T_{c,j})}{(T_{c,i} \cdot T_{c,j})^{0.5}} \tag{39}$$

with $\beta_{v,ij}$ and $\beta_{T,ij}$ set to 1 (see eqs 34 and 35). It should be noted that the structure of eqs 34 and 35 is maintained for all binary subsystems, and no additional numerical effort is required when the results calculated from eq 39 are used. The use of different combining rules is superfluous when data are used to adjust the binary parameters.

4.4.1.1. Invariance Condition and Alternative Reducing Functions. The predictive capability of a multi-fluid approximation in the description of mixture properties for multi-component systems strongly depends on the mathematical form of the reducing functions for density and temperature. The restriction to binary reducing equations and the simple extension to multi-component mixtures (double summation over all binary subsystems) leads, however, to a loss in accuracy for the prediction of the thermodynamic properties of multi-component mixtures.

The restriction to binary reducing equations is unavoidable due to the comparatively poor data that are available for ternary, quaternary, and other multi-component mixtures. Consequently, a more accurate description of the properties of multi-component mixtures can only be realized by minimizing the loss in accuracy when extending from binary to multi-component mixtures. In mixture models based on multi-fluid approximations, the mathematical structure of the reducing functions has a large influence on this loss in accuracy.

The suitability of a mathematical structure for the extension from binary to multi-component mixtures is connected to certain physically founded conditions. Such a condition is the invariance condition, which was reported by Michelsen and Kistenmacher[149] (Aside from the invariance condition, an additional problem, which is called the "dilution" effect, was investigated by the authors for GERG-2008 and by Kunz et al.[1] for GERG-2004. See also Mathias et al.[148] and Avlonitis et al.[150]). The authors state that mixture parameters calculated from mixing rules have to be invariant when a component is partitioned into a number of identical subcomponents. This requirement must also be valid for the composition-dependent parameters of multi-fluid mixture models. The invariance condition is, however, not fulfilled for the reducing functions of all existing multi-fluid mixture models that contain expressions for modeling asymmetric shapes, including the model presented in this work. According to Michelsen and Kistenmacher,[149] these theoretical considerations are of practical relevance, for example, for mixtures containing very similar components.

A solution to this problem is based on a mixing rule suggested by Mathias et al.[148] and was proposed by Klimeck[22] for the reducing functions of multi-fluid approximations. The corresponding invariant reducing functions for density and temperature were introduced by Kunz et al.[1] for the development of a second (alternative) mixture model and can be written as

$$Y_r(\bar{x}) = \sum_{i=1}^{N}\sum_{j=1}^{N} x_i x_j \phi_{Y,ij} Y_{c,ij} + \sum_{i=1}^{N} x_i \left(\sum_{j=1}^{N} x_j \lambda_{Y,ij}^{1/3} Y_{c,ij}^{1/3}\right)^3 \tag{40}$$

where Y corresponds to either the molar volume v or the temperature T, and ϕ and λ are adjustable binary parameters. The very flexible structure of eq 40 enables asymmetric shapes, and the values calculated for $Y_r(\bar{x})$ are invariant when a mixture component is divided in two or more pseudocomponents. Further details on the use of these alternative reducing functions and the alternative mixture model are provided by Kunz et al.[1]

The results of the comprehensive investigations[1] showed that the reducing functions used in the GERG-2008 equation of state according to eqs 16 and 17 are more suitable for the description of, for example, natural gases rich in carbon dioxide and natural gas dew points. The nonfulfillment of the invariance condition by the reducing functions of GERG-2008 seems to be of minor importance and does not affect the accuracy in the description of the available data for the thermal and caloric properties of multi-component mixtures.

4.4.2. Departure Functions. The purpose of a departure function is to improve the accuracy of the mixture model in the description of the thermodynamic properties of nonideal mixtures in situations where fitting the parameters of the reducing functions to accurate experimental data does not yield a sufficiently accurate result. This concept was independently developed by Tillner-Roth[12] and Lemmon.[13]

Compared to the reducing functions for density and temperature, the departure function $\Delta\alpha^r(\delta,\tau,\bar{x})$ in eq 7 is in general of minor importance for modeling the residual mixture behavior since it only describes an additional small residual deviation to the real mixture behavior. The development of such a function is associated with considerable effort, which was, however, necessary to fulfill the high demands on the accuracy of

the GERG-2008 equation of state in the description of the thermodynamic properties of natural gases and other mixtures.

4.4.2.1. Binary Specific Departure Functions. Originally, the departure function developed by Tillner-Roth[12] was designed to describe the behavior of individual binary mixtures for which a large amount of accurate experimental data is available. Such a binary specific departure function can be written in the form

$$\Delta\alpha^{r}(\delta, \tau, \bar{x}) = f^{\Delta}(x_1, x_2)\cdot\alpha_{12}^{r}(\delta, \tau) \tag{41}$$

In eq 41, the composition dependence in the form of the factor f^{Δ} is clearly separated from a function that only depends on the reduced mixture density δ and the inverse reduced mixture temperature τ. For a given composition dependence, the structure of the function $\alpha_{12}^{r}(\delta,\tau)$ that yields the best representation of the thermodynamic properties of the mixture can be determined by means of a suitable structure optimization procedure (e.g., Setzmann and Wagner[151]). The composition-dependent factor f^{Δ} has to equal zero for a pure component.

4.4.2.2. Generalized Departure Functions. The model of Lemmon and Jacobsen[21] was developed to describe the thermodynamic properties of multi-component mixtures. To achieve a sufficiently accurate representation, these authors also used a departure function. The structure of this function is similar to the one of the binary specific function of Tillner-Roth,[12] but generalized for all considered binary systems. In this way, an accurate description is achieved for a number of well-measured binary mixtures as well as for binary mixtures for which only limited data are available. Such a generalized departure function is given by

$$\Delta\alpha^{r}(\delta, \tau, \bar{x}) = \sum_{i=1}^{N-1}\sum_{j=i+1}^{N} x_i x_j F_{ij}\alpha_{gen}^{r}(\delta, \tau) \tag{42}$$

Similar to eq 41, the composition dependence in eq 42 is separated from a function that only depends on the reduced mixture density δ and the inverse reduced mixture temperature τ. The structure of this function can also be determined by use of structure-optimization methods[151] and is identical for all binary mixtures. Only the parameter F_{ij} in eq 42 is binary-specific. The composition dependence of the factor

$$f^{\Delta} = x_i x_j F_{ij} \tag{43}$$

is quadratic. Provided that the composition-dependent factor vanishes for a pure component, any arbitrary structure can be used, which may, for example, result in asymmetric shapes.

4.4.2.3. Combined Strategy Used for the Departure Functions of GERG-2008. Binary specific and generalized departure functions have their respective advantages and disadvantages. Provided that a relatively large amount of accurate experimental data for thermal and caloric properties of binary mixtures is available, binary specific departure functions enable a more accurate description of mixture properties than generalized formulations. On the other hand, generalized departure functions can be used to model the residual behavior of mixtures characterized by poor or limited data.

For the development of the GERG-2004 equation of state of Kunz et al.,[1] a combined strategy was pursued. For binary mixtures consisting of the main natural gas components (see Table 1), binary specific departure functions were developed. For many other binary systems, the data situation does not allow for the development of binary specific departure functions. Hence, a generalized departure function was developed for binary mixtures consisting of important hydrocarbons. Binary mixtures characterized by very limited data or of minor importance for the description of natural gas properties (the mole fractions of several components contained in natural gases are small) were considered without a departure function, that is, $\Delta\alpha_{ij}^{r} = 0$.

In the mixture model developed by Kunz et al.,[1] which is also used in this work, the departure function $\Delta\alpha^{r}$ of multi-component mixtures is the sum of all binary specific and generalized departure functions of the involved binary subsystems (see also eq 10):

$$\Delta\alpha^{r}(\delta, \tau, \bar{x}) = \sum_{i=1}^{N-1}\sum_{j=i+1}^{N} \Delta\alpha_{ij}^{r}(\delta, \tau, \bar{x}) \tag{44}$$

with

$$\Delta\alpha_{ij}^{r}(\delta, \tau, \bar{x}) = x_i x_j F_{ij}\alpha_{ij}^{r}(\delta, \tau) \tag{45}$$

The parameter F_{ij} equals unity for binary specific departure functions and is fitted for binary mixtures that use a generalized departure function, where $\Delta\alpha_{ij}^{r} = \Delta\alpha_{gen}^{r}$. This structure of the departure function for the multi-component mixture was used first by Klimeck[22] for the preliminary equation of state for natural gases.

The GERG-2008 equation of state contains a total of seven binary specific departure functions and one generalized departure function for a total of eight binary hydrocarbon mixtures (see Table 5 and Figure 1). The functions $\alpha_{ij}^{r}(\delta,\tau)$ were developed using procedures that are based on the fitting and structure-optimization methods as described by Kunz et al.[1] Since the mixture model is not limited to the number of binary specific and generalized formulations presented in this work, the expansion of the model by developing additional departure functions, for example, for binary mixtures of air components and mixtures containing carbon dioxide and water, may be worthwhile for future expansions (see also Section 6).

4.4.2.4. Functional Forms for α_{ij}^{r}. As mentioned before, the structure of the function $\alpha_{ij}^{r}(\delta,\tau)$ of a binary specific or generalized departure function (see eq 45) can be determined by means of modern structure-optimization methods.[151] A survey of the type of terms used for the departure functions of multi-fluid mixture models reported in the literature is given in ref 1.

Basically, two different types of terms, namely, polynomial terms and polynomial terms in combination with exponential expressions (for simplicity, referred to in the following as exponential terms), form the structure of the departure functions of the multi-fluid mixture models reported in the literature. Driven by the need for a functional term that on the one hand enables the accurate description of the thermal and caloric properties of binary and multi-component mixtures within the uncertainty of the best measured data and on the other hand ensures a reasonable behavior of the mixture model in regions characterized by poor data, a comprehensive investigation on the suitability of exponential functions was performed for the first time by Kunz et al.[1] As a result of these investigations, a new functional form was introduced.[1] The new functional form resulted in a fundamentally improved formulation as compared to the preliminary natural gas model of Klimeck[22] that showed physically unreasonable shapes in the description

dx.doi.org/10.1021/je300655b | J. Chem. Eng. Data 2012, 57, 3032−3091

of vapor−liquid equilibrium states. This special term, which replaced the ordinary exponential term, can be written as

$$\alpha^{r}_{ij,k} = n_{ij,k}\delta^{d_{ij,k}}\tau^{t_{ij,k}}\cdot\exp[-\eta_{ij,k}(\delta - \varepsilon_{ij,k})^2 - \beta_{ij,k}(\delta - \gamma_{ij,k})] \quad (46)$$

where $\eta_{ij,k}$, $\varepsilon_{ij,k}$, $\beta_{ij,k}$, and $\gamma_{ij,k}$ are adjustable parameters used to model the shape of the term. Their values are based on comprehensive precalculations and determined prior to the optimization and nonlinear fitting process. The new functional form enables the description of the thermodynamic properties of binary mixtures in the homogeneous gas, liquid, and supercritical regions with the same high accuracy as with the ordinary exponential form, while demonstrating physically correct behavior along the phase boundary. Additional details are given by Kunz et al.[1]

Based on the ordinary polynomial terms and the new exponential term, binary specific departure functions were developed for the binary mixtures methane−nitrogen, methane−carbon dioxide, methane−ethane, methane−propane, nitrogen−carbon dioxide, and nitrogen−ethane as described by Kunz et al.[1] (see also Table 5).

4.4.3. Basic Information on the Development of the Binary Correlation Equations. The basic principles for the development of mixture models based on multi-fluid approximations are strongly related to the development of empirical equations of state for pure substances, where the development of the final form of an equation for the residual part of the Helmholtz free energy α^r requires the following steps (see Wagner and Pruß[146]):

- selection of the final data set;
- weighting of the data;
- precorrelation of auxiliary quantities;
- linear least-squares fitting in connection with the structure-optimization method;
- nonlinear least-squares fitting.

The residual part of the Helmholtz free energy for pure substances is described by one equation that has the same mathematical structure independent of the various substances. However, for mixtures, several correlation equations of different structure have to be developed to take into account the residual behavior of a mixture. The tools used for the development of the multi-fluid mixture model presented here were developed and reported by Klimeck.[22] Some of the basic principles of the development of multi-fluid mixture models are briefly summarized in the following sections. Additional details are given by Kunz et al.[1] and Klimeck.[22]

The GERG-2008 equation of state, eq 8, describes multi-component mixtures based only on formulations developed for the binary mixtures of the components in the model. For most of the binary systems, only the parameters of the reducing functions for density and temperature given as eqs 16 and 17 were adjusted. The binary mixtures for which, in addition, binary specific departure functions or a generalized departure function were developed are listed separately in Table 5. For binary mixtures for which only poor data, neither allowing for the development of a departure function nor the fitting of the parameters of the reducing functions, are available, either the parameters of the reducing functions were set to unity or the linear combining rules for the critical parameters of the respective pure components were used (instead of the combining rules of Lorentz and Berthelot) as described in Section 4.4.1. The linear combining rules are used for binary mixtures consisting of secondary alkanes and also for binary mixtures that are composed of a secondary alkane and either hydrogen or carbon monoxide as the second component. For the remaining subsystems, for which only poor data are available, the combining rules of Lorentz and Berthelot are used (which is the default when the parameters of the reducing functions are set to unity). The use of different combining rules is immaterial if data are used to adjust the binary parameters of the reducing functions (see Section 4.4.1).

For the binary mixtures methane−nitrogen, methane−carbon dioxide, methane−ethane, methane−propane, methane−hydrogen, nitrogen−carbon dioxide, and nitrogen−ethane, the data situation is quite satisfactory,[1] and binary specific departure functions were developed for these mixtures. To develop a mixture model that is able to accurately describe the properties of a variety of natural gases (of typical and unusual compositions), a generalized departure function was developed for binary mixtures of important secondary alkanes. The experimental data for these mixtures do not allow for the development of binary specific departure functions. For the development of the generalized departure function for secondary alkanes, selected data for the well-measured binary alkane mixtures of methane−ethane and methane−propane were also used.

In the first step, for fitting GERG-2008 to any binary mixture, the binary parameters of the reducing functions for density and temperature were fitted to selected data. Subsequently, the departure functions, which consist of 4 to 12 individual terms, were developed. The development of departure functions involves considerable but worthwhile effort. The pursued strategy for this development is briefly described in the following. Details on the development of a new functional form and the different banks of terms used for the development of the different binary departure functions are given by Kunz et al.[1]

4.4.3.1. Fitting of the Reducing Functions for Density and Temperature. The fitting of the binary parameters of the reducing functions according to eqs 16 and 17 to the different (linear and nonlinear) data types was generally performed using nonlinear fitting procedures. For VLE properties, linearized data were used in the initial cycles of the iterative fitting process. Subsequently, direct (nonlinear) fitting to VLE data was applied. Since the reducing functions only depend on the mixture composition, the use of VLE data that uniformly cover large composition ranges proved to be advantageous.

For several binary mixtures consisting of secondary and minor components, the data sets are either limited with respect to the covered temperature, pressure, and composition ranges or the number of available data. The development of equations for these systems was carried out very carefully, and occasionally only the (symmetric) parameters $\gamma_{v,ij}$ and $\gamma_{T,ij}$ were fitted to the data to avoid unreasonable behavior in regions not covered by data. Thus, the parameters $\beta_{v,ij}$ and $\beta_{T,ij}$ remain at unity for these systems. Additional details are given by Kunz et al.[1]

4.4.3.2. Development of Binary Specific Departure Functions. After the parameters of the reducing functions have been determined for a binary mixture, the development of a departure function, which only depends on the reduced mixture density δ and the inverse reduced mixture temperature τ, can be performed.

The structure of a departure function was optimized based on the linear structure-optimization method of Setzmann and Wagner.[151] The coefficients of the resulting structure-optimized equation were then redetermined by direct (nonlinear) fitting to the selected (linear and nonlinear) binary data. For direct fitting of vapor−liquid equilibrium properties, measured vapor pressures and vapor-phase compositions (as functions of the

given saturation temperature and liquid-phase composition) were usually used. When available, experimental data for saturated-liquid densities (at a given temperature and composition) were additionally considered. Due to the linearization of the nonlinear binary data, the entire process of optimizing the structure of a departure function is an iterative process and is repeated until convergence is obtained. For certain binary mixtures, such as the binary systems methane−carbon dioxide and methane−ethane, it was advantageous to repeatedly determine the parameters of the reducing functions with subsequent fitting. This can be done separately or simultaneously together with the coefficients of the departure function.

4.4.3.3. Development of a Generalized Departure Function. Since the data sets for most of the binary hydrocarbon mixtures (both components are hydrocarbons) are limited, binary specific departure functions were only developed for methane−ethane and methane−propane. Methane is the main constituent of virtually all natural gases. Aside from nitrogen, carbon dioxide, ethane, and propane, *n*-butane and isobutane are further common components. To achieve an accurate description of the thermodynamic properties of natural gases and similar mixtures, it is necessary to develop departure functions for (at least) the binary mixtures methane−*n*-butane and methane−isobutane. Since the data sets for these and other binary hydrocarbon mixtures are limited, a generalized departure function for the eight binary hydrocarbon mixtures listed in Table 5 was developed. Aside from the experimental data available for the limited mixtures, selected data for the well-measured binary mixtures methane−ethane and methane−propane were also used to accurately describe the thermodynamic properties of all binary hydrocarbon mixtures for which the generalized departure function is valid.

In addition to optimizing the structure of the part of the departure function that only depends on the reduced mixture variables δ and τ (see Section 4.4.2), the development of a generalized departure function involves fitting the binary parameters of the reducing functions and the binary specific parameters F_{ij} of the departure function (see eq 10) to experimental data for each mixture in the group of generalized binary mixtures.

The final structure of the generalized departure function for secondary binary hydrocarbon mixtures is almost entirely based on the accurate and comprehensive data sets available for the three binary systems methane−ethane, methane−propane, and methane−*n*-butane. Within intermediate optimization steps, selected data for the binary systems ethane−propane and propane−*n*-butane were also used. They have, however, only a minor influence on the structure of the equation because of their limited accuracy, which is also true for the other secondary hydrocarbon mixtures. For the additional binary hydrocarbon mixtures listed in Table 5, the parameters of the reducing functions and the F_{ij} parameters were fitted to selected data for each binary mixture, where the final structure of the generalized departure function previously determined was used. Additional details are given by Kunz et al.[1]

4.4.3.4. Overview of the Use of the Different Types of Functions for the Binary Mixtures in the GERG-2008 Equation of State. Figure 1 presents an overview of the 210 binary combinations that result from the 21 natural gas components considered for the development of the GERG-2008 equation of state, eq 8. It also shows the form in which the departure functions (binary specific or generalized) and reducing functions [adjusted, linear combining rules (no fitting), or Lorentz−Berthelot combining rules (no fitting)] were applied. Furthermore, the additional components included in the GERG-2008 equation of state, eq 8, are marked.

5. COMPARISONS OF CALCULATED MIXTURE PROPERTIES TO EXPERIMENTAL DATA

In this section, the quality of the GERG-2008 equation of state, eq 8, is discussed based on comparisons with selected experimental data used in the development of the mixture model and with further experimental data used for the validation of the equation (see Section 3). Several figures also show results that were calculated from the AGA8-DC92 equation of state of Starling and Savidge[6] (see Section 2.1.1). Since AGA8-DC92 was developed on the IPTS-68 temperature scale, all input temperatures were converted to the IPTS-68 scale before values were calculated from this equation. Values calculated from the cubic equation of state of Peng and Robinson[3] with binary interaction parameters taken from Knapp et al.[152] are also included in several figures. The multi-fluid mixture models developed by Lemmon and Jacobsen[21] and Klimeck,[22] which are limited to a smaller number of natural gas components than considered in this work, are used for comparison as well. Additional graphical and also detailed statistical comparisons are given by Kunz et al.[1] for the GERG-2004 equation of state. These comparisons are also valid for the GERG-2008 equation of state, since both equations yield virtually the same results for mixtures composed from the 18 components covered by GERG-2004 (see Section 1).

The GERG-2008 equation of state covers binary and multi-component mixtures that consist of the 21 natural gas components listed in Table 1. The huge number of data for the various thermal and caloric properties, which were measured over wide ranges of temperature, pressure, and composition, do not allow for a detailed graphical comparison of GERG-2008 with all of the available experimental information. Therefore, the representation of data for binary mixtures by GERG-2008 is exemplified by deviation plots for selected binary systems that are strongly related to multi-component natural gas mixtures. The selected data represent, in general, the most accurate measurements that are available for the respective mixture property. In this context, it should be noted that the actual number of data used for the development and evaluation of GERG-2008 far exceeds the selected experimental information shown in the figures of this section (the comparisons are limited to certain ranges of temperature, pressure, and composition).

Section 5.1 focuses on the description of thermal and caloric properties of binary mixtures consisting of the main natural gas components methane, nitrogen, carbon dioxide, and ethane, and the secondary hydrocarbons propane and *n*-butane.

The quality of GERG-2008 in the description of various types of natural gases and other multi-component mixtures is discussed in Section 5.2.

The baseline in all of the following deviation plots corresponds to the values calculated from GERG-2008, unless otherwise explicitly stated. If values calculated from other equations of state are additionally displayed (together with the experimental data and GERG-2008 as the baseline), they are calculated for the lowest temperature written at the top of each small plot, unless otherwise indicated. Data points shown at the upper or lower vertical limits of the graph indicate that the points are off-scale. In the following text, absolute values of the deviations are used in the discussions of maximum errors or systematic offsets.

5.1. Representation of Thermal and Caloric Properties of Selected Binary Mixtures. *5.1.1. pρT Relation in the*

dx.doi.org/10.1021/je300655b | J. Chem. Eng. Data 2012, 57, 3032−3091

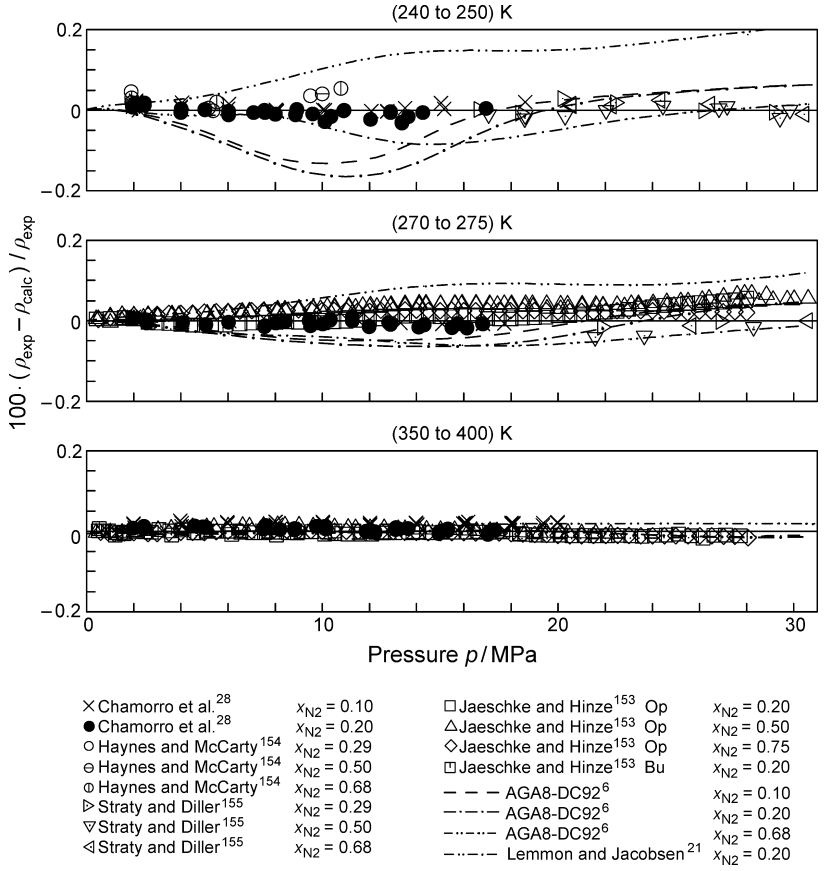

Figure 2. Percentage density deviations of experimental $p\rho T$ data for the binary mixture methane−nitrogen from values calculated with GERG-2008, eq 8. Values calculated with the AGA8-DC92 equation of Starling and Savidge[6] and the mixture model of Lemmon and Jacobsen[21] are plotted for comparison. Bu: Burnett apparatus, Op: optical interferometry method.

Homogeneous Region. In this section, the representation of experimental $p\rho T$ data of four very well measured binary mixtures by the GERG-2008 equation of state is described.

5.1.1.1. Methane−Nitrogen and Methane−Ethane. Experimental measurements of gas-phase densities for the binary mixture methane−nitrogen and their percentage deviations from the GERG-2008 equation of state, eq 8, are shown in Figure 2 for temperatures ranging from (240 to 400) K. The selected data cover a large range of nitrogen mole fractions from 0.10 to 0.75. The $p\rho T$ data published by Chamorro et al.[28] for nitrogen mole fractions of 0.10 and 0.20 represent the most accurate measurements in the gas phase. The data were measured using a single-sinker densimeter, and their uncertainty is estimated to be $\Delta\rho/\rho$ = 0.03 %. The uncertainty in density of the measurements of Jaeschke and Hinze,[153] which cover mole fractions from 0.20 to 0.75 of nitrogen and temperatures ranging from (270 to 353) K, amounts to approximately 0.07 %. For the liquid-phase data of Haynes and McCarty[154] and Straty and Diller,[155] the uncertainty in density is assumed to be about (0.1 to 0.3) %. The deviation plots clearly demonstrate that GERG-2008 is able to represent all of the data, independently of the mixture composition, to within their experimental uncertainty for all temperatures and at pressures up to 30 MPa. The data measured by Straty and Diller[155] at pressures above 30 MPa are described by GERG-2008 to within the experimental uncertainty as well.

Important improvements compared to the AGA8-DC92 equation of state[6] and the mixture model of Lemmon and Jacobsen[21] are achieved for temperatures below 275 K. At 240 K, the deviations of values calculated from AGA8-DC92 for nitrogen mole fractions of 0.10, 0.20, and 0.68 clearly exceed the uncertainty of the measurements with density deviations of up to 0.14 % (x_{N_2} = 0.10), up to 0.15 % (x_{N_2} = 0.20), and more than 0.2 % (x_{N_2} = 0.68, p > 30 MPa). Even at pipeline conditions (for pressures below 12 MPa), the deviations exceed 0.1 % in density for AGA8-DC92. Also at 270 K, this equation is not able to represent the different data sets as accurately as GERG-2008. The composition dependence of the deviations is particularly of concern. Values calculated from AGA8-DC92 for the mixture with a nitrogen mole fraction of 0.68 deviate by more than 0.1 % from the measurements of Straty and Diller[155] at elevated pressures, and densities calculated for the mixtures with x_{N_2} = 0.10 and x_{N_2} = 0.20 do not agree within the experimental uncertainty with the very accurate data of Chamorro et al.[28] This is also true for the mixture model of Lemmon and Jacobsen[21] as shown for the mixture containing a nitrogen mole fraction of 0.20. However, it should be noted here (and also for other comparisons shown in the following) that the measurements of Chamorro et al.[28] were not available at the time the previous equations were developed. Preliminary measurements from Chamorro et al. with x_{N_2} = 0.20 were used for the development of GERG-2008. The experimental results for x_{N_2} = 0.10 were available prior to the publication of the data but were only used for comparison. At higher temperatures of 350 K and above, all equations yield quite similar results.

For the binary mixtures methane−nitrogen and methane−ethane, accurate $p\rho T$ data covering wide ranges of pressure and composition were measured in the liquid phase. Figure 3 shows

dx.doi.org/10.1021/je300655b | J. Chem. Eng. Data 2012, 57, 3032−3091

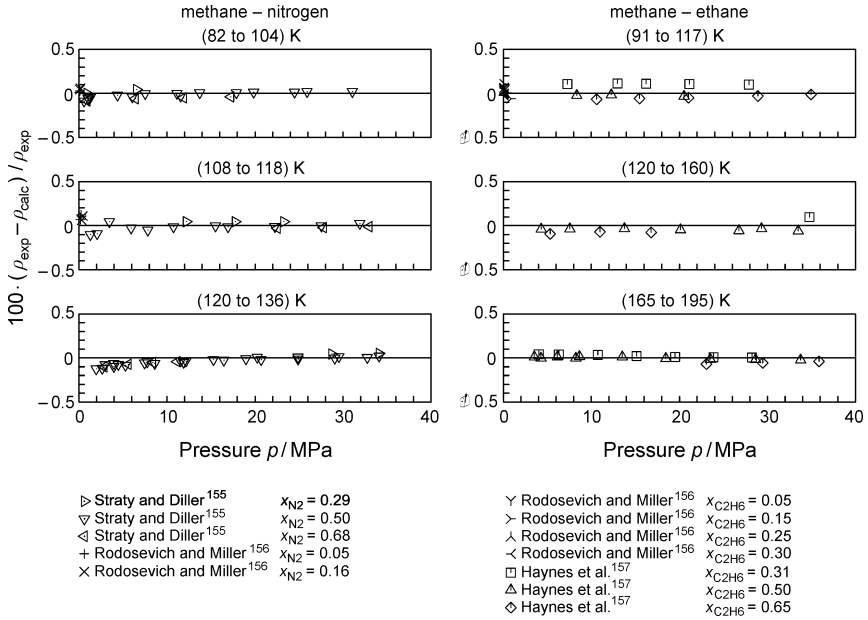

Figure 3. Percentage density deviations of experimental $p\rho T$ data for the binary mixtures methane−nitrogen and methane−ethane from values calculated with GERG-2008, eq 8.

deviations of these data from values calculated with GERG-2008 over temperature ranges that are important for applications with liquefied natural gas (LNG). The comparisons for the binary system methane−nitrogen are based on the data of Straty and Diller[155] and Rodosevich and Miller.[156] The data of Rodosevich and Miller were measured in the vicinity of the vapor−liquid phase boundary at nitrogen mole fractions of 0.05 and 0.16 and temperatures of (91 to 115) K, and the data of Straty and Diller cover pressures up to about 35 MPa at nitrogen mole fractions of 0.29, 0.50, and 0.68 over a wide temperature range down to 82 K. The GERG-2008 equation of state represents all of the selected data to within 0.15 % (generally to within 0.1 %) in density. For the binary system methane−ethane, similar results are obtained as exemplified by the deviation plots in Figure 3. The data of Rodosevich and Miller[156] were measured over virtually the same temperature range as for the methane−nitrogen mixture and also near the phase boundary, but they cover a wider range of compositions. The measurements of Haynes et al.[157] cover pressures up to about 35 MPa at ethane mole fractions of 0.31, 0.50, and 0.65 and at temperatures down to 100 K. Similar to the methane−nitrogen binary system, all of the selected methane−ethane binary data are represented by GERG-2008 to within about 0.1 % in density.

The GERG-2008 equation of state achieves a very accurate description of the $p\rho T$ relation in the liquid phase. As mentioned in Section 2.1.1, AGA8-DC92[6] is not valid in the liquid phase. Values calculated from cubic equations of state, which are still widely used in many technical applications, deviate from the measurements by several percents. Compared to GERG-2008, only the mixture model of Lemmon and Jacobsen[21] yields comparable accuracies in the description of liquid-phase densities. Values calculated from this model deviate from the measurements shown in Figure 3 by up to 0.3 % in density.

5.1.1.2. Methane−Propane and Methane−n-Butane. Deviations of selected experimental measurements for gas-phase densities of the binary mixtures methane−propane and methane−*n*-butane calculated from the GERG-2008 equation of state, eq 8, are shown in Figure 4. The data for the propane of 0.07 and the *n*-butane mole fraction of 0.015 of Ruhrgas (1990)[158] and those for the mole fraction of 0.15 of propane and 0.05 of *n*-butane of Ruhrgas (1999)[159] were measured with the use of an optical interferometry method and a Burnett apparatus. The data cover temperatures from (280 to 353) K for methane−propane and (270 to 353) K for methane−*n*-butane at pressures up to 30 MPa. The new equation of state represents all of the data to within 0.1 % in density. Most of the measurements are described with deviations of clearly less than 0.07 %. In contrast to GERG-2008, the AGA8-DC92 equation[6] and the model of Lemmon and Jacobsen[21] are not able to accurately describe the data. Both equations deviate from the measurements for the two binary mixtures at a propane mole fraction of 0.15 and a *n*-butane mole fraction of 0.05 by more than 0.3 % in density, even at moderate temperatures around 310 K. Considerably higher deviations between the data and values calculated from these two equations of state are observed at lower temperatures, exceeding 1 % for the methane−*n*-butane binary mixture in the case of AGA8-DC92. Even at higher temperatures around 350 K and elevated pressures, values calculated from the model of Lemmon and Jacobsen deviate from the measurements by more than 0.3 % for the methane−propane mixture and by more than 0.2 % for the methane−*n*-butane mixture.

Aside from the improvements achieved in the description of the $p\rho T$ relation of the selected examples discussed above, the description of the $p\rho T$ data of other binary mixtures composed of the natural gas main constituents, such as nitrogen−carbon dioxide and nitrogen−ethane, is also improved compared to the previous equations of state mentioned above. Moreover, data available at pressures above 30 or 40 MPa are accurately described as well. Reamer et al. measured densities on the mixtures (CH_4−C_3H_8),[160] (CH_4−*n*-C_4H_{10}),[161] (CH_4−CO_2),[162] (N_2−C_2H_6),[163] (CO_2−C_2H_6),[164] and (CO_2−C_3H_8)[165] at pressures up to 69 MPa and temperatures up to 511 K. Seitz et al.[166] and Seitz and Blencoe[167] took density data on the mixtures CH_4−N_2, CH_4−CO_2, and N_2−CO_2 for pressures up to 100 MPa

dx.doi.org/10.1021/je300655b | J. Chem. Eng. Data 2012, 57, 3032−3091

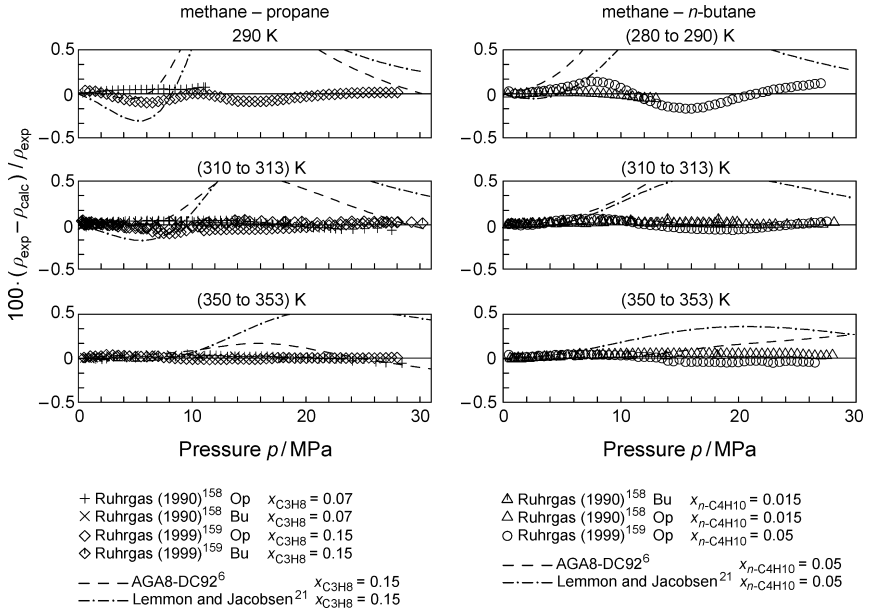

Figure 4. Percentage density deviations of experimental $p\rho T$ data for the binary mixtures methane−propane and methane−*n*-butane from values calculated with GERG-2008, eq 8. Values calculated with the AGA8-DC92 equation of Starling and Savidge[6] and the mixture model of Lemmon and Jacobsen[21] are plotted for comparison. Bu: Burnett apparatus, Op: optical interferometry method.

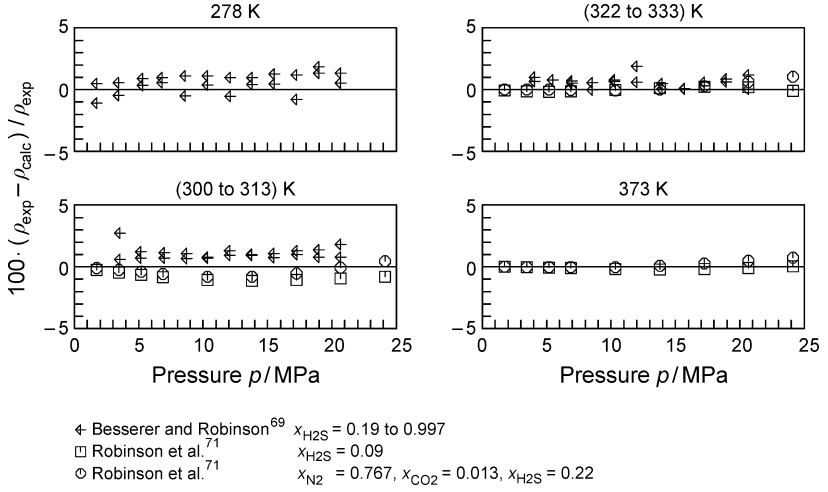

Figure 5. Percentage density deviations of experimental saturated liquid and saturated vapor densities measured by Besserer and Robinson[69] for the binary mixture nitrogen−hydrogen sulfide and of the $p\rho T$ data (compression-factor measurements) of Robinson et al.[71] for the binary mixture nitrogen−hydrogen sulfide and the ternary mixture nitrogen−carbon dioxide−hydrogen sulfide from values calculated with GERG-2008, eq 8.

and temperatures up to 673 K. All of these data cover wide ranges of composition. Comparisons with measurements, which are known to be very accurate, show that the data of these authors are associated with considerably higher uncertainties. Typical deviations between the data and values calculated from GERG-2008 are within (0.5 to 1) % in density, which agrees well with the assumed uncertainty of the measurements.

5.1.1.3. Binary Mixtures Containing the Components n-Nonane, n-Decane, and Hydrogen Sulfide. Comparisons between experimental $p\rho T$ data for binary mixtures containing at least one of the three mentioned components with densities calculated from GERG-2008, eq 8, are carried out for selected examples and are summarized in Figures 5 to 7. It should be noted that there are no highly accurate measurements for these mixtures (see Section 3 and Sections 5.1.1.1 and 5.1.1.2).

For the binary mixture nitrogen−hydrogen sulfide, Figure 5 shows differences of densities measured on the bubble and dew lines and differences of gas-phase densities (compression-factor measurements) from values calculated with GERG-2008. Corresponding differences for the ternary mixture nitrogen−carbon dioxide−hydrogen sulfide (with only a small content of CO_2) are also presented. The saturation densities were measured by Besserer and Robinson[69] (for the binary mixture) and the compression factors by Robinson et al.[71] (for the binary and ternary mixtures). They cover the temperature range of (278 to 373) K. Only very few data deviate from the calculated values by more than 1 %, which corresponds to about the experimental uncertainty. For the mixture methane−*n*-decane, Figure 6 illustrates how the experimental densities in the homogeneous liquid (for all compositions given) and gas (at a mole fraction of 0.34 *n*-decane at 511 K and pressures up to 1.5 MPa)

dx.doi.org/10.1021/je300655b | J. Chem. Eng. Data 2012, 57, 3032−3091

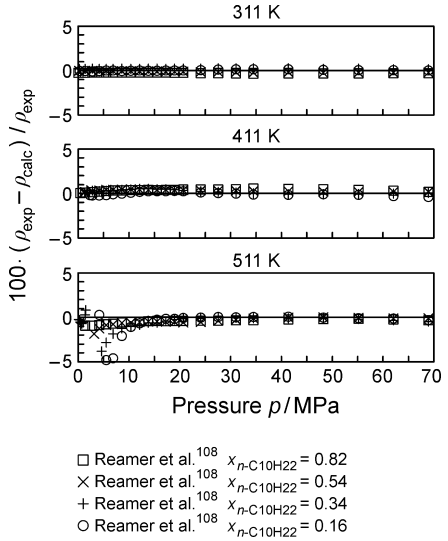

Figure 6. Percentage density deviations of experimental $p\rho T$ data for the binary mixture methane−*n*-decane from values calculated with GERG-2008, eq 8. These are liquid-phase data except for the data with the *n*-decane mole fraction of 0.34 at T = 511 K and $p \leq$ 1.5 MPa, which are in the gas phase.

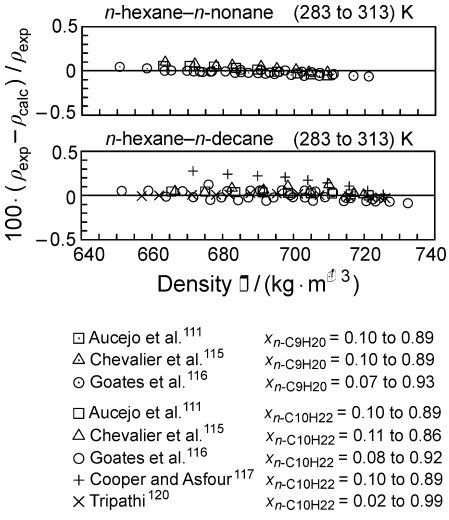

Figure 7. Percentage density deviations of experimental liquid-phase $p\rho T$ data for the binary mixtures *n*-hexane−*n*-nonane and *n*-hexane−*n*-decane from values calculated with GERG-2008, eq 8.

of Reamer[108] are represented by GERG-2008. The differences between the liquid densities and the calculated values are less than 0.5 % for most of the measurements. The representation of liquid-phase density data by GERG-2008 for the mixtures *n*-hexane−*n*-nonane and *n*-hexane−*n*-decane measured by Aucejo at al.,[111] Chevalier et al.,[115] and Goates et al.[116] and for the mixture *n*-hexane−*n*-decane measured by Cooper and Asfour[117] and Tripathi[120] can be seen in Figure 7. These data cover practically the entire composition range of these binary mixtures and are represented to within 0.1 % by GERG-2008, except for the limited data of Cooper and Asfour,[117] which are not consistent with the data of the other authors. This shows that these accurate data are also very accurately reproduced by GERG-2008.

5.1.2. Caloric Properties in the Homogeneous Region. Accurate data for caloric properties of binary mixtures, suitable for discussion, are primarily available for sound speeds and enthalpy differences in the gas phase. Isochoric and isobaric heat capacity data, which also cover the liquid phase, are available for only a few binary mixtures.

5.1.2.1. Methane−Nitrogen. For the binary mixture methane−nitrogen, very accurate sound speeds were measured by Estela-Uribe,[30] Trusler,[31] and Estela-Uribe et al.[168] The measurements cover temperatures from (220 to 400) K at pressures up to 30 MPa for nitrogen mole fractions of 0.10 and 0.20 and temperatures from (170 to 400) K at pressures up to 16 MPa for a nitrogen mole fraction of 0.54. The mixture was studied along pseudoisochores at molar densities between 0.2 mol·dm^{-3} and 5 mol·dm^{-3}. The data cover large reduced temperature ranges of $1.20 \leq T/T_r \leq 2.19$ for the mixture with $x_{N_2} = 0.10$, of $1.25 \leq T/T_r \leq 2.28$ for $x_{N_2} = 0.20$, and of $1.12 \leq T/T_r \leq 2.62$ for $x_{N_2} = 0.54$. For the measurements at nitrogen mole fractions of 0.10 and 0.20, and for almost all of the data measured for $x_{N_2} = 0.54$, the uncertainty in sound speed is estimated to be (0.02 to 0.05) %. Additional accurate sound-speed data were measured by Younglove et al.[169] for nitrogen mole fractions of 0.05, 0.15, and 0.29 at temperatures from (250 to 350) K and pressures up to 11 MPa. The uncertainty in sound speed of these data is estimated to be 0.1 %, which is higher than that of the measurements of Estela-Uribe et al.[168]

The GERG-2008 equation of state, eq 8, represents (almost) all of the sound-speed measurements, regardless of the mixture composition, to within very low deviations of less than 0.05 % as shown in the deviation plots of Figure 8. The very accurate data sets of Estela-Uribe et al.[168] are described by GERG-2008 well within their low experimental uncertainty. The few data points for $x_{N_2} = 0.54$ that exceed deviations of 0.05 % were all measured on the pseudoisochore of the highest molar density and are associated with an increased uncertainty as reported by the authors.

Values calculated from the AGA8-DC92 equation[6] deviate from the measurements of Estela-Uribe et al.[168] for nitrogen mole fractions of 0.10 and 0.20 and 220 K by clearly more than 0.1 % in sound speed at pressures around 11 MPa and above 17 MPa (with a maximum deviation of 0.4 % for $x_{N_2} = 0.20$ at about 30 MPa). Even at a considerably higher temperature of 300 K and moderate pressures, AGA8-DC92 is not able to describe all of the data to within their experimental uncertainty. The model of Lemmon and Jacobsen[21] significantly deviates from the measurements over a wide range of pressures. The maximum deviations amount to about 0.3 % in sound speed for $x_{N_2} = 0.10$ around 15 MPa and 220 K and about 0.4 % for $x_{N_2} = 0.20$ around 16 MPa for the same temperature. Even at higher temperatures of 300 K, the deviations calculated from this model exceed values of two to four times the experimental uncertainty of the data. However, these new data were not available when either equation was developed.

The temperature and pressure ranges covered by the sound speeds of Estela-Uribe et al.[168] for nitrogen mole fractions of 0.10 and 0.20 include those covered by the very accurate $p\rho T$ data of Chamorro et al.,[28] which were measured at virtually the same mixture compositions (see Section 5.1.1). The data sets of these two sources are represented by GERG-2008 well within their low experimental uncertainty. This indicates a very high degree of thermodynamic consistency between various types of properties.

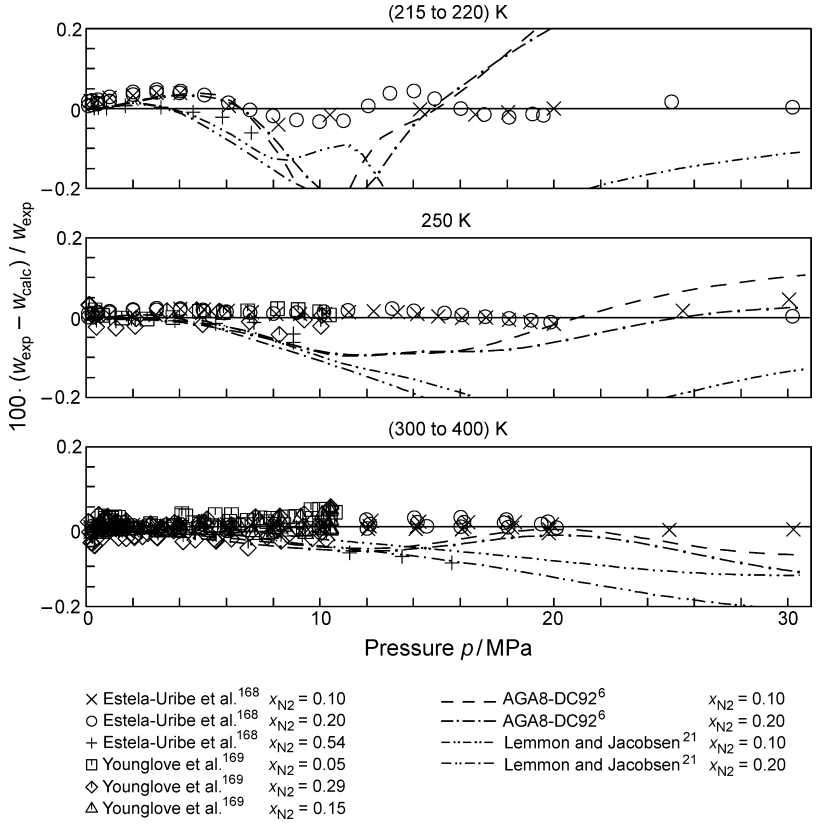

Figure 8. Percentage deviations of experimental sound-speed data for the binary mixture methane−nitrogen from values calculated with GERG-2008, eq 8. Values calculated with the AGA8-DC92 equation of Starling and Savidge[6] and the mixture model of Lemmon and Jacobsen[21] are plotted for comparison at temperatures of (220, 250, and 300) K.

5.1.2.2. Methane−Ethane. Experimental measurements of gas phase sound speeds for the binary mixture methane−ethane and their percentage deviations from the GERG-2008 equation of state, eq 8, for temperatures ranging from (250 to 350) K are shown in Figure 9. The selected data cover ethane mole fractions from 0.05 to 0.31. The very accurate and wide-ranging data measured by Costa Gomes and Trusler[29] for an ethane mole fraction of 0.15 cover pressures up to 20 MPa. According to the authors, the uncertainty of these data at 250 K amounts to $\Delta w/w$ = 0.05 %, and an uncertainty of $\Delta w/w$ = 0.03 % is estimated for higher temperatures. The accurate measurements of Trusler[170] for $x_{C_2H_6}$ = 0.20 cover pressures up to 13 MPa (at 375 K), and the data reported by Younglove et al.[169] for ethane mole fractions of 0.05, 0.15, and 0.31 are limited to pressures up to 11 MPa. Most of the data are represented by GERG-2008 to within very low deviations of less than 0.05 % in sound speed. The maximum deviations do not exceed 0.1 %, except for one data point on the 250 K isotherm at 20 MPa. This single point, for which the sound-speed value from GERG-2008, eq 8, deviates by 0.28 %, is most likely associated with an increased uncertainty since no equation that resulted from the optimization and fitting procedures was able to better reproduce this particular point. Moreover, this assumption is supported by the fact that the authors mention experimental difficulties along this isotherm.

The accurate representation of the sound-speed data with an ethane mole fraction of 0.15 along the 250 K isotherm (T/T_r = 1.19) at pressures between (5 and 10) MPa (where the sound speed exhibits a minimum followed by a comparatively steep increase toward higher pressures) is of major importance for the accurate description of the sound speed of natural gases at such relatively low temperatures. During the development of the GERG-2008 equation of state it was observed that even a slightly less accurate description of the binary data would adversely affect the representation of the available multi-component sound

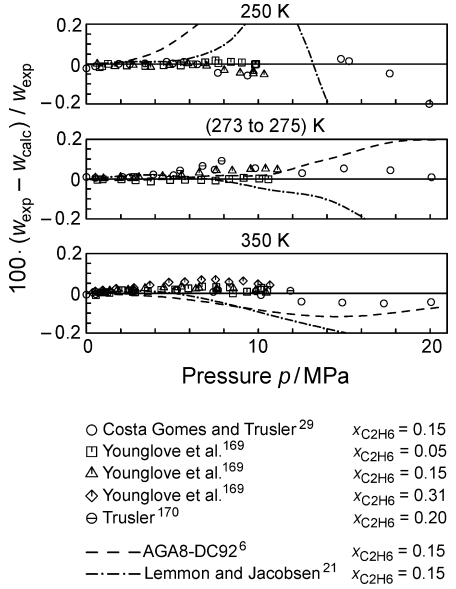

Figure 9. Percentage deviations of experimental sound-speed data for the binary mixture methane−ethane from values calculated with GERG-2008, eq 8. Values calculated with the AGA8-DC92 equation of Starling and Savidge[6] and the mixture model of Lemmon and Jacobsen[21] are plotted for comparison at temperatures of (250, 275, and 350) K.

dx.doi.org/10.1021/je300655b | J. Chem. Eng. Data 2012, 57, 3032−3091

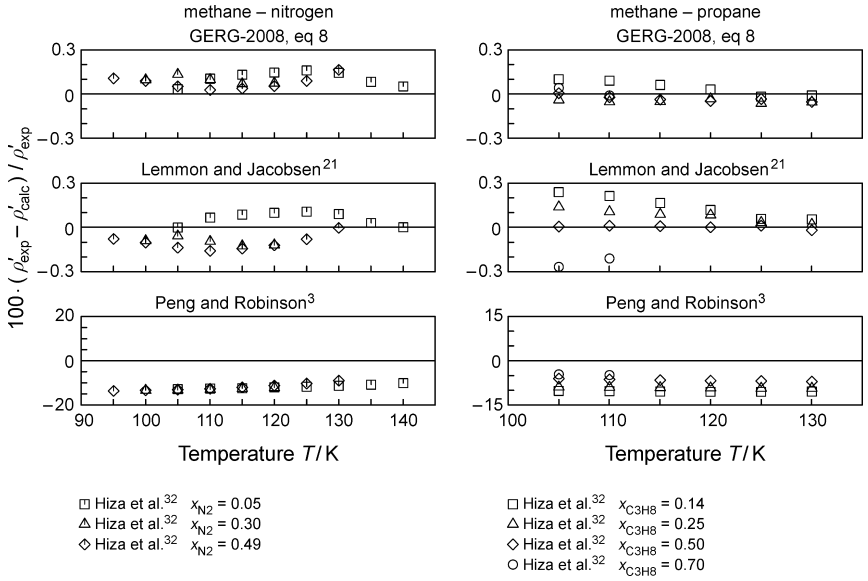

Figure 10. Percentage deviations of the experimental saturated-liquid densities measured by Hiza et al.[32] for the binary mixtures methane−nitrogen and methane−propane from values calculated with GERG-2008, eq 8, the mixture model of Lemmon and Jacobsen,[21] and the cubic equation of state of Peng and Robinson.[3]

speeds (see also Section 5.2.2). This underlines the importance of accurate and wide-ranging binary sound-speed data for the development of accurate equations of state for multi-component mixtures.

Neither the AGA8-DC92 equation[6] nor the model of Lemmon and Jacobsen[21] is able to describe the available sound-speed data as accurately as GERG-2008. Significant improvements compared to the previous equations are achieved by GERG-2008 at temperatures of $T \leq 275$ K, but also at higher temperatures as exemplified by the 350 K isotherm in Figure 9. Deviations between the accurate measurements of Costa Gomes and Trusler[31] for an ethane mole fraction of 0.15 and values calculated from both previous equations clearly exceed the experimental uncertainty of the data over wide ranges of temperature and pressure as shown in this figure. At 250 K, values calculated from AGA8-DC92 deviate by more than (0.3 to 0.8) % from the data, and the model of Lemmon and Jacobsen shows deviations of more than (0.3 to 0.5) % in sound speed. Even at 350 K, the model of Lemmon and Jacobsen deviates from the measurements by more than 0.1 %.

The accurate and improved description of the sound speed of binary mixtures and natural gases (see Sections 5.1.2 and 5.2.2) is of considerable practical importance for the precise determination of mass flow-rates by means of sonic nozzles. Due to the specific mathematical relation between this caloric property and the various derivatives of the reduced Helmholtz free energy α with respect to δ and τ (see Table B.1), the experimental information contained in accurate sound speeds is very useful for the development of multi-fluid mixture models. It also advantageously contributes to the description of other caloric properties, such as enthalpy, entropy, and isobaric heat capacity, which are needed (and of much more interest) for compressor and heat exchanger design in standard and advanced technical applications for natural gases, including pipeline transport, natural gas storage, and processes with liquefied natural gas.

Compared to both AGA8-DC92[6] and the mixture model of Lemmon and Jacobsen,[21] the examples above prove that GERG-2008, eq 8, achieves major and important improvements in the description of caloric properties of binary mixtures of the natural gas main constituents. Even the most accurate sound-speed data are represented by GERG-2008 to within their very low experimental uncertainties over wide ranges of mixture conditions. This is also true for data measured for other caloric properties, including particularly those measured in the liquid phase, where AGA8-DC92 is not applicable. Cubic equations of state deviate from accurate caloric data in the gas and liquid regions by several percent (frequently considerably more than 5 %; see also Section 2.1.2).

5.1.3. Vapor−Liquid Equilibrium Properties. Apart from $p\rho T$ measurements and experimental data for caloric properties of binary mixtures in the homogeneous gas, liquid, and supercritical regions, experimental data for vapor−liquid equilibrium (VLE) states were used for the development of the different binary equations as described in Section 4.4.3. As mentioned in Section 3, accurate VLE data are available for saturated-liquid densities of several binary (and also multi-component) mixtures. Experimental $pTxy$ data (i.e., simultaneous measurements of vapor pressure, saturation temperature, and equilibrium-phase compositions) are in general associated with an increased uncertainty mainly resulting from errors in the measured phase compositions.

5.1.3.1. Saturated-Liquid Densities. Figure 10 shows deviations of experimental saturated-liquid densities for the binary mixtures methane−nitrogen and methane−propane from values calculated from the GERG-2008 equation of state, eq 8, the multi-fluid mixture model of Lemmon and Jacobsen,[21] and the cubic equation of state of Peng and Robinson.[3] The data were measured by Hiza et al.[32] and cover wide ranges of composition at temperatures between (95 to 140) K. The uncertainty of the measurements of the saturated-liquid density is estimated to be $\Delta\rho'/\rho' = (0.1 \text{ to } 0.2)$ %. All of the data (for both mixtures) are represented by GERG-2008 to within low deviations of less than (0.1 to 0.15) %, which is well within the experimental uncertainty. For the methane−nitrogen mixture, the mixture model of Lemmon and Jacobsen achieves a comparable accuracy. The data for the methane−propane mixture are represented by this model to within (0.1 to 0.3) %, and the maximum deviations occur for propane mole fractions of 0.14, 0.25, and 0.70 at the

dx.doi.org/10.1021/je300655b | J. Chem. Eng. Data 2012, 57, 3032−3091

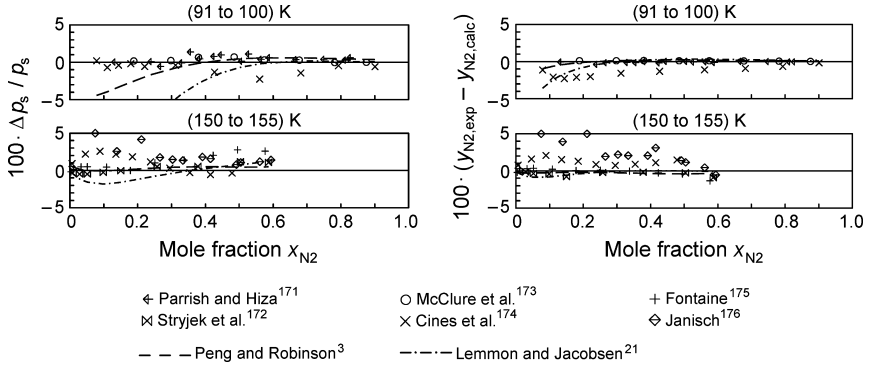

Figure 11. Percentage deviations of experimental bubble-point pressures and nitrogen mole fractions in the saturated vapor phase for the binary mixture methane−nitrogen from values calculated with GERG-2008, eq 8. Values calculated with the cubic equation of state of Peng and Robinson[3] and the mixture model of Lemmon and Jacobsen[21] are plotted for comparison at temperatures of (100 and 150) K.

lowest measured temperatures, indicating a stronger composition dependence compared to GERG-2008. Deviations of more than 10 % for the methane−nitrogen data, obtained from the cubic equation of Peng and Robinson,[3] are nearly independent of the mixture composition. For the methane−propane data, the cubic equation deviates from the measurements by approximately (5 to 10) %, where the deviations strongly depend on the propane concentration. Thus, the deviations between values calculated from the cubic equation of Peng and Robinson and the experimental data are 50 to 100 times larger than those obtained from GERG-2008. The poor representation of saturated-liquid densities (and also compressed-liquid densities) by cubic equations of state can be observed for many binary and multicomponent mixtures (see also Section 5.2.3).

For other binary mixtures, for example, nitrogen−ethane and nitrogen−propane, GERG-2008 achieves similarly high accuracies in the description of saturated-liquid densities; for further details see Kunz et al.[1]

5.1.3.2. The pTxy Relation. Figure 11 shows the representation of selected experimental vapor pressures for the binary mixture methane−nitrogen by the GERG-2008 equation of state, eq 8, at subcritical temperatures [(91 to 100) K] and in the critical region of the mixture [(150 to 155) K]. The displayed deviations were calculated at a given temperature and a given liquid-phase composition (bubble-point pressure calculation). The available binary data for this mixture cover the complete composition range for temperatures from (78 to 190) K (which is close to the critical temperature of pure methane). The GERG-2008 equation of state represents the most reliable vapor-pressure measurements, assumed to be those of Parrish and Hiza,[171] Stryjek et al.,[172] and McClure et al.,[173] to within (1 to 2) %, which agrees well with the experimental uncertainty of the data. It should be noted that the total uncertainty in vapor pressure is generally estimated to be $\Delta p_s/p_s$ = (1 to 3) % or higher (see also Section 3). From the plots shown in Figure 11 it is obvious that data measured by different authors deviate among one another by (partly) more than (2 to 3) % in vapor pressure at virtually the same mixture conditions. Similar (or even worse) experimental situations are observed for most binary systems.[1] Compared to other binary mixtures, the data situation for VLE properties of methane−nitrogen is very satisfactory. However, the poor consistency between the data sets of different authors—and also within single data sets—complicates the development of equations of state for mixtures. To a certain extent, these difficulties are compensated for when accurate experimental data are available for properties in the homogeneous gas, liquid, and supercritical regions or for saturated-liquid densities (see above). Nevertheless, due to the flexible structure of mixture models based on a multi-fluid approximation, the representation of binary *pTxy* data by such an equation of state strongly depends on the data sets chosen by the correlator for use in the development of the equation. The use of "wrong" VLE measurements can adversely affect the description of data measured in the homogeneous region and vice versa.

In the critical region of the mixture (at temperatures above the critical temperature of nitrogen), the cubic equation of state of Peng and Robinson[3] yields quite similar results compared to GERG-2008 as shown for the 150 K isotherm in Figure 11. At lower temperatures, values calculated from the cubic equation significantly deviate from the measurements by more than 2 % in vapor pressure, exceeding the uncertainty of the data. Even higher deviations of more than 5 % are obtained for the mixture model of Lemmon and Jacobsen.[21]

The vapor pressure at a given temperature and liquid-phase composition is not the only VLE property of a *pTxy* data set that was used in the development (nonlinear fitting) of the binary correlation equations of the new mixture model. Further important experimental information can additionally be utilized by nonlinearly fitting the measured vapor-phase composition. Deviations between experimentally determined vapor-phase compositions (mole fractions) and values calculated from GERG-2008, eq 8, for given temperatures and liquid-phase compositions are also shown in Figure 11. Those data that are assumed to be the most reliable for this mixture (see above) are represented by GERG-2008 to within deviations of less than (0.005 to 0.01) mole fractions, which is well in agreement with the experimental uncertainty of such measurements (as estimated from experience). Frequently, the scatter in a single data set significantly exceeds mole fractions of 0.01, and deviations between data sets of different authors can even exceed mole fractions of 0.02 (or more) as shown in Figure 11 for the data of Cines et al.[174] and Janisch.[176] Only the best, that is, most accurate and consistent, *pTxy* measurements are accurate to within (1 to 2) % in vapor pressure and (0.005 to 0.01) mole fractions in vapor-phase composition. Other authors are able to accurately measure the vapor pressure but show inconsistencies in the measured vapor-phase composition and vice versa.

Comparisons between experimental VLE data in the form of *pTxy* data for binary mixtures containing at least one of the components *n*-nonane, *n*-decane, or hydrogen sulfide with values calculated from GERG-2008 are carried out for selected

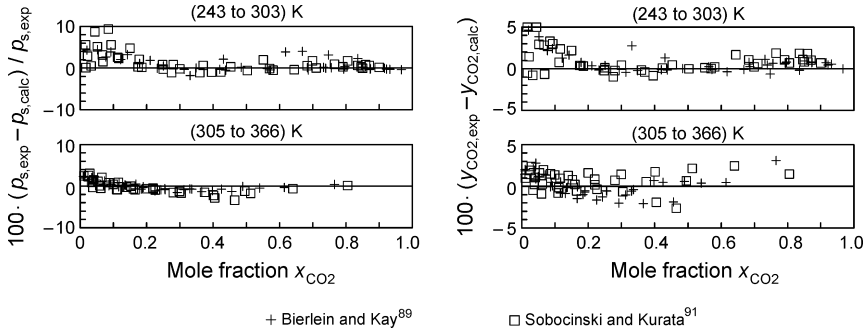

Figure 12. On the left, percentage deviations of experimental bubble-point pressures and, on the right, carbon dioxide vapor-phase compositions for the binary mixture carbon dioxide−hydrogen sulfide from values calculated with GERG-2008, eq 8.

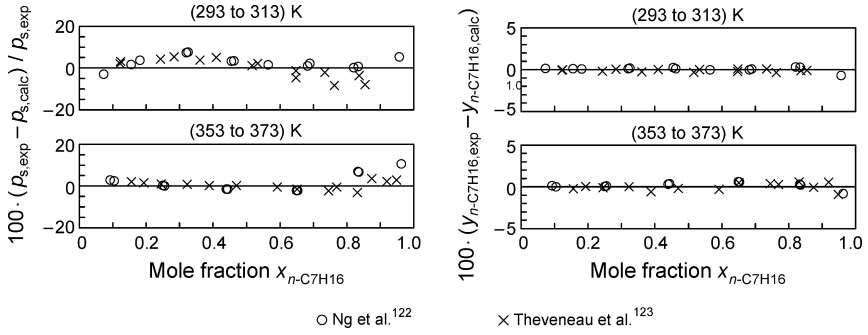

Figure 13. On the left, percentage deviations of experimental bubble-point pressures and, on the right, *n*-heptane vapor-phase compositions for the binary mixture *n*-heptane−hydrogen sulfide from values calculated with GERG-2008, eq 8.

examples and are summarized in two figures. The two deviation diagrams on the left of Figure 12 show how vapor pressures calculated from GERG-2008 for the mixture carbon dioxide−hydrogen sulfide deviate from the measurements of Bierlein and Kay[89] and Sobocinski and Kurata[91] for temperatures from (243 to 366) K. For carbon dioxide mole fractions of (0.18 to 1.0), the data are represented by GERG-2008 to within 2 % in vapor pressure. For temperatures from (243 to 303) K and lower mole fractions, the maximum deviations increase up to about 10 %, where the deviations greater than 5 % are only in the temperature range from (243 to 255) K. The corresponding differences of the VLE data for this mixture to GERG-2008 expressed as differences in vapor-phase compositions (mole fractions) can be seen in the two diagrams on the right of Figure 12. Aside from carbon dioxide mole fractions below about 0.15, the differences between the data and the values from GERG-2008 remain within mole fractions of 0.02 for $T \leq 303$ K and within mole fractions of 0.03 for temperatures from (305 to 366) K. Based on the *pTxy* measurements of Ng et al.[122] and Theveneau et al.,[123] the VLE behavior of GERG-2008 for the mixture *n*-heptane−hydrogen sulfide, expressed again in vapor pressure and vapor-phase composition, is illustrated in Figure 13 for temperatures from (293 to 373) K. Vapor pressures are reproduced by GERG-2008 to within about 7.5 %. The two deviation diagrams on the right show the differences for the same mixture now expressed again in vapor-phase compositions. Except for two points, the data are reproduced by GERG-2008 within 0.005 mole fraction. Comparisons between the deviation diagrams on the left and on the right show that vapor pressures are usually much more sensitive than vapor-phase compositions with regard to differences between experimental VLE data and calculated values.

An example for the representation of VLE states of the binary mixture methane-nitrogen by GERG-2008 is illustrated in Figure 11. In comparison with the cubic equation of Peng and Robinson,[3] GERG-2008 achieves a more accurate description of bubble-point pressures at temperatures below about 110 K. Compared to the mixture model of Lemmon and Jacobsen,[21] there are significant improvements for bubble-point pressures at temperatures below about 150 K, and the description of vapor-phase compositions less than nitrogen mole fractions of 0.2 is improved as well.

As a full mixture model, GERG-2008 is not only able to accurately describe common VLE behavior as shown for the examples discussed above but also for mixtures exhibiting unusual phase behavior, for example, an azeotrope, as described by Kunz et al.[1]

5.2. Representation of Thermal and Caloric Properties of Natural Gases and Other Multi-Component Mixtures.

The quality of the GERG-2008 equation of state, eq 8, in the description of thermal and caloric properties of different types of natural gases and other multi-component mixtures is presented in the following discussions. It should be noted that the experimental data selected for the comparisons were not used for the development (fitting and structure optimization) of GERG-2008.

5.2.1. The pρT Relation in the Homogeneous Gas Region. As described in Section 3, a huge amount of the *pρT* measurements is available for natural gases and similar mixtures covering temperatures from (270 to 350) K at pressures up to about 30 MPa. Comparatively few (but accurate) data were measured at temperatures below 270 K. Together with the accurate and wide-ranging data for binary mixtures that are strongly related to natural gases, such as methane−nitrogen and methane−ethane, the present data situation allows for a well-founded estimation of the uncertainty in gas-phase densities at temperatures below 270 K.

dx.doi.org/10.1021/je300655b | J. Chem. Eng. Data 2012, 57, 3032−3091

Table 7. Molar Compositions of the Round-Robin Natural Gases[a]

	composition (100·mole fraction)									
mixture	CH_4	N_2	CO_2	C_2H_6	C_3H_8	n-C_4	i-C_4	n-C_5	i-C_5	n-C_6
NIST1	96.522	0.260	0.596	1.819	0.460	0.101	0.098	0.032	0.047	0.066
NIST2	90.672	3.128	0.468	4.528	0.828	0.156	0.104	0.044	0.032	0.039
RG2	85.906	1.007	1.495	8.492	2.302	0.351	0.349	0.048	0.051	
GU1	81.441	13.465	0.985	3.300	0.605	0.104	0.100			
GU2	81.212	5.702	7.585	4.303	0.895	0.152	0.151			

[a]The mixtures were prepared in two batches (one for laboratories in Europe and one for those in the U.S.). The values given here belong to the batch distributed to laboratories in Europe. The minor differences in the compositions between the two batches have no influence on the representation of the $p\rho T$ measurements by equations of state.

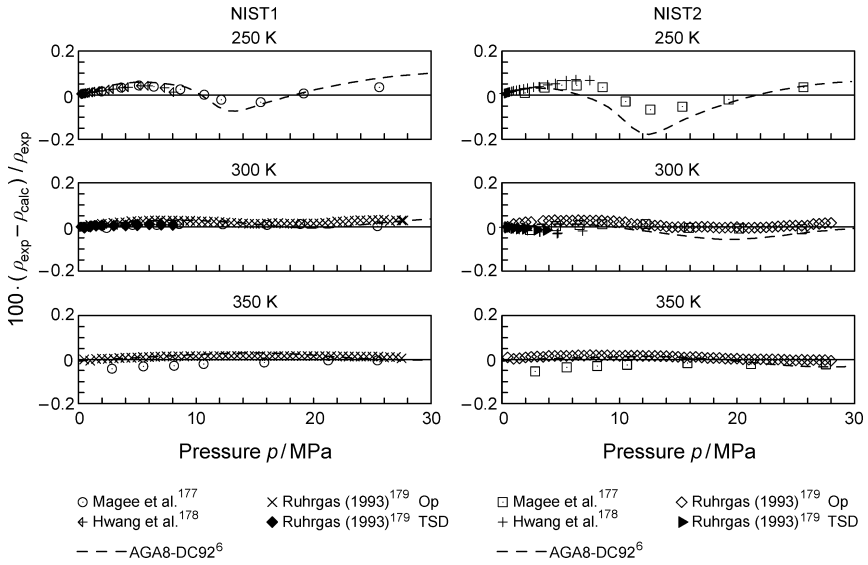

Figure 14. Percentage density deviations of experimental $p\rho T$ data for the round-robin natural gases "NIST1" and "NIST2" from values calculated with GERG-2008, eq 8; for the mixture compositions see Table 7. Values calculated with the AGA8-DC92 equation of Starling and Savidge[6] are plotted for comparison. TSD: two-sinker densimeter, Op: optical interferometry method.

Most of the measurements used for the following comparisons were taken from the databank GERG TM7 of Jaeschke et al.,[26] which comprises accurate density data for synthetic multicomponent mixtures, simulated and true natural gases, and natural gases with different admixtures (i.e., natural gases diluted or enriched with one or more natural gas components). The majority of these data were measured at Ruhrgas using an optical interferometry method or a Burnett apparatus. The uncertainty in density of these measurements is generally estimated to be $\Delta\rho/\rho$ = (0.07 to 0.1) %. A few very accurate density data were measured with a two-sinker densimeter at pressures up to about 8 MPa. For these measurements, the uncertainty in density is estimated to be 0.03 %.

A number of data measured in a round-robin series of $p\rho T$ measurements (see Magee et al.[177]) exist for a selection of five simulated natural gases. The measurements were performed by different laboratories using five different experimental techniques. The gases are designated by "NIST1", "NIST2", "RG2", "GU1", and "GU2". They cover the range of compositions normally encountered in gas industry operations in North America and Europe. Each mixture was prepared gravimetrically to the (approximate) molar compositions given in Table 7. Aside from the measurements carried out at Ruhrgas, reliable data were also measured by Magee et al.[177] and Hwang et al.[178] using a Burnett apparatus. Measurements that appear to be associated with an increased or questionable uncertainty, such as data measured using a pycnometer method, are not included in the comparisons. In addition to the round-robin measurements, experimental data for the mixtures listed in Table 8 were selected for the comparisons discussed below.

To demonstrate important improvements compared to the previous equations of state, the comparisons frequently focus on the representation of data at lower to medium temperatures. In general, toward higher temperatures, for example, (330 and 350) K, the deviations decrease.

5.2.1.1. Methane-Rich and Pipeline-Quality Natural Gases. Experimental measurements of gas-phase densities for the round-robin gases NIST1 and NIST2 and their percentage deviations from the GERG-2008 equation of state, eq 8, are shown in Figure 14.

The round-robin gas NIST1 consists of 10 components and represents a simulated Gulf Coast natural gas containing a methane mole fraction of about 0.965, an ethane mole fraction of about 0.018, and low to small fractions of nitrogen, carbon dioxide, and hydrocarbons from propane to *n*-hexane. Such a natural gas, which is almost entirely composed of methane, is typical for Russian gas. The selected data cover temperatures from (250 to 350) K and wide ranges of pressure. As shown in Figure 14, all of the data are represented by GERG-2008 to within very low deviations of less than 0.05 % in density, which is

dx.doi.org/10.1021/je300655b | J. Chem. Eng. Data 2012, 57, 3032−3091

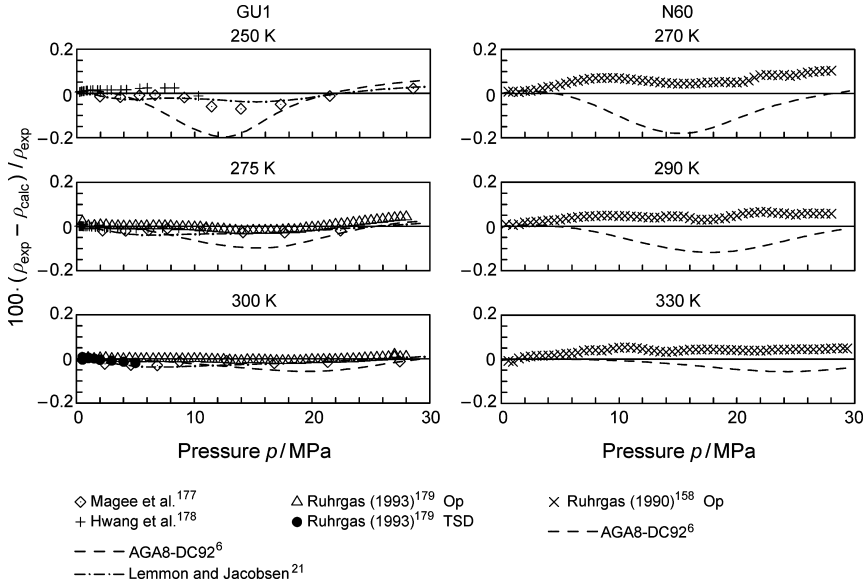

Figure 15. Percentage density deviations of experimental $p\rho T$ data for the nitrogen-rich natural gases "GU1" and "N60" from values calculated with GERG-2008, eq 8; for the mixture compositions see Tables 7 and 8. Values calculated with the AGA8-DC92 equation of Starling and Savidge[6] are plotted for comparison. TSD: two-sinker densimeter, Op: optical interferometry method.

clearly within the uncertainty of the measurements. The AGA8-DC92 equation of state[6] yields a quite similar accurate description for this type of natural gas.

The round-robin gas NIST2 consists of 10 components and represents a simulated Amarillo gas. The mixture contains medium fractions of methane (about 0.907), nitrogen (about 0.031), and ethane (about 0.045). The mole fraction of carbon dioxide amounts to approximately 0.005, which is typical for natural gases of pipeline quality. The mixture contains a propane mole fraction of about 0.008 and small amounts of the further hydrocarbons from *n*-butane to *n*-hexane (see also Table 7). The selected data cover a wide range of temperatures from (250 to 350) K at pressures up to 29 MPa. All of the density measurements are represented by GERG-2008 well within their experimental uncertainty, which is estimated to be $\Delta\rho/\rho$ = 0.07 % for the measurements of Ruhrgas[179] and $\Delta\rho/\rho$ = 0.1 % for Magee et al.[177] and Hwang et al.[178] In contrast to GERG-2008, AGA8-DC92 deviates from the measurements at 250 K and pressures around 12 MPa by slightly more than 0.1 % (see Figure 14). A similar description of the data is achieved at higher temperatures. Since the mixture model reported by Lemmon and Jacobsen[21] is not applicable for mixtures containing fractions of *n*-pentane, isopentane, and *n*-hexane, no comparison is possible here.

5.2.1.2. Natural Gases Rich in Nitrogen. As mentioned in Section 2.1.1, a known weakness of the AGA8-DC92 equation of state[6] is its less accurate description of natural gases containing a relatively high fraction of nitrogen. A nitrogen mole fraction of more than 0.10 is typical for Dutch natural gases of pipeline quality. Figure 15 shows density measurements for two nitrogen-rich natural gases and their percentage deviations from the GERG-2008 equation of state, eq 8. The mixture designated by "GU1" consists of seven components and represents a simulated Slochteren gas. This natural gas mixture is composed of mole fractions of methane (about 0.814), nitrogen (about 0.135), carbon dioxide (about 0.01), ethane (about 0.033), and low to small fractions of heavier hydrocarbons (see Table 7). GERG-2008 is able to describe all of the selected data to within low deviations of (0.05 to 0.07) % over the entire covered temperature and pressure ranges. Values calculated from AGA8-DC92 deviate from the measurements at 250 K by clearly more than 0.1 %, which exceeds the estimated uncertainty in density for the data. A quite similar poor description is obtained from AGA8-DC92 for the $p\rho T$ relation of the binary mixture methane−nitrogen discussed in Section 5.1.1.1 (see the results for nitrogen mole fractions of 0.10 and 0.20 displayed in Figure 2), which underlines the observations for this natural gas.

The AGA8-DC92 equation[6] yields an even worse description of the measurements of Ruhrgas[158] for the 13-component mixture designated by "N60", exemplifying another nitrogen-rich natural gas (see Figure 15). The nitrogen mole fraction for this mixture amounts to about 0.117. In contrast to the mixture GU1, N60 additionally contains small fractions of the hydrocarbons from *n*-pentane to *n*-octane and helium. Values calculated from AGA8-DC92 deviate from the data by more than 0.1 % at 290 K and even exceed 0.2 % at 270 K. The GERG-2008 equation of state represents all measurements to well within (0.07 to 0.1) % for all measured temperatures and pressures. These examples indicate that GERG-2008 is clearly superior to AGA8-DC92 in the description of nitrogen-rich natural gases and achieves a significantly lower uncertainty in calculated densities.

5.2.1.3. Natural Gases Rich in Carbon Dioxide. Important and substantial improvements compared to all previous equations of state are achieved by the GERG-2008 equation of state, eq 8, for natural gas mixtures rich in carbon dioxide. Figure 16 shows density deviations between data for the round-robin gas GU2 in the temperature range from (250 to 325) K at pressures up to 30 MPa and values calculated from the new equation of state. The mixture has a methane concentration of about 0.812 mole fraction and contains medium mole fractions of nitrogen (0.057), ethane (0.043), and propane (0.009) and a comparatively high mole fraction of carbon dioxide of about 0.076 (see Table 7). All of the selected data measured by Ruhrgas[179] and Magee et al.[177] are well-represented by GERG-2008 to within low deviations of (0.05 to 0.07) %, which agrees with the experimental uncertainty of the data.

dx.doi.org/10.1021/je300655b | J. Chem. Eng. Data 2012, 57, 3032−3091

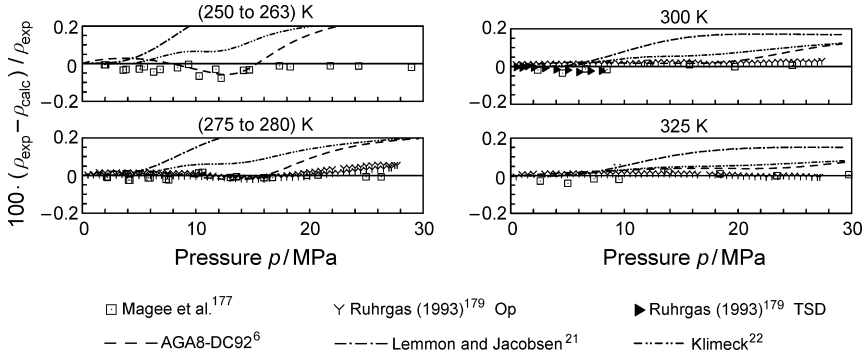

Figure 16. Percentage density deviations of experimental $p\rho T$ data for the round-robin natural gas "GU2" from values calculated with GERG-2008, eq 8; for the mixture composition see Table 7. Values calculated with the AGA8-DC92 equation of Starling and Savidge[6] and the mixture models of Lemmon and Jacobsen[21] and Klimeck[22] are plotted for comparison. TSD: two-sinker densimeter, Op: optical interferometry method.

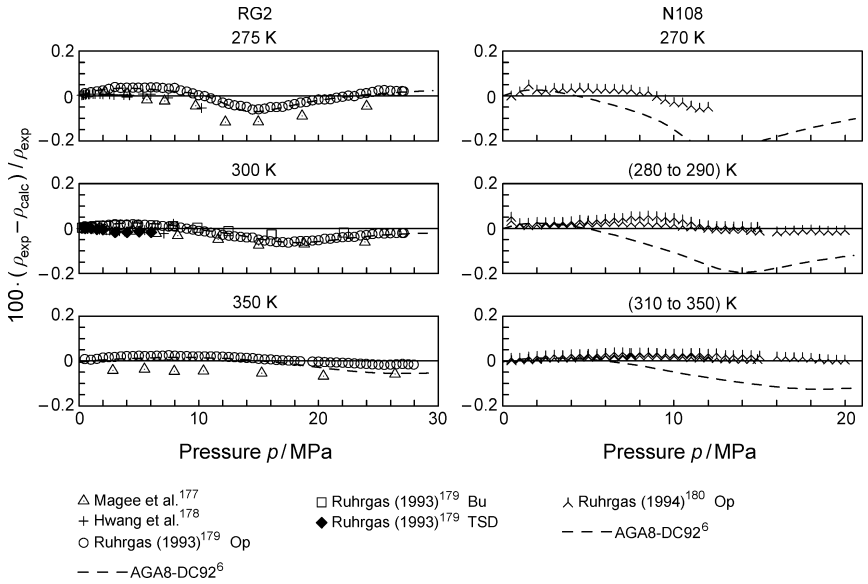

Figure 17. Percentage density deviations of experimental $p\rho T$ data for the natural gas mixtures "RG2" and "N108" from values calculated with GERG-2008, eq 8; for the mixture compositions see Tables 7 and 8. Values calculated with the AGA8-DC92 equation of Starling and Savidge[6] are plotted for comparison. Bu: Burnett apparatus, TSD: two-sinker densimeter, Op: optical interferometry method.

At lower temperatures, density deviations exceeding 0.1 % or even 0.2 % exist for the AGA8-DC92 equation[6] as well as for the preliminary equation of state of Klimeck.[22] A worse description comes from the mixture model of Lemmon and Jacobsen,[21] which shows greater deviations from the measurements over wide ranges of temperature and pressure. Values calculated from this model deviate from the experimental data by more than 0.1 % at 300 K (and also 325 K) and by more than 0.2 % at lower temperatures.

5.2.1.4. Natural Gases Containing Substantial Amounts of Ethane and Propane, And Natural Gases Rich in Ethane. Natural gases containing substantial amounts of ethane and propane are typical for North Sea gas. Percentage density deviations of selected measurements for such natural gas mixtures from the GERG-2008 equation of state, eq 8, are displayed in Figure 17. The round-robin mixture designated by "RG2" consists of nine components and contains an ethane mole fraction of about 0.085 and a propane mole fraction of 0.023 (see also Table 7). The mixture designated by "N108" is composed of 15 components and represents an Ekofisk gas enriched with ethane. This mixture contains only about 0.80 mole fraction methane but 0.16 mole fraction ethane (see also Table 8).

The most reliable measurements for the mixture RG2 are represented by GERG-2008 to within low deviations of (0.05 to 0.07) %, which is well within the experimental uncertainty of the data. The measurements of Magee et al.[177] show a systematic offset of about 0.05 % in density from the optical interferometry measurements of Ruhrgas[179] at temperatures of (275 and 350) K and from the Burnett measurements of Ruhrgas[179] at 300 K. Similar systematic offsets can also be observed for the data of Magee et al. measured for the other round-robin gases. However, a number of further data for natural gas mixtures of nearly the same composition are accurately described by GERG-2008 supporting the impression that the measurements of Magee et al.[177] seem to be associated with an increased uncertainty. The AGA8-DC92 equation[6] almost exactly follows the optical interferometry measurements of Ruhrgas.[179] This behavior follows the assumption that the experimental data were used for the development of the equation.

Substantial improvements are achieved by GERG-2008 for natural gas mixtures that contain even higher fractions of ethane than contained in typical Ekofisk gases. This is exemplified by the comparisons shown in Figure 17 for the mixture N108. The GERG-2008 equation of state represents all of the data measured

dx.doi.org/10.1021/je300655b | J. Chem. Eng. Data 2012, 57, 3032−3091

Table 8. Molar Compositions of Selected Synthetic Multi-Component Mixtures, True Natural Gases, Natural Gases with Different Admixtures, and Simulated Rich Natural Gas Mixtures[a,b,c]

	composition (100·mole fraction)											
mixture	CH_4	N_2	CO_2	C_2H_6	C_3H_8	n-C_4	i-C_4	n-C_5	i-C_5	n-C_6	H_2	CO
D18	61.77	12.66	12.60	12.97								
N60[a]	82.52	11.73	1.11	3.46	0.76	0.15	0.10	0.04	0.03	0.02		
N108[b]	79.95	1.13	1.02	16.01	1.40	0.26	0.13	0.03	0.03	0.02	<0.01	
N116[c]	28.89	28.00	2.02	0.84	0.16	0.07		0.03	<0.01	<0.01	26.99	13.00
RNG3	59.00	4.99	5.99	18.00	8.02	3.30		0.49		0.21		
RNG5	63.98	2.02	7.99	11.97	10.01	3.31		0.51		0.20		

[a]The mixture contains small fractions of *n*-heptane, *n*-octane, and helium. [b]The mixture contains small fractions of *n*-heptane, *n*-octane, *n*-nonane, and helium. [c]The mixture contains a small fraction of *n*-heptane.

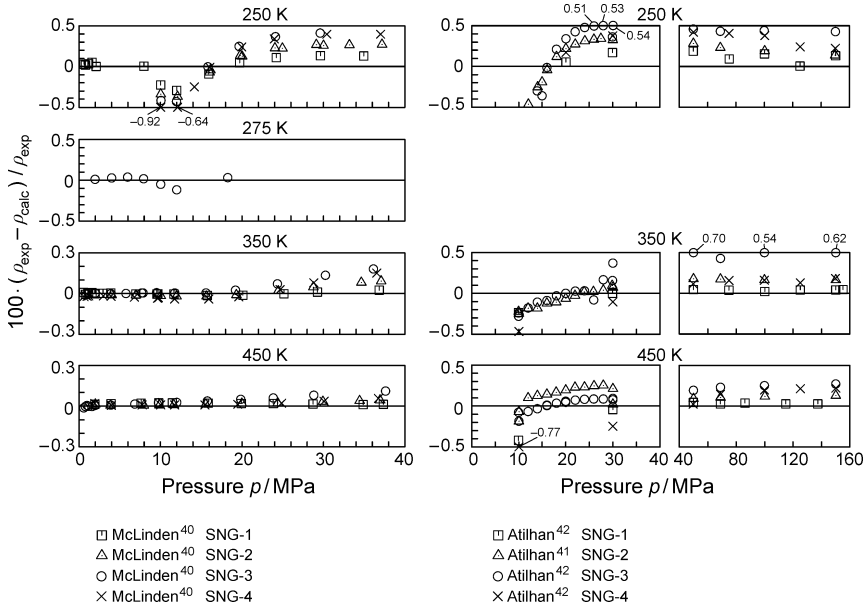

Figure 18. Percentage density deviations of experimental gas-phase $p\rho T$ data of McLinden[40] (diagrams on the left) and of Atilhan et al.[41,42] (diagrams on the right) for four synthetic natural-gas-like mixtures from values calculated with GERG-2008, eq 8. These mixtures contain comparatively high fractions of butanes and pentanes. The mixtures used by the two experimenters have exactly the same composition (they are from the same bottles), which is given in Table 3. It should be noted that the mixture described in ref 41 corresponds to the mixture SNG-2 in ref 40 and the mixture SNG-2 described in ref 42 corresponds to the mixture SNG-1 in ref 40; here the notations of ref 40 are used. There are no measurements of Atilhan et al. for T = 275 K.

by Ruhrgas[180] to within low deviations of about 0.05 % in density. Values calculated from AGA8-DC92 deviate from the measurements at 310 K by up to 0.09 % and by up to about 0.2 % at (280 and 270) K.

5.2.1.5. Natural Gases Containing Substantial Fractions of Butanes and Pentanes. As described in Section 3.1.2, McLinden[40] and Atilhan et al.[41,42] performed gas-phase density measurements for four synthetic natural-gas-like mixtures. Due to the comparatively high fractions of butanes and pentanes (see Table 3), these mixtures can be classified as natural gases rich in these components. The representation of these $p\rho T$ data by the GERG-2008 equation of state, eq 8, is summarized in Figure 18. The differences between McLinden's data for (275, 350, and 450) K and those calculated from GERG-2008 are less than 0.1 %. Only at 350 K for pressures above 30 MPa, the deviations increase to 0.2 % for the two mixtures with the highest mole fractions of butanes and pentanes, namely, SNG-3 and SNG-4 (see Table 3). For 250 K and pressures above 20 MPa, the differences increase to 0.4 % for SNG-3 and SNG-4. All of these data are represented well within the uncertainty of GERG-2008. This is also true for 250 K, in particular, when realizing that these two mixtures belong to the group of rich natural gases (at least regarding the high fractions of the butanes and pentanes), and the highest pressure is at the limit of the normal range of validity of GERG-2008. A special situation can be seen in the pressure range of about (10 to 12) MPa where the differences between the experimental and calculated densities extend to about −0.9 %. However, this range is a part of the critical region or near to it (dependent on composition) where the uncertainties of both GERG-2008 and the measurements are clearly greater than those for the "normal" fluid region. For experiments in this region, very small changes in composition by, for example, adsorption and precondensation, causes significant changes in the measured density.

The diagrams on the right of Figure 18 show for the same mixtures the differences in density of the $p\rho T$ measurements of Atilhan et al.[41,42] in comparison to values from GERG-2008. These data cover pressures up to 150 MPa. For a better comparison with McLinden's data, the deviation diagrams for Atilhan et al.'s data are separated into the pressure ranges up to

dx.doi.org/10.1021/je300655b | J. Chem. Eng. Data 2012, 57, 3032−3091

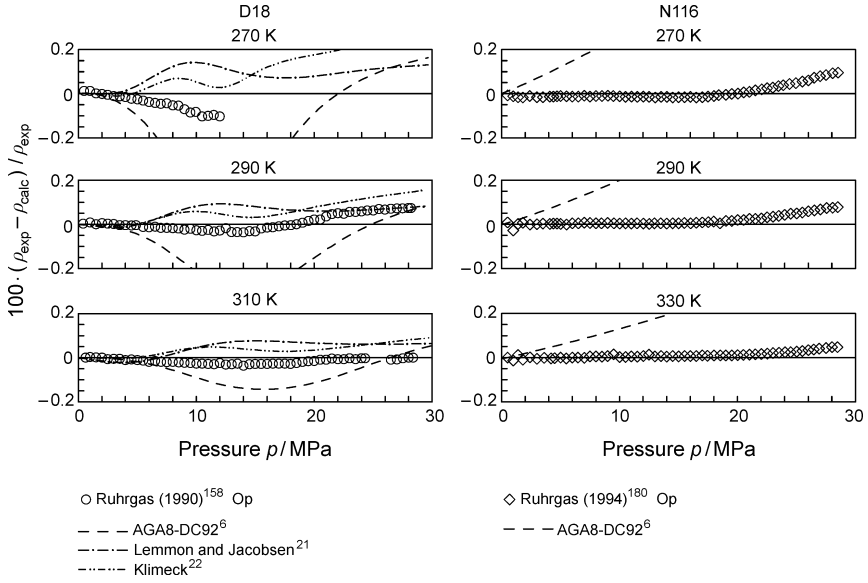

Figure 19. Percentage density deviations of experimental $p\rho T$ data for the natural gas mixtures "D18" and "N116" from values calculated with GERG-2008, eq 8; for the mixture compositions see Table 8. Values calculated with the AGA8-DC92 equation of Starling and Savidge[6] and the mixture models of Lemmon and Jacobsen[21] and Klimeck[22] are plotted for comparison. Op: optical interferometry method.

40 MPa and from (40 to 150) MPa. For pressures below 40 MPa, there are systematic differences in density of up to 0.54 % at 250 K (SNG-3) and up to −0.77 % at 450 K (SNG-1) between their data and values from GERG-2008. The reason for these differences is probably the higher experimental uncertainties in the data than claimed by these authors for this pressure range. Moreover, the data are also not consistent either with McLinden's densities (see the diagrams on the left side of Figure 18). The density differences between the data and the GERG-2008 values for the pressure range from (40 to 150) MPa are mostly within the given experimental uncertainty of 0.3 % (see Section 3.1.2). The differences increase to 0.7 % only for the mixture SNG-3 at T = 350 K. This is very good agreement when keeping in mind that this large pressure range is far beyond the extended range of validity of GERG-2008.

5.2.1.6. Natural Gas Mixtures of Uncommon Composition. The comparisons displayed in Figures 15 to 18 have shown important and substantial improvements for the $p\rho T$ relation of natural gases containing high fractions of either nitrogen, carbon dioxide, ethane, or higher hydrocarbons. Figure 19 illustrates comparisons for two mixtures of uncommon composition. The comparisons demonstrate the enormous predictive power of the GERG-2008 equation, eq 8, resulting from the accurate and improved description of the respective binary subsystems. The four-component mixture designated by "D18" contains high fractions of nitrogen, carbon dioxide, and ethane and a comparatively low mole fraction of methane of only about 0.618. The mole fractions of nitrogen, carbon dioxide, and ethane amount to approximately 0.13 for each component (see Table 8). For the mixture D18, the measurements were carried out by Ruhrgas[158] using an optical interferometry method.

The data for the mixture D18 are represented by GERG-2008 to within low deviations of less than (0.05 to 0.1) %. The AGA8-DC92 equation[6] deviates from the measurements at 270 K by more than 0.4 % and at 290 K by more than 0.2 %. Even at higher temperatures AGA8-DC92 is not as accurate as GERG-2008. The comparisons for the mixture D18 show that the mixture models of Lemmon and Jacobsen[21] and Klimeck[22] yield more accurate results than AGA8-DC92. But both models are clearly not able to represent the measurements as accurately as GERG-2008. The model of Klimeck deviates from the measurements at 270 K by more than 0.1 %, and the model of Lemmon and Jacobsen shows deviations of more than 0.2 %. Also at higher temperatures, both models are less accurate than GERG-2008.

The GERG-2008 equation not only accurately describes the $p\rho T$ relation of various types of pipeline quality natural gases and similar mixtures but also accurately handles natural gas−hydrogen mixtures, natural gases diluted with oxygen, and other special gases. This is exemplified by the comparisons shown in Figure 19 for the rather untypical gas mixture designated by "N116". The 12-component mixture represents a low calorific natural gas containing large amounts of coke-oven constituents. The mixture contains very low mole fractions of methane (only about 0.289), but high fractions of nitrogen (0.28), hydrogen (0.27), and carbon monoxide (0.13). All data were measured by Ruhrgas[180] using an optical interferometry method. They are represented by GERG-2008 to within low density deviations of less than 0.07 % (most of the measurements are clearly represented to within 0.05 %), except for a few data points, which are, however, well within 0.1 %. Large systematic deviations are obtained from AGA8-DC92, which is not able to accurately describe this rather special mixture. Values calculated from this equation deviate from the measurements at 270 K by up to approximately 0.7 % and at 330 K by up to about 0.35 %.

5.2.1.7. Rich Natural Gases. In general, natural gas produced at the wellhead contains varying (and large) amounts of ethane, propane, *n*-butane, isobutane, and heavier hydrocarbons, which are also called "natural gas liquids" (NGL). In its raw form, this "rich" natural gas is usually not acceptable for transportation in natural gas pipeline systems or for commercial use as a fuel. Moreover, NGLs usually have more value on their own than when left in the natural gas. Therefore, rich natural gas is processed to meet pipeline-quality specifications and to remove the NGLs, which are then reprocessed in a fractionation unit to be broken up for individual sale as ethane, propane, LPG, and other products. The new mixture model can be used for the calculation of such separation processes since it accurately describes the phase behavior of natural gases and hydrocarbon

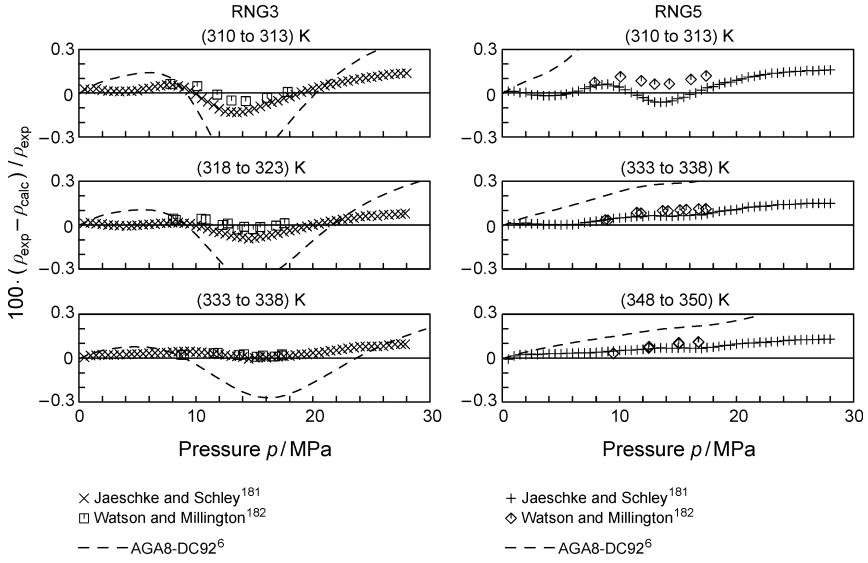

Figure 20. Percentage density deviations of experimental $p\rho T$ data for the rich natural gases "RNG3" and "RNG5" from values calculated with GERG-2008, eq 8; for the mixture compositions see Table 8. Values calculated from the AGA8-DC92 equation of Starling and Savidge[6] are plotted for comparison.

mixtures and also their liquid-phase properties (see Sections 5.2.3 and 5.2.4).

A number of accurate $p\rho T$ data for seven differently composed simulated rich natural gas mixtures are available, which were independently measured by Jaeschke and Schley[181] and Watson and Millington.[182] These mixtures contain up to 0.18 mole fraction ethane, 0.14 propane, 0.06 *n*-butane, 0.005 *n*-pentane, 0.002 *n*-hexane, 0.05 nitrogen, and up to 0.20 mole fraction carbon dioxide. Their low content of methane ranges from only about (0.52 to 0.64) mole fraction. The measurements of Jaeschke and Schley[181] were carried out using an optical interferometry method and cover the gas phase and gas-like supercritical region for temperatures from (280 to 350) K at pressures up to 30 MPa. The high content of the hydrocarbons from ethane to *n*-hexane causes the cricondentherm of the rich natural gas to be located at considerably higher temperatures [in the approximate range from (300 to 310) K] than for typical natural gases. Thus, the measurements at the lower temperatures are limited to pressures below the two-phase boundary. The densities of Watson and Millington[182] complement those of Jaeschke and Schley[181] for virtually the same mixture compositions. They were measured using a two-sinker densimeter and cover temperatures ranging from about (313 to 353) K at pressures from around (8 to 18) MPa. The uncertainty in density of the data of Watson and Millington is claimed by the authors to be 0.04 %. For the data measured by Jaeschke and Schley, which are generally in good agreement with those of Watson and Millington, the uncertainty in density is assumed to be 0.1 %. A systematic offset of (slightly) more than 0.1 % can be observed between some data in these two sources, indicating an increased uncertainty for at least some of the measurements (see also Figure 20).

The comparisons in Figure 20 show selected data in these sources for two differently composed rich natural gases. The mixture designated by "RNG3" consists of about 0.59 mole fraction methane, 0.05 nitrogen, 0.06 carbon dioxide, 0.18 ethane, 0.08 propane, 0.033 *n*-butane, 0.005 *n*-pentane, and 0.002 *n*-hexane. The mixture designated by "RNG5" consists of about 0.64 mole fraction methane, 0.02 nitrogen, 0.08 carbon dioxide, 0.12 ethane, 0.10 propane, 0.033 *n*-butane, 0.005 *n*-pentane, and 0.002 *n*-hexane. The GERG-2008 equation of state, eq 8, represents the selected measurements to within deviations of (0.1 to 0.15) % in density. A similarly accurate description is obtained for the measurements of Jaeschke and Schley[181] at lower temperatures (not shown here). Comparisons with the data measured for additional simulated rich natural gases show that the new equation of state generally yields similarly accurate results for the mixtures that contain mole fractions of about (0.10 to 0.18) ethane, (0.08 to 0.14) propane, (0.033 to 0.06) *n*-butane, and (0.06 to 0.08) carbon dioxide [with or without the smaller fractions of *n*-pentane and *n*-hexane of (0.005 and 0.002) mole fraction, respectively]. Noticeably higher systematic deviations are observed for only two rich natural gas mixtures containing carbon dioxide mole fractions of about 0.14 and 0.20, which are obviously more difficult to describe. However, the maximum deviations obtained for these mixtures never exceed 0.5 % in density.

Although there seems to be potential for further improvements (see also Section 6), the description currently achieved by GERG-2008 is very satisfactory and represents a major improvement compared to AGA8-DC92, which is not able to describe any of the data as accurately as the new mixture model. Values calculated from AGA8-DC92 deviate from the measurements for the mixture RNG3 by more than 0.3 % at 310 K and by more than 0.2 % at higher temperatures. For the rich natural gas mixture RNG5, deviations of up to approximately 0.7 % at 310 K and of about (0.2 to 0.4) % at higher temperatures are obtained from AGA8-DC92. Maximum deviations of up to 1 % are obtained from AGA8-DC92 for other rich natural gas mixtures.

As exemplified by all of the comparisons above, GERG-2008 achieves a very accurate description of the $p\rho T$ relation for binary mixtures and natural gases over a much wider range of mixture conditions (temperature, pressure, and composition) than any of the previously developed equations. Since no multi-component mixture data were used for the development of the new mixture model, the improvements achieved for natural gases, similar gases, and other multi-component mixtures (see also the

dx.doi.org/10.1021/je300655b | J. Chem. Eng. Data 2012, 57, 3032−3091

Table 9. Molar Compositions of Selected Natural Gas Mixtures Investigated by Younglove et al.[169]

	composition (100·mole fraction)									
mixture	CH_4	N_2	CO_2	C_2H_6	C_3H_8	*n*-C_4	*i*-C_4	*n*-C_5	*i*-C_5	*n*-C_6
Gulf Coast	96.561	0.262	0.597	1.829	0.410	0.098	0.098	0.032	0.046	0.067
Amarillo	90.708	3.113	0.500	4.491	0.815	0.141	0.106	0.065	0.027	0.034
Statoil Dry	83.980	0.718	0.756	13.475	0.943	0.067	0.040	0.008	0.013	

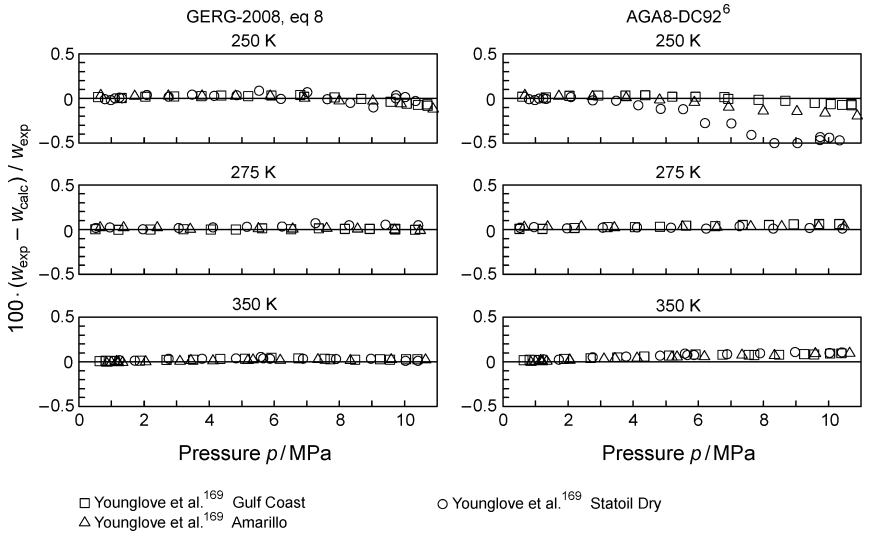

Figure 21. Percentage deviations of experimental sound-speed data for the natural gases "Gulf Coast", "Amarillo", and "Statoil Dry" from values calculated with GERG-2008, eq 8, and the AGA8-DC92 equation of Starling and Savidge;[6] for the mixture compositions see Table 9.

comparisons given by Kunz et al.[1]) result from the accurate description of the different binary subsystems.

5.2.2. Caloric Properties in the Homogeneous Gas Region. This section discusses the representation of caloric properties by the GERG-2008 equation of state, eq 8, for natural gases and other multi-component mixtures. Compared to the gas-phase $p\rho T$ data sets, measurements for caloric properties of natural gases are scarce. For pipeline-quality natural gases, the uncertainty of GERG-2008 in gas-phase sound speed needed to be $\Delta w/w$ = 0.1 %. Modern technical applications require the prediction of isobaric enthalpy differences to within $\Delta(\Delta h)/\Delta h$ = 1 %. The investigations of Klimeck et al.[9] showed that the AGA8-DC92 equation[6] is not able to fulfill these requirements. A significant shortcoming of this equation concerns the description of caloric properties at lower temperatures. The following comparisons demonstrate the results and improvements achieved by GERG-2008.

5.2.2.1. Sound Speed. Younglove et al.[169] reported accurate caloric data for gas-phase sound speeds of different natural gas mixtures consisting of eight to 10 components. The data were measured over the temperature range from (250 to 350) K for pressures up to 11 MPa. The mixture compositions are representative of commercially available or naturally occurring natural gases in North America and Europe (see Table 9). Comparisons between data for binary mixtures measured by these authors and those of other sources (as shown in Figures 8 and 9) conclude that the uncertainty in sound speed of the multi-component data of Younglove et al.[169] is likely to be (0.05 to 0.1) %.

Figure 21 shows percentage deviations of sound-speed data for three natural gases from the GERG-2008 equation of state, eq 8, and the AGA8-DC92 equation.[6] The data were measured by Younglove et al.[169] The different mixtures represent a methane-rich natural gas (Gulf Coast), a natural gas containing medium fractions of methane, nitrogen, and ethane (Amarillo), and an ethane-rich natural gas (Statoil Dry). Table 9 lists the respective molar compositions (prepared gravimetrically) of these mixtures. The measurements of all three mixtures are represented by GERG-2008 well within low deviations in sound speed of (0.05 to 0.1) % over the entire measured temperature and pressure ranges, which are well within the estimated uncertainty of the data. The AGA8-DC92 equation shows similar deviations at temperatures of (275 and 350) K. At 250 K, this equation shows weaknesses in the description of the sound speeds for the ethane-rich natural gas mixture, which contains an ethane mole fraction of about 0.135. Here, deviations of up to 0.5 % in sound speed are observed. AGA8-DC92 also yields less accurate results for the Amarillo gas mixture, where systematic deviations of more than 0.1 % (up to about 0.2 % at the highest measured pressures) are obtained. The comparisons show that the results achieved by GERG-2008 are well within the targeted uncertainty for gas-phase sound speeds.

5.2.2.2. Enthalpy Differences. Very accurate gas-phase isobaric enthalpy differences were measured by Owren et al.[183] for a five-component synthetic natural gas mixture. The uncertainty in enthalpy differences of the measurements is estimated to be (0.2 to 0.5) %. The synthetic mixture consists of about 0.80 mole fraction methane, 0.10 nitrogen, 0.02 carbon dioxide, 0.05 ethane, and 0.03 propane. Figure 22 shows percentage deviations of selected experimental isobaric enthalpy differences from the GERG-2008 equation of state, eq 8, and the AGA8-DC92 equation of state.[6] Almost all measurements are represented to within deviations of (0.2 to 0.5) % by GERG-2008, which is in good agreement with the uncertainty of the data. There are only two points, located in the lower temperature range from (243 to 257) K, for which the deviations from the

dx.doi.org/10.1021/je300655b | J. Chem. Eng. Data 2012, 57, 3032−3091

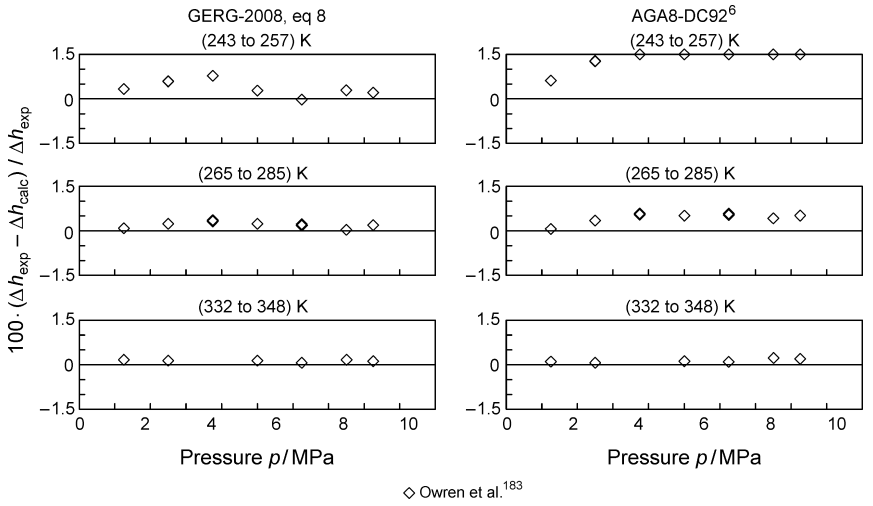

Figure 22. Percentage deviations of experimental (isobaric) enthalpy differences measured by Owren et al.[183] for a five-component synthetic natural gas mixture from values calculated with GERG-2008, eq 8, and the AGA8-DC92 equation of Starling and Savidge;[6] the mixture composition in mole fractions is as follows: 0.79969 CH_4, 0.09946 N_2, 0.02013 CO_2, 0.05065 C_2H_6, and 0.03007 C_3H_8.

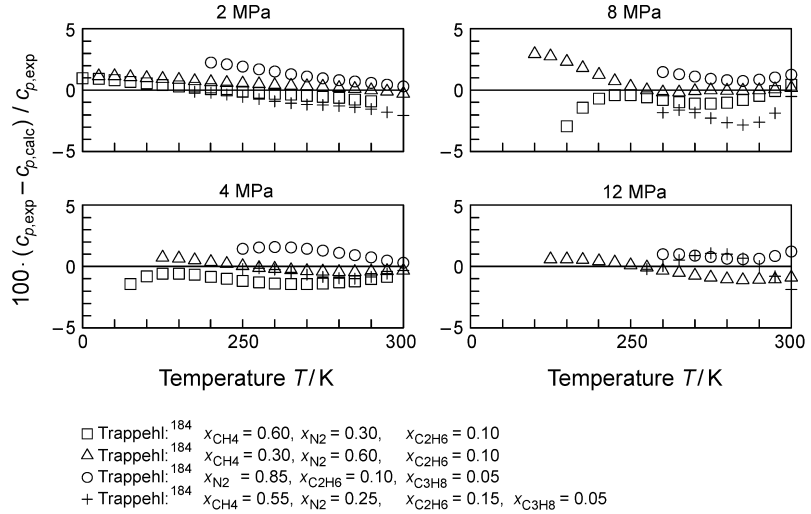

Figure 23. Percentage deviations of the experimental isobaric heat-capacity data measured by Trappehl[184] for two ternary mixtures and a quaternary mixture composed of methane, nitrogen, ethane, and propane from values calculated with GERG-2008, eq 8.

GERG-2008 values slightly exceed 0.5 % in enthalpy differences, but stay clearly within the targeted uncertainty of $\Delta(\Delta h)/\Delta h = 1$ %.

Significant weaknesses in the description of the selected isobaric enthalpy differences can be observed for the AGA8-DC92 equation, which deviates from the data at the lower temperatures from (243 to 257) K by (slightly) more than 1.5 %. Compared to GERG-2008, the AGA8-DC92 equation is even less accurate in the temperature range from (265 to 285) K. Similar accurate results are only obtained at higher temperatures. The comparisons demonstrate that GERG-2008 yields substantial improvements in the description of isobaric enthalpy differences over the temperature and pressure ranges of most interest for pipeline applications. Deviations of up to about 4 % in the medium temperature range and of more than 5 % in enthalpy differences at lower temperatures are obtained from the cubic equation of state of Peng and Robinson[3] (not shown here).

5.2.2.3. Isobaric Heat Capacity. Measurements for isobaric heat capacities of natural gases and other multi-component mixtures are scarce. However, comparisons with the few available multi-component data show that the GERG-2008 equation of state achieves a very similar accuracy in the description of isobaric heat capacities as obtained for binary mixtures (see also Kunz et al.[1]).

Figure 23 shows percentage deviations of isobaric heat capacities for three different ternary mixtures and a quaternary mixture consisting of methane, nitrogen, ethane, and propane from GERG-2008, eq 8. The data were measured by Trappehl[184] and cover the gas phase and gas-like supercritical region at temperatures from (200 to 300) K along isobars of (2, 4, 8, and 12) MPa (some of the data for the lowest measured temperatures are located near the phase boundary of the respective mixture). As claimed by the author, the uncertainty in isobaric heat capacity of the measurements is 2.5 %, which seems to be a quite realistic estimation. Most of the measurements are represented by GERG-2008 to within deviations of (1 to 2) %, which is well within the experimental uncertainty. Slightly higher systematic deviations of up to 3 % occur for only a few measurements. The achieved description is supported by the mixture model of

dx.doi.org/10.1021/je300655b | J. Chem. Eng. Data 2012, 57, 3032−3091

Lemmon and Jacobsen,[21] which yields similarly accurate results (not shown here).

5.2.3. Saturated Liquid Densities of LNG-like Mixtures. Experimental data for liquid-phase densities of multi-component natural gas mixtures are scarce. Very accurate data, however, exist for saturated-liquid densities of a variety of simulated commercial LNG mixtures consisting of up to eight components. The data cover the temperature range from (100 to 140) K, which corresponds to reduced temperatures T/T_r ranging from about 0.4 to 0.6. The measurements were performed by Haynes et al.[185] as part of an extensive experimental program carried out at the National Bureau of Standards (NBS) [today the National Institute of Standards and Technology (NIST)] in Boulder, Colorado, USA. The uncertainty of the data is claimed by the authors to be $\Delta\rho'/\rho' = 0.1$ %. Since the pressure dependence of the $p\rho T$ relation in the liquid phase is small for reduced temperatures such as these, the accurately measured saturated-liquid densities provide a suitable basis for the approximate evaluation of the quality of the GERG-2008 equation of state in the description of homogeneous liquid-phase densities of LNG-like mixtures. Table 10 summarizes the data sets that are discussed in the following (see Figure 24) and lists the compositions of the corresponding mixtures.

Table 10. Molar Compositions of Selected Multi-Component LNG-like Mixtures

		composition (100·mole fraction)							
	author	CH_4	N_2	C_2H_6	C_3H_8	*n*-C_4	*i*-C_4	*n*-C_5	*i*-C_5
	Five- to six-component mixtures								
◫	Haynes[34]	90.613	0.601	6.026	2.154	0.306	0.300	–	–
⊕	Haynes[34]	88.225	0.973	7.259	2.561	0.492	0.490	–	–
○	Haynes[34]	85.934	1.383	8.477	2.980	0.707	0.519	–	–
⋈	Haynes[34]	85.892	–	11.532	1.341	0.705	0.530	–	–
Y	Hiza and Haynes[33]	85.442	–	5.042	4.038	2.901	2.577	–	–
✳	Haynes[34]	84.558	–	8.153	4.778	1.252	1.259	–	–
Z	Hiza and Haynes[33]	81.300	4.250	4.750	4.870	2.420	2.410	–	–
	Seven- to eight-component mixtures								
□	Haynes[34]	90.068	0.599	6.537	2.200	0.284	0.291	0.011	0.010
◇	Haynes[34]	85.341	–	7.898	4.729	0.992	0.854	0.089	0.097
+	Haynes[34]	75.713	0.859	13.585	6.742	1.326	1.336	0.216	0.223
○	Haynes[34]	75.442	–	15.401	6.950	1.057	0.978	0.083	0.089
×	Haynes[34]	74.275	0.801	16.505	6.547	0.893	0.843	0.067	0.069

The left part of Figure 24 exemplifies the high quality of the GERG-2008 equation of state, eq 8, in the description of saturated-liquid densities for multi-component LNG-like mixtures. Displayed are percentage deviations between selected experimental data for five different mixtures measured by Haynes[34] and values calculated from GERG-2008 and the cubic equation of state of Peng and Robinson.[3] The seven- to eight-component mixtures are composed of methane, nitrogen, ethane, propane, *n*-butane, isobutane, *n*-pentane, and isopentane. The mixture compositions are representative for commercial LNG mixtures. The GERG-2008 equation of state describes all measurements well within deviations of (0.1 to 0.4) %. Most of the measurements are represented to within (0.1 to 0.3) %. Slightly higher systematic deviations of up to about 0.4 % are only obtained for the data of the mixture containing comparatively large amounts of *n*-butane and isobutane (mole fractions of about 0.013 each) and *n*-pentane and isopentane (about 0.002 each). The cubic equation of state of Peng and Robinson[3] is not able to represent the data to within acceptable deviations and deviates from the measurements for the five selected mixtures by approximately 10 %. On average, the deviations between the densities from GERG-2008 and the experimental values are about 50 times smaller than when calculating these densities from ordinary cubic equations of state, which are still widely applied in the natural gas industry. GERG-2008 thus enables a substantial improvement in the description of natural gases in the liquid phase. The comparisons with the data for binary mixtures of LNG components measured by Hiza et al.[32] showed similar results (see Figure 10 and also Kunz et al.[1]).

The right-hand side of Figure 24 shows deviations of selected experimental saturated-liquid densities of Hiza and Haynes[33] and Haynes[34] for LNG-like mixtures consisting of five to six components from GERG-2008 and the mixture model of Lemmon and Jacobsen.[21] The GERG-2008 equation of state represents almost all of the measurements to within deviations of (0.1 to 0.3) % (maximum deviations are clearly below 0.4 %). Larger systematic deviations, partially exceeding (0.4 to 0.5) %, are observed for the mixture model of Lemmon and Jacobsen. The cubic equation of Peng and Robinson[3] again deviates from the measurements for the seven selected mixtures by approximately 10 %.

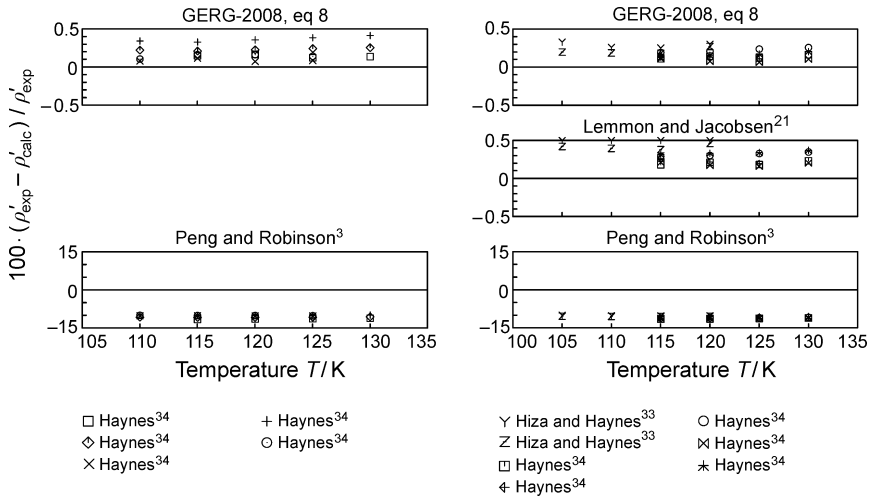

Figure 24. Percentage deviations of experimental saturated-liquid densities for different LNG-like mixtures consisting of seven to eight components (on the left) and five to six components (on the right) from values calculated with GERG-2008, eq 8, the mixture model of Lemmon and Jacobsen,[21] and the cubic equation of state of Peng and Robinson;[3] for the mixture compositions see Table 10.

dx.doi.org/10.1021/je300655b | J. Chem. Eng. Data 2012, 57, 3032−3091

Table 11. Comparisons between the VLE Measurements of VonNiederhausern and Giles[38] on Two Multi-Component Hydrocarbon Mixtures and Values Calculated from GERG-2008, eq 8

component	experimental overall and phase compositions (mole fraction)			calculated phase compositions and total differences (mole fraction)[a]			
i	x_i	$x'_{i,\mathrm{exp}}$	$x''_{i,\mathrm{exp}}$	$x'_{i,\mathrm{calc}}$	$x''_{i,\mathrm{calc}}$	$\Delta x'_i$	$\Delta x''_i$
Four-Component Mixture at 322.04 K and 1.713 MPa							
ethane	0.02	0.0197	0.0467	0.0193	0.0458	0.0004	0.0009
propane	0.96	0.9567	0.9423	0.9604	0.9448	−0.0037	−0.0025
n-butane	0.01	0.0112	0.00461	0.0102	0.00424	0.0010	0.00037
isobutane	0.01	0.0124	0.00639	0.0101	0.00511	0.0023	0.00128
Five-Component Mixture at 366.48 K and 1.039 MPa							
propane	0.01	0.0089	0.0229	0.0089	0.0240	0.0000	−0.0011
n-butane	0.50	0.5008	0.6032	0.4927	0.5921	0.0081	0.0111
isobutane	0.15	0.1436	0.2169	0.1444	0.2206	−0.0008	−0.0037
n-pentane	0.20	0.2061	0.1159	0.2063	0.1200	−0.0002	−0.0041
n-hexane	0.14	0.1406	0.0411	0.1477	0.0433	−0.0071	−0.0022

[a]The total mole fraction differences are calculated as $\Delta x'_i = x'_{i,\mathrm{exp}} - x'_{i,\mathrm{calc}}$ and $\Delta x''_i = x''_{i,\mathrm{exp}} - x''_{i,\mathrm{calc}}$.

The new multi-fluid mixture model, GERG-2008, allows for the accurate calculation of saturated-liquid densities of LNG mixtures, which is underlined by the comparisons given here. Unfortunately, (virtually) no accurate experimental data are available for compressed-liquid densities of natural gases, but such density measurements are planned at the Chair of Thermodynamics of the Ruhr-University Bochum using a specially designed single-sinker densimeter.[196,197] Due to the small pressure dependence in liquid-phase densities and the very accurate description of compressed-liquid densities for binary mixtures, exemplified in Figure 3, a comparable accuracy as achieved for saturated-liquid densities can be assumed for compressed-liquid densities of natural gases calculated from GERG-2008.

5.2.4. The pTxy Relation and Dew Points of Natural Gases. The accurate description of the *pTxy* relation is of indispensable importance for the design of any separation process. Measurements of the *pTxy* relation of natural gases and other multi-component mixtures are rather scarce. Various but generally not wide-ranging measurements are available for the *pTxy* relation of ternary mixtures of natural gas components and also of air; a comparison of some of these data with the GERG-2004 equation of state is given by Kunz et al.[1]

Virtually no accurate experimental information is available for bubble-point pressures of natural gases. Compared to the very accurate saturated-liquid densities of Hiza and Haynes[33] and Haynes[34] discussed in the previous section, their reported pressure measurements are much less accurate and can only be considered as approximate bubble-point pressures (see also Section 3). The data show quite large systematic deviations from different equations of state as demonstrated by the investigations of Klimeck.[22]

A number of accurate VLE measurements for mixtures of hydrocarbons from ethane through *n*-hexane, which are encountered in the design of depropanizers (depropanization is a continuous distillation process to remove propane from the gas mixture), were reported by VonNiederhausern and Giles.[38] The measurements were performed on the binary mixtures propane−*n*-butane and propane−isobutane (see also Kunz et al.[1]) and three multi-component mixtures (a ternary mixture of propane, *n*-butane, and isobutane, a four-component mixture of ethane, propane, *n*-butane, and isobutane, and a five-component mixture of propane, *n*-butane, isobutane, *n*-pentane, and *n*-hexane). For each multi-component system, the authors measured only one data point at a defined temperature and pressure. However, the data provide accurate and valuable information for testing the quality of the GERG-2008 equation of state, eq 8, in flash operations for multi-component hydrocarbon mixtures. Table 11 lists the results of the *pTxy* measurements of VonNiederhausern and Giles[38] on the four- and five-component mixtures and the values calculated from GERG-2008. The results show that deviations between the experimentally determined and the calculated molar phase compositions are very small (in general clearly less than 0.01 mole fraction).

A number of comparatively accurate dew-point data for synthetic natural gases and similar mixtures were measured by several authors (e.g., Avila et al.,[186−189] Jarne et al.,[190,191] and Mørch et al.[192]) and are accurately represented by GERG-2008, as exemplified in Figures 25 and 26. The compositions of the three selected mixtures are given in Table 12.

Multi-fluid mixture models do not only enable the accurate calculation of the thermal and caloric properties of multi-component mixtures in the homogeneous gas, liquid, and supercritical regions, but they also accurately describe the phase behavior of the mixtures. Figure 25 shows *pT* plots of the phase boundaries of a four-component hydrocarbon mixture and a 12-component synthetic natural gas. Aside from the phase envelopes calculated from GERG-2008 and the cubic equation of state of Peng and Robinson,[3] the plots include the experimental dew-point data of Mørch et al.[192] and Avila et al.[186] (see Figure 25). Jarne et al.[190] measured dew points for two synthetic natural gases and their mixtures with water. Selected results of these measurements and phase boundaries calculated from GERG-2008 are shown in Figure 26 for 0.00154 mole fraction of water in addition to the dry mixture, which consists of 10 components. The comparisons demonstrate that the new mixture model, GERG-2008, is able to accurately predict the dew-point conditions of very different types of natural gases, even for mixtures containing certain amounts of water or, for example, about 0.26 mole fraction of carbon dioxide[190] (not shown here).

Since the phase behavior of multi-component mixtures is considerably sensitive to errors in the mixture composition, especially when heavier hydrocarbons (e.g., *n*-octane and *n*-decane) are involved, one has to be very careful in assessing the data and their representation by mixture models. Even small amounts of secondary or minor components frequently result in a significantly different phase behavior. Compared to other equations of state (e.g., cubic equations of state), the

dx.doi.org/10.1021/je300655b | J. Chem. Eng. Data 2012, 57, 3032−3091

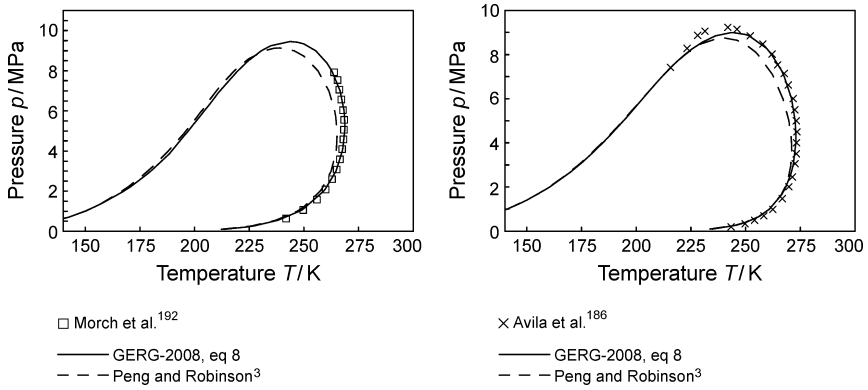

Figure 25. Vapor−liquid phase boundary of a four-component hydrocarbon mixture (on the left) and a 12-component synthetic natural gas (on the right) calculated with GERG-2008, eq 8, and the cubic equation of state of Peng and Robinson[3] in comparison with experimental dew-point data. The mixture compositions are given in Table 12.

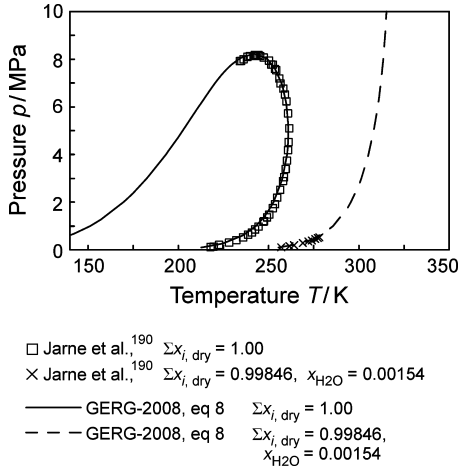

Figure 26. Vapor−liquid phase boundaries of a 10-component synthetic natural gas and its mixture with water as calculated with GERG-2008, eq 8, in comparison with experimental dew-point data. The mixture composition of the dry gas is given in Table 12.

Table 12. Molar Compositions of Selected Synthetic Natural Gas Mixtures

component	mixture composition (mole fraction) Mørch et al.[192]	Avila et al.[186]	Jarne et al.[190]
methane	0.96611	0.833482	0.84446
nitrogen		0.056510	0.00772
carbon dioxide		0.002840	0.01700
ethane		0.075260	0.08683
propane		0.020090	0.03297
n-butane	0.01475	0.005200	0.00589
isobutane	0.01527	0.003050	0.00293
n-pentane	0.00385	0.001440	0.00086
isopentane		0.001200	0.00084
n-hexane		0.000680	0.00050
n-heptane		0.000138	
n-octane		0.000110	

representation of multi-component dew-point data by GERG-2008 yields, on average, similar or better results, which is shown by comprehensive investigations. Figures 25 shows that the cubic equation of state of Peng and Robinson[3] with binary interaction parameters taken from Knapp et al.[152] significantly deviates from the experimental data, especially at elevated pressures. In this context, it should be noted that GERG-2008 was not fitted to any multi-component mixture data. It is also interesting to note that none of the equations used by the authors for comparisons are able to reproduce the measurements considerably better than GERG-2008, even if they are fitted to the data (see, for example, Mørch et al.[192]).

5.3. General Conclusions of the Comparisons for Binary and Multi-Component Mixtures. As underlined by the comparisons and discussions above, the new mixture model, the GERG-2008 equation of state, eq 8, achieves a very accurate description of the thermal and caloric properties of natural gases, similar gases, and other multi-component mixtures and also of their constituent binary mixtures over much wider ranges of temperature, pressure, and composition than any of the previously developed equations of state.

The statements on the ranges of validity as well as the conservative uncertainty estimations for the different thermodynamic properties, given in Section 4.3, are based on detailed graphical comparisons with all available experimental data (see Section 3). The following passages briefly summarize the main conclusions that follow from these comparisons.

5.3.1. Binary Mixtures. The GERG-2008 equation of state, eq 8, achieves substantial improvements in the description of gas-phase densities and sound speeds (including gas-like supercritical states) of binary mixtures consisting of methane and further important natural gas constituents. Very accurate experimental gas-phase densities and sound speeds are represented by GERG-2008 to within their low experimental uncertainty of (0.05 to 0.1) %. The GERG-2008 equation of state achieves a very accurate description of these properties over a much wider range of temperatures, pressures, and compositions than any of the previously developed equations, including the AGA8-DC92 equation of state of Starling and Savidge[6] and the multi-fluid mixture model of Lemmon and Jacobsen.[21] Accurate experimental gas-phase enthalpy differences are represented by GERG-2008 to within deviations of (0.2 to 0.5) %, which is in agreement with the experimental uncertainty of the measurements.

The GERG-2008 equation of state accurately represents the properties in the liquid phase and liquid-like supercritical region. Typical deviations between experimental compressed-liquid densities and values calculated from GERG-2008 are within (0.1 to 0.2) % (e.g., methane−nitrogen, methane−ethane, ethane−propane, and binary mixtures of propane, *n*-butane, and isobutane), (0.1 to 0.3) % (e.g., *n*-pentane−*n*-hexane, *n*-hexane−*n*-heptane),

dx.doi.org/10.1021/je300655b | J. Chem. Eng. Data 2012, 57, 3032−3091

or (0.1 to 0.5) % (e.g., *n*-pentane−*n*-heptane). In general, the deviations obtained from GERG-2008 are smaller than those from the model of Lemmon and Jacobsen.[21] Isobaric and isochoric heat capacities are well-represented by GERG-2008 to within (1 to 2) % in the homogeneous gas, liquid, and supercritical regions.

The vapor−liquid phase equilibrium is accurately described as well. It is interesting to see that the deviations observed for saturated-liquid densities are very consistent to those obtained for compressed-liquid densities. The achieved description for the *pTxy* relation is in agreement with the experimental uncertainty of the measurements (which are often of relatively poor quality). Accurate bubble- and dew-point pressure data for binary mixtures consisting of the main natural gas components or light hydrocarbons are represented to within (1 to 2) %. However, frequently a scatter in the measurements of (1 to 3) % or more can be observed. Typical deviations between the simultaneously measured vapor-phase compositions and values calculated from GERG-2008 are within (0.005 to 0.02) mole fraction, which agree with the accuracy of the measurements.

Aside from the accurate representation of the properties of binary mixtures of the main natural gas components and binary hydrocarbon mixtures, GERG-2008 accurately describes the thermodynamic properties of many binary mixtures containing the secondary natural gas components hydrogen, oxygen, carbon monoxide, water, hydrogen sulfide, helium, and argon.

5.3.2. Multi-Component Mixtures. The new equation of state, GERG-2008, eq 8, fulfills the high demands on the accuracy in the description of thermal and caloric properties of natural gases and similar mixtures in the custody transfer region. Important improvements compared to the AGA8-DC92 equation of state[6] are particularly achieved for temperatures below 290 K and also for mixtures of unusual composition. Thus, the known weaknesses of the current internationally accepted standard for this region are eliminated by the GERG-2008 equation of state.

In contrast to AGA8-DC92, GERG-2008 is valid (and yields very accurate results) over the entire fluid region (i.e., in the homogeneous gas, liquid, and supercritical regions and for vapor−liquid equilibrium states). Additionally, GERG-2008 is able to represent the most accurate experimental data for gas-phase and gas-like supercritical densities, sound speeds, and enthalpy differences to within their low experimental uncertainty, which is not true for AGA8-DC92. Accurate experimental gas-phase densities for a broad variety of natural gases and similar mixtures are represented by GERG-2008 to within (0.05 to 0.1) % for temperatures down to 250 K and at pressures up to 30 MPa. The same accuracy is achieved for gas-phase sound speeds over the temperature range from (250 to 350) K at pressures up to 11 MPa. Accurate experimental enthalpy differences covering almost the same temperature range at pressures up to 17 MPa are mostly represented by GERG-2008 to within (0.2 to 0.5) %. Accurate experimental gas-phase densities for rich natural gases are generally described with deviations of less than (0.1 to 0.3) % over a wide temperature range and at pressures up to 30 MPa. In addition, isobaric heat capacities of natural gases and other multi-component mixtures are well represented to within (1 to 2) %, which is in agreement with the experimental uncertainty of the available data.

In summary, it can be stated that, compared to AGA8-DC92,[6] the GERG-2008 equation of state, eq 8, achieves important and fundamental improvements in the description of gas-phase and gas-like supercritical densities of natural gas mixtures containing

- high fractions of nitrogen,
- high fractions of carbon dioxide,
- high fractions of ethane,
- substantial amounts of ethane, propane, and heavier hydrocarbons,
- high fractions of hydrogen,
- considerable amounts of carbon monoxide, or
- noticeable fractions of oxygen.

The GERG-2008 equation of state is much more accurate for rich natural gases and in the description of all caloric properties.

Moreover, GERG-2008 enables the accurate calculation of liquid-phase and vapor−liquid equilibrium properties. Compared to ordinary cubic equations of state, major improvements are achieved for saturated-liquid densities of LNG-like multi-component mixtures. The accurate experimental saturated-liquid densities are represented well by the GERG-2008 equation of state to within (0.1 to 0.5) %. These deviations are on average about 50 times less than when calculating these densities from ordinary cubic equations of state. Due to the small pressure dependence of the $p\rho T$ relation in the temperature range from (100 to 140) K, a similar accurate description can be expected for compressed-liquid densities of natural gas mixtures. This assumption is supported by the very accurate description achieved for compressed-liquid densities of important binary mixtures, such as methane−nitrogen and methane−ethane. Moreover, experimental liquid-phase densities for ternary mixtures consisting of the natural gas main constituents or only hydrocarbons are accurately described as well. For many cases, the deviations obtained from the new mixture model, GERG-2008, are smaller than those from the model of Lemmon and Jacobsen.[21]

For liquid-phase isobaric and isochoric heat capacities, a similarly accurate description as that for binary mixtures can also be expected for multi-component mixtures. Experimental liquid-phase isobaric enthalpy differences are represented to within (0.5 to 1) %.

For bubble- and dew-point pressures and vapor-phase compositions of multi-component mixtures, a similarly accurate description like that for binary mixtures is achieved by GERG-2008. Accurate bubble- and dew-point pressures are represented to within (1 to 3) %, and vapor-phase compositions are represented to within (0.01 to 0.02) mole fraction. The achieved description is supported by the results obtained from the cubic equation of state of Peng and Robinson.[3] Cubic equations generally achieve an accurate description of (only) the *pTxy* relation of mixtures. In general, GERG-2008 yields similar or even more accurate results as shown by the comparisons.

5.3.3. General Comments. Due to the basic structure of the new multi-fluid mixture model GERG-2008, eq 8, the representation of multi-component mixture data is based on the description of thermal and caloric properties of binary mixtures. Thus, the model only considers the binary interactions of the molecules in the multi-component mixture. This restriction, mostly resulting from the limited data sets, obviously does not affect the accuracy in the description of multi-component mixtures, implying that ternary and higher order interactions between molecules in the mixture are negligible for the components considered in the developed model (this is confirmed by comparisons with ternary and quaternary data). For an accurate description of the properties of multi-component mixtures, the development of accurate equations for the constituent binaries is necessary and sufficient.

In general, the quality and the extent of the available experimental data limit the achievable accuracy of any empirical equation of state. Many of the improvements achieved in this work are due to the use of recently measured accurate experimental data. However, the structure of the mixture model is also of considerable importance for the accurate description of binary and multi-component mixtures. Aside from the use of suitable (flexible and efficient) reducing functions for density and temperature, the development of binary specific departure functions is indispensable to represent the most accurate binary data to within their low experimental uncertainty. Generalized departure functions allow for an improved description of binary mixtures for which only limited or poor data are available. The combined strategy pursued in this work and the work of Kunz et al.[1] proved to be clearly superior to the one of Lemmon and Jacobsen,[21] who used a single generalized departure function for all considered binary mixtures. However, their work provided a foundation from which this work and the work of Kunz et al.[1] was able to build on, and a basis to which the new model, GERG-2008, could be compared to supersede it with increased accuracies and a more fundamental functional form.

The following statement should be a hint not to overestimate the high performance of the equation of state GERG-2008. Formally, GERG-2008 should cover (all) mixtures consisting of an arbitrary combination of the 21 considered components. Of course, there are a number of mixtures for which GERG-2008 does not yield a satisfactory property description. Reasons for this might be, for example, the lack of accurate measurements (at the time the equation of state was developed), mixture conditions that are far beyond the range of validity of GERG-2008 (e.g., mixtures with large amounts of helium or hydrogen at cryogenic temperatures), and mixtures that were not in the main focus of this work (e.g., carbon dioxide−water and other gaseous components dissolved in liquid water); see also the statement in the next to the last paragraph in Section 6.

6. OUTLOOK AND FUTURE CHALLENGES

The GERG-2008 equation of state for natural gases, similar gases, and other mixtures, eq 8, satisfies the high demands on the accuracy in the description of thermal and caloric properties as shown by the comparisons presented in Section 5. However, based on experiences gained during this work and the preceding study of Kunz et al.,[1] it is worthwhile to discuss the further expansion of the current mixture model. Some of the main ideas and recommendations will be summarized in the following passages.

6.1. Expansion to Further Components. One of the main recommendations concerns the expansion of the present multi-fluid mixture model to further components since its structure basically allows for an expansion to any arbitrary number of components without affecting the achieved high accuracy for mixtures consisting of the 21 already considered natural gas components.

For example, natural gases may contain small amounts of ethylene, propylene, benzene, and toluene. To inhibit the undesired formation of gas hydrates (hydrocarbon ice), which can lead to blockage of transport pipelines, alcohols such as methanol and monoethylene glycol are commonly used as an antifreeze added to the wellstream. With regard to flue-gas mixtures, the inclusion of sulfur dioxide as a further component might be of certain interest. Fortunately, accurate technical equations of state in the form of fundamental equations that fit well to the currently pursued structure of the mixture model are available for a number of these components and are listed in Table 13.

Table 13. Accurate Technical Equations of State Used for the Listed Further Components

pure substance	reference	range of validity: temperature T/K	range of validity: pressure p_{max}/MPa	no. terms
ethylene	Span and Wagner[23]	104 to 473	100	12
cyclohexane	Span and Wagner[23]	279 to 473	100	12
toluene	Lemmon and Span[24]	178 to 700	500	12
n-dodecane	Lemmon and Huber[193]	263 to 700	500	12
sulfur dioxide	Lemmon and Span[24]	197 to 523	35	12

Aside from the pure substance equations of state, binary data are required to (at least) fit the parameters of the reducing functions for density and temperature. However, for binary mixtures for which only limited or poor data are available, different combining rules for the critical parameters of the pure components can be used without any fitting (see Section 4.4.1).

6.2. Expansion of the Mixture Model to User-Definable (Pseudo-)Components. In addition to the number of considered distinct and well-defined mixture components, the implementation of one or more pseudocomponents that can be individually defined by the user seems to be worthwhile. Such a development is relevant for many applications in the chemical and petrochemical industry. Uncommon mixture constituents and heavy hydrocarbons, which have a great influence on the phase behavior of natural gases even when only present in very small amounts, can be handled in this way.

For this development, a generalized equation of state in the form of a fundamental equation with substance-specific (adjustable) parameters is required that can be used like a usual substance-specific equation of state. Such an equation was developed by Span[194] and can be expressed as follows:

$$\frac{a(\rho, T)}{RT} = \alpha^{o}(\rho, T) + \alpha^{r}(\delta, \tau) = \alpha^{o}(\rho, T) + \sum_{i=1}^{5} n_i \delta^{d_i} \tau^{t_i} + \sum_{i=6}^{10} n_i \delta^{d_i} \tau^{t_i} e^{-\delta^{p_i}} \quad (47)$$

with

$$n_i = c_{1,i} + c_{2,i}\omega + c_{3,i}\omega^4, \quad \delta = \rho/\rho_r, \quad \text{and} \quad \tau = T_r/T \quad (48)$$

In eq 48, ρ_r, T_r, and ω are substance-dependent adjustable parameters. The structure of the equation for α^r in eq 48 was determined by a simultaneous optimization method (see Span et al.[195]) considering data sets for 13 non- and weakly polar substances. The generalized coefficients $c_{j,i}$ in eq 47 were determined by a fit to data sets for methane, ethane, propane, *n*-butane, isobutane, *n*-pentane, *n*-hexane, *n*-heptane, *n*-octane, oxygen, and argon. The values for the exponents d_i, t_i, and p_i, and the coefficients $c_{j,i}$ are tabulated in ref 194. With these parameters, eq 47 becomes an empirical three-parameter equation of state for nonpolar fluids.

To specify a pseudocomponent, values for ρ_r (an approximate critical density), T_r (an approximate critical temperature), and ω (an approximate acentric factor) are required. Normally, these parameters can be fitted to experimental data to compensate for the limited accuracy of this kind of corresponding states

Table A1. Coefficients and Parameters of α^{o}_{oi}, eq 12, for the Considered 21 Components

k	$n^{o}_{oi,k}$	$\vartheta^{o}_{oi,k}$	k	$n^{o}_{oi,k}$	$\vartheta^{o}_{oi,k}$
		Methane			
1	19.597508817		5	0.00460	0.936220902
2	−83.959667892		6	8.74432	5.577233895
3	3.00088		7	−4.46921	5.722644361
4	0.76315	4.306474465			
		Nitrogen			
1	11.083407489		5	−0.14660	−5.393067706
2	−22.202102428		6	0.90066	13.788988208
3	2.50031		7		
4	0.13732	5.251822620			
		Carbon Dioxide			
1	11.925152758		5	−1.06044	−2.844425476
2	−16.118762264		6	2.03366	1.589964364
3	2.50002		7	0.01393	1.121596090
4	2.04452	3.022758166			
		Ethane			
1	24.675437527		5	1.23722	0.731306621
2	−77.425313760		6	13.19740	3.378007481
3	3.00263		7	−6.01989	3.508721939
4	4.33939	1.831882406			
		Propane			
1	31.602908195		5	3.19700	0.543210978
2	−84.463284382		6	19.19210	2.583146083
3	3.02939		7	−8.37267	2.777773271
4	6.60569	1.297521801			
		n-Butane			
1	20.884143364		5	6.89406	0.431957660
2	−91.638478026		6	24.46180	4.502440459
3	3.33944		7	14.78240	2.124516319
4	9.44893	1.101487798			
		Isobutane			
1	20.413726078		5	5.25156	0.485556021
2	−94.467620036		6	25.14230	4.671261865
3	3.06714		7	16.13880	2.191583480
4	8.97575	1.074673199			
		n-Pentane			
1	14.536611217		5	21.83600	1.789520971
2	−89.919548319		6	33.40320	3.777411113
3	3.00000		7		
4	8.95043	0.380391739			
		Isopentane			
1	15.449907693		5	20.11010	1.977271641
2	−101.298172792		6	33.16880	4.169371131
3	3.00000		7		
4	11.76180	0.635392636			
		n-Hexane			
1	14.345969349		5	26.81420	1.691951873
2	−96.165722367		6	38.61640	3.596924107
3	3.00000		7		
4	11.69770	0.359036667			
		n-Heptane			
1	15.063786601		5	30.47070	1.548136560
2	−97.345252349		6	43.55610	3.259326458
3	3.00000		7		
4	13.72660	0.314348398			
		n-Octane			
1	15.864687161		5	33.80290	1.431644769
2	−97.370667555		6	48.17310	2.973845992
3	3.00000		7		
4	15.68650	0.279143540			
		n-Nonane			
1	16.313913248		5	38.12350	1.370586158
2	−102.160247463		6	53.34150	2.848860483
3	3.00000		7		
4	18.02410	0.263819696			

dx.doi.org/10.1021/je300655b | *J. Chem. Eng. Data* 2012, 57, 3032−3091

Table A1. continued

k	$n^{o}_{oi,k}$	$\vartheta^{o}_{oi,k}$	k	$n^{o}_{oi,k}$	$\vartheta^{o}_{oi,k}$
		n-Decane			
1	15.870791919		5	43.49310	1.353835195
2	−108.858547525		6	58.36570	2.833479035
3	3.00000		7		
4	21.00690	0.267034159			
		Hydrogen			
1	13.796443393		5	0.45444	9.847634830
2	−175.864487294		6	1.56039	49.765290750
3	1.47906		7	−1.37560	50.367279301
4	0.95806	6.891654113			
		Oxygen			
1	10.001843586		5	1.01334	7.223325463
2	−14.996095135		6		
3	2.50146		7		
4	1.07558	14.461722565			
		Carbon Monoxide			
1	10.813340744		5	0.00493	5.302762306
2	−19.834733959		6		
3	2.50055		7		
4	1.02865	11.669802800			
		Water			
1	8.203520690		5	0.98763	1.763895929
2	−11.996306443		6	3.06904	3.874803739
3	3.00392		7		
4	0.01059	0.415386589			
		Hydrogen Sulfide			
1	9.336197742		5	1.00243	2.270653980
2	−16.266508995		6		
3	3.00000		7		
4	3.11942	4.914580541			
		Helium			
1	13.628409737		5		
2	−143.470759602		6		
3	1.50000		7		
4					
		Argon			
1	8.316631500		5		
2	−4.946502600		6		
3	1.50000		7		
4					

Table A2. Coefficients and Exponents of α^{r}_{oi}, eq 14, for Propane, *n*-Butane, Isobutane, *n*-Pentane, Isopentane, *n*-Hexane, *n*-Heptane, *n*-Octane, *n*-Nonane, *n*-Decane, Oxygen, Carbon Monoxide, Hydrogen Sulfide, and Argon[a]

k	$n_{oi,k}$		
	Propane	*n*-Butane	Isobutane
1	$0.10403973107358\cdot10^{1}$	$0.10626277411455\cdot10^{1}$	$0.10429331589100\cdot10^{1}$
2	$-0.28318404081403\cdot10^{1}$	$-0.28620951828350\cdot10^{1}$	$-0.28184272548892\cdot10^{1}$
3	0.84393809606294	0.88738233403777	0.86176232397850
4	$-0.76559591850023\cdot10^{-1}$	−0.12570581155345	−0.10613619452487
5	$0.94697373057280\cdot10^{-1}$	0.10286308708106	$0.98615749302134\cdot10^{-1}$
6	$0.24796475497006\cdot10^{-3}$	$0.25358040602654\cdot10^{-3}$	$0.23948208682322\cdot10^{-3}$
7	0.27743760422870	0.32325200233982	0.30330004856950
8	$-0.43846000648377\cdot10^{-1}$	$-0.37950761057432\cdot10^{-1}$	$-0.41598156135099\cdot10^{-1}$
9	−0.26991064784350	−0.32534802014452	−0.29991937470058
10	$-0.69313413089860\cdot10^{-1}$	$-0.79050969051011\cdot10^{-1}$	$-0.80369342764109\cdot10^{-1}$
11	$-0.29632145981653\cdot10^{-1}$	$-0.20636720547775\cdot10^{-1}$	$-0.29761373251151\cdot10^{-1}$
12	$0.14040126751380\cdot10^{-1}$	$0.57053809334750\cdot10^{-2}$	$0.13059630303140\cdot10^{-1}$
	n-Pentane	Isopentane	*n*-Hexane
1	$0.10968643098001\cdot10^{1}$	$0.10963\cdot10^{1}$	$0.10553238013661\cdot10^{1}$
2	$-0.29988888298061\cdot10^{1}$	$-0.30402\cdot10^{1}$	$-0.26120615890629\cdot10^{1}$
3	0.99516886799212	$0.10317\cdot10^{1}$	0.76613882967260
4	−0.16170708558539	−0.15410	−0.29770320622459

dx.doi.org/10.1021/je300655b | J. Chem. Eng. Data 2012, 57, 3032−3091

Table A2. continued

k	$n_{oi,k}$		
	n-Pentane	Isopentane	*n*-Hexane
5	0.11334460072775	0.11535	0.11879907733358
6	$0.26760595150748 \cdot 10^{-3}$	$0.29809 \cdot 10^{-3}$	$0.27922861062617 \cdot 10^{-3}$
7	0.40979881986931	0.39571	0.46347589844105
8	$-0.40876423083075 \cdot 10^{-1}$	$-0.45881 \cdot 10^{-1}$	$0.11433196980297 \cdot 10^{-1}$
9	−0.38169482469447	−0.35804	−0.48256968738131
10	−0.10931956843993	−0.10107	$-0.93750558924659 \cdot 10^{-1}$
11	$-0.32073223327990 \cdot 10^{-1}$	$-0.35484 \cdot 10^{-1}$	$-0.67273247155994 \cdot 10^{-2}$
12	$0.16877016216975 \cdot 10^{-1}$	$0.18156 \cdot 10^{-1}$	$-0.51141583585428 \cdot 10^{-2}$
	n-Heptane	*n*-Octane	*n*-Nonane
1	$0.10543747645262 \cdot 10^{1}$	$0.10722544875633 \cdot 10^{1}$	$0.11151 \cdot 10^{1}$
2	$-0.26500681506144 \cdot 10^{1}$	$-0.24632951172003 \cdot 10^{1}$	$-0.27020 \cdot 10^{1}$
3	0.81730047827543	0.65386674054928	0.83416
4	−0.30451391253428	−0.36324974085628	−0.38828
5	0.12253868710800	0.12713269626764	0.13760
6	$0.27266472743928 \cdot 10^{-3}$	$0.30713572777930 \cdot 10^{-3}$	$0.28185 \cdot 10^{-3}$
7	0.49865825681670	0.52656856987540	0.62037
8	$-0.71432815084176 \cdot 10^{-3}$	$0.19362862857653 \cdot 10^{-1}$	$0.15847 \cdot 10^{-1}$
9	−0.54236895525450	−0.58939426849155	−0.61726
10	−0.13801821610756	−0.14069963991934	−0.15043
11	$-0.61595287380011 \cdot 10^{-2}$	$-0.78966330500036 \cdot 10^{-2}$	$-0.12982 \cdot 10^{-1}$
12	$0.48602510393022 \cdot 10^{-3}$	$0.33036597968109 \cdot 10^{-2}$	$0.44325 \cdot 10^{-2}$
	n-Decane	Oxygen	Carbon Monoxide
1	$0.10461 \cdot 10^{1}$	0.88878286369701	0.90554
2	$-0.24807 \cdot 10^{1}$	$-0.24879433312148 \cdot 10^{1}$	$-0.24515 \cdot 10^{1}$
3	0.74372	0.59750190775886	0.53149
4	−0.52579	$0.96501817061881 \cdot 10^{-2}$	$0.24173 \cdot 10^{-1}$
5	0.15315	$0.71970428712770 \cdot 10^{-1}$	$0.72156 \cdot 10^{-1}$
6	$0.32865 \cdot 10^{-3}$	$0.22337443000195 \cdot 10^{-3}$	$0.18818 \cdot 10^{-3}$
7	0.84178	0.18558686391474	0.19405
8	$0.55424 \cdot 10^{-1}$	$-0.38129368035760 \cdot 10^{-1}$	$-0.43268 \cdot 10^{-1}$
9	−0.73555	−0.15352245383006	−0.12778
10	−0.18507	$-0.26726814910919 \cdot 10^{-1}$	$-0.27896 \cdot 10^{-1}$
11	$-0.20775 \cdot 10^{-1}$	$-0.25675298677127 \cdot 10^{-1}$	$-0.34154 \cdot 10^{-1}$
12	$0.12335 \cdot 10^{-1}$	$0.95714302123668 \cdot 10^{-2}$	$0.16329 \cdot 10^{-1}$
	Hydrogen Sulfide	Argon	
1	0.87641	0.85095714803969	
2	$-0.20367 \cdot 10^{1}$	$-0.24003222943480 \cdot 10^{1}$	
3	0.21634	0.54127841476466	
4	$-0.50199 \cdot 10^{-1}$	$0.16919770692538 \cdot 10^{-1}$	
5	$0.66994 \cdot 10^{-1}$	$0.68825965019035 \cdot 10^{-1}$	
6	$0.19076 \cdot 10^{-3}$	$0.21428032815338 \cdot 10^{-3}$	
7	0.20227	0.17429895321992	
8	$-0.45348 \cdot 10^{-2}$	$-0.33654495604194 \cdot 10^{-1}$	
9	−0.22230	−0.13526799857691	
10	$-0.34714 \cdot 10^{-1}$	$-0.16387350791552 \cdot 10^{-1}$	
11	$-0.14885 \cdot 10^{-1}$	$-0.24987666851475 \cdot 10^{-1}$	
12	$0.74154 \cdot 10^{-2}$	$0.88769204815709 \cdot 10^{-2}$	

k	$c_{oi,k}$	$d_{oi,k}$	$t_{oi,k}$
1		1	0.250
2		1	1.125
3		1	1.500
4		2	1.375
5		3	0.250
6		7	0.875
7	1	2	0.625
8	1	5	1.750
9	2	1	3.625
10	2	4	3.625
11	3	3	14.500
12	3	4	12.000

[a] $K_{Pol,i} = 6$, $K_{Exp,i} = 6$.

dx.doi.org/10.1021/je300655b | J. Chem. Eng. Data 2012, 57, 3032−3091

Table A3. Coefficients and Exponents of α^r_{oi}, eq 14, for Methane, Nitrogen, and Ethane[a]

k	$n_{oi,k}$		
	Methane	Nitrogen	Ethane
1	0.57335704239162	0.59889711801201	0.63596780450714
2	$-0.16760687523730\cdot10^{1}$	$-0.16941557480731\cdot10^{1}$	$-0.17377981785459\cdot10^{1}$
3	0.23405291834916	0.24579736191718	0.28914060926272
4	−0.21947376343441	−0.23722456755175	−0.33714276845694
5	$0.16369201404128\cdot10^{-1}$	$0.17954918715141\cdot10^{-1}$	$0.22405964699561\cdot10^{-1}$
6	$0.15004406389280\cdot10^{-1}$	$0.14592875720215\cdot10^{-1}$	$0.15715424886913\cdot10^{-1}$
7	$0.98990489492918\cdot10^{-1}$	0.10008065936206	0.11450634253745
8	0.58382770929055	0.73157115385532	$0.10612049379745\cdot10^{1}$
9	−0.74786867560390	−0.88372272336366	$-0.12855224439423\cdot10^{1}$
10	0.30033302857974	0.31887660246708	0.39414630777652
11	0.20985543806568	0.20766491728799	0.31390924682041
12	$-0.18590151133061\cdot10^{-1}$	$-0.19379315454158\cdot10^{-1}$	$-0.21592277117247\cdot10^{-1}$
13	−0.15782558339049	−0.16936641554983	−0.21723666564905
14	0.12716735220791	0.13546846041701	−0.28999574439489
15	$-0.32019743894346\cdot10^{-1}$	$-0.33066712095307\cdot10^{-1}$	0.42321173025732
16	$-0.68049729364536\cdot10^{-1}$	$-0.60690817018557\cdot10^{-1}$	$0.46434100259260\cdot10^{-1}$
17	$0.24291412853736\cdot10^{-1}$	$0.12797548292871\cdot10^{-1}$	−0.13138398329741
18	$0.51440451639444\cdot10^{-2}$	$0.58743664107299\cdot10^{-2}$	$0.11492850364368\cdot10^{-1}$
19	$-0.19084949733532\cdot10^{-1}$	$-0.18451951971969\cdot10^{-1}$	$-0.33387688429909\cdot10^{-1}$
20	$0.55229677241291\cdot10^{-2}$	$0.47226622042472\cdot10^{-2}$	$0.15183171583644\cdot10^{-1}$
21	$-0.44197392976085\cdot10^{-2}$	$-0.52024079680599\cdot10^{-2}$	$-0.47610805647657\cdot10^{-2}$
22	$0.40061416708429\cdot10^{-1}$	$0.43563505956635\cdot10^{-1}$	$0.46917166277885\cdot10^{-1}$
23	$-0.33752085907575\cdot10^{-1}$	$-0.36251690750939\cdot10^{-1}$	$-0.39401755804649\cdot10^{-1}$
24	$-0.25127658213357\cdot10^{-2}$	$-0.28974026866543\cdot10^{-2}$	$-0.32569956247611\cdot10^{-2}$

k	$c_{oi,k}$	$d_{oi,k}$	$t_{oi,k}$	k	$c_{oi,k}$	$d_{oi,k}$	$t_{oi,k}$
1		1	0.125	13	2	2	4.500
2		1	1.125	14	2	3	4.750
3		2	0.375	15	2	3	5.000
4		2	1.125	16	2	4	4.000
5		4	0.625	17	2	4	4.500
6		4	1.500	18	3	2	7.500
7	1	1	0.625	19	3	3	14.000
8	1	1	2.625	20	3	4	11.500
9	1	1	2.750	21	6	5	26.000
10	1	2	2.125	22	6	6	28.000
11	1	3	2.000	23	6	6	30.000
12	1	6	1.750	24	6	7	16.000

[a] $K_{Pol,i} = 6$, $K_{Exp,i} = 18$.

approach. Due to its optimized functional form, eq 47 is numerically very stable. Therefore, a very small number of accurate experimental data is sufficient to adjust the substance-specific parameters and to obtain equations of state that yield satisfyingly accurate results for a variety of substances. If data are not available, the critical density ρ_c, the critical temperature T_c, and the acentric factor ω can be used for ρ_r, T_r, and ω. Whether the limited accuracy of this corresponding states approach (without fitting the parameters to experimental data) is sufficient to obtain at least reasonably accurate results for the properties of the desired substance, and for those of mixtures containing small amounts of such a component, remains to be investigated.

6.3. Development of Further Binary Departure Functions. The present mixture model uses equations of state in the form of fundamental equations for each considered mixture component along with binary correlation equations to take into account the residual mixture behavior. Most of the binary mixtures are represented using only adjusted reducing functions for density and temperature. Binary specific and generalized departure functions were additionally developed for binary mixtures consisting of important main and secondary natural gas components (see Section 4.4.3). This approach enabled a very accurate description of the properties of various types of natural gases, similar gases, and other mixtures over a wide range of mixture conditions (temperature, pressure, and composition) as underlined by the comparisons presented in Section 5. Potential further improvements were identified during the development of the GERG-2008 equation of state, also resulting from very recent measurements or other data that were not available at the time this equation of state was developed.

A very accurate description of the thermal and caloric properties of binary mixtures is achieved by the use of binary-specific departure functions. Such a development requires a sufficiently comprehensive and comparatively accurate data set. This precondition is, however, not fulfilled for most of the considered binary systems. Aside from new measurements for mixtures where accurate experimental data are currently not available, further improvements can possibly be achieved by the development of additional generalized departure functions. Based on the experiences gained during this work, it seems to

Table A4. Coefficients and Exponents of α^{r}_{oi}, eq 14, for Carbon Dioxide, Hydrogen, Water, and Helium

k	$c_{oi,k}$	$d_{oi,k}$	$t_{oi,k}$	$n_{oi,k}$
			Carbon Dioxide[a]	
1		1	0.000	0.52646564804653
2		1	1.250	$-0.14995725042592\cdot10^{1}$
3		2	1.625	0.27329786733782
4		3	0.375	0.12949500022786
5	1	3	0.375	0.15404088341841
6	1	3	1.375	−0.58186950946814
7	1	4	1.125	−0.18022494838296
8	1	5	1.375	$-0.95389904072812\cdot10^{-1}$
9	1	6	0.125	$-0.80486819317679\cdot10^{-2}$
10	1	6	1.625	$-0.35547751273090\cdot10^{-1}$
11	2	1	3.750	−0.28079014882405
12	2	4	3.500	$-0.82435890081677\cdot10^{-1}$
13	3	1	7.500	$0.10832427979006\cdot10^{-1}$
14	3	1	8.000	$-0.67073993161097\cdot10^{-2}$
15	3	3	6.000	$-0.46827907600524\cdot10^{-2}$
16	3	3	16.000	$-0.28359911832177\cdot10^{-1}$
17	3	4	11.000	$0.19500174744098\cdot10^{-1}$
18	5	5	24.000	−0.21609137507166
19	5	5	26.000	0.43772794926972
20	5	5	28.000	−0.22130790113593
21	6	5	24.000	$0.15190189957331\cdot10^{-1}$
22	6	5	26.000	$-0.15380948953300\cdot10^{-1}$
			Hydrogen[b]	
1		1	0.500	$0.53579928451252\cdot10^{1}$
2		1	0.625	$-0.62050252530595\cdot10^{1}$
3		2	0.375	0.13830241327086
4		2	0.625	$-0.71397954896129\cdot10^{-1}$
5		4	1.125	$0.15474053959733\cdot10^{-1}$
6	1	1	2.625	−0.14976806405771
7	1	5	0.000	$-0.26368723988451\cdot10^{-1}$
8	1	5	0.250	$0.56681303156066\cdot10^{-1}$
9	1	5	1.375	$-0.60063958030436\cdot10^{-1}$
10	2	1	4.000	−0.45043942027132
11	2	1	4.250	0.42478840244500
12	3	2	5.000	$-0.21997640827139\cdot10^{-1}$
13	3	5	8.000	$-0.10499521374530\cdot10^{-1}$
14	5	1	8.000	$-0.28955902866816\cdot10^{-2}$
			Water[c]	
1		1	0.500	0.82728408749586
2		1	1.250	$-0.18602220416584\cdot10^{1}$
3		1	1.875	$-0.11199009613744\cdot10^{1}$
4		2	0.125	0.15635753976056
5		2	1.500	0.87375844859025
6		3	1.000	−0.36674403715731
7		4	0.750	$0.53987893432436\cdot10^{-1}$
8	1	1	1.500	$0.10957690214499\cdot10^{1}$
9	1	5	0.625	$0.53213037828563\cdot10^{-1}$
10	1	5	2.625	$0.13050533930825\cdot10^{-1}$
11	2	1	5.000	−0.41079520434476
12	2	2	4.000	0.14637443344120
13	2	4	4.500	$-0.55726838623719\cdot10^{-1}$
14	3	4	3.000	$-0.11201774143800\cdot10^{-1}$
15	5	1	4.000	$-0.66062758068099\cdot10^{-2}$
16	5	1	6.000	$0.46918522004538\cdot10^{-2}$
			Helium[d]	
1		1	0.000	−0.45579024006737
2		1	0.125	$0.12516390754925\cdot10^{1}$
3		1	0.750	$-0.15438231650621\cdot10^{1}$
4		4	1.000	$0.20467489707221\cdot10^{-1}$
5	1	1	0.750	−0.34476212380781
6	1	3	2.625	$-0.20858459512787\cdot10^{-1}$
7	1	5	0.125	$0.16227414711778\cdot10^{-1}$
8	1	5	1.250	$-0.57471818200892\cdot10^{-1}$
9	1	5	2.000	$0.19462416430715\cdot10^{-1}$
10	2	2	1.000	$-0.33295680123020\cdot10^{-1}$
11	3	1	4.500	$-0.10863577372367\cdot10^{-1}$
12	3	2	5.000	$-0.22173365245954\cdot10^{-1}$

[a] $K_{Pol,i}$ = 4, $K_{Exp,i}$ = 18. [b] $K_{Pol,i}$ = 5, $K_{Exp,i}$ = 9. [c] $K_{Pol,i}$ = 7, $K_{Exp,i}$ = 9. [d] $K_{Pol,i}$ = 4, $K_{Exp,i}$ = 8.

Table A5. Critical Parameters and Molar Masses of the Considered 21 Components

component i	formula	$\rho_{c,i}/(\mathrm{mol\cdot dm^{-3}})$	$T_{c,i}/\mathrm{K}$	$M_i/(\mathrm{g\cdot mol^{-1}})$[a]
methane	CH_4	10.139342719	190.564	16.04246
nitrogen	N_2	11.1839	126.192	28.0134
carbon dioxide	CO_2	10.624978698	304.1282	44.0095
ethane	C_2H_6	6.870854540	305.322	30.06904
propane	C_3H_8	5.000043088	369.825	44.09562
n-butane	*n*-C_4H_{10}	3.920016792	425.125	58.1222
isobutane	*i*-C_4H_{10}	3.860142940	407.817	58.1222
n-pentane	*n*-C_5H_{12}	3.215577588	469.7	72.14878
isopentane	*i*-C_5H_{12}	3.271	460.35	72.14878
n-hexane	*n*-C_6H_{14}	2.705877875	507.82	86.17536
n-heptane	*n*-C_7H_{16}	2.315324434	540.13	100.20194
n-octane	*n*-C_8H_{18}	2.056404127	569.32	114.22852
n-nonane	*n*-C_9H_{20}	1.81	594.55	128.2551
n-decane	*n*-$C_{10}H_{22}$	1.64	617.7	142.28168
hydrogen	H_2	14.94	33.19	2.01588
oxygen	O_2	13.63	154.595	31.9988
carbon monoxide	CO	10.85	132.86	28.0101
water	H_2O	17.873716090	647.096	18.01528
hydrogen sulfide	H_2S	10.19	373.1	34.08088
helium	He	17.399	5.1953	4.002602
argon	Ar	13.407429659	150.687	39.948

[a] According to Wieser.[137]

Table A6. Non-Zero F_{ij} Parameters of α^{r}, eq 10, for the Binary Mixtures Taken into Account by Binary Specific and Generalized Departure Functions[a]

mixture i–j	F_{ij}
methane–nitrogen	1.0
methane–carbon dioxide	1.0
methane–ethane	1.0
methane–propane	1.0
methane–*n*-butane	1.0
methane–isobutane	0.771035405688
methane–hydrogen	1.0
nitrogen–carbon dioxide	1.0
nitrogen–ethane	1.0
ethane–propane	0.130424765150
ethane–*n*-butane	0.281570073085
ethane–isobutane	0.260632376098
propane–*n*-butane	$0.312572600489\cdot10^{-1}$
propane–isobutane	$-0.551609771024\cdot10^{-1}$
n-butane–isobutane	$-0.551240293009\cdot10^{-1}$

[a] The values of F_{ij} equal zero for all other binary combinations.

be worthwhile to develop different generalized departure functions for the following groups of (somehow) related binary mixtures:

dx.doi.org/10.1021/je300655b | J. Chem. Eng. Data 2012, 57, 3032−3091

Table A7. Coefficients and Exponents of α^{r}_{ij}, eq 15, for the Binary Mixtures Taken into Account by Binary Specific and Generalized Departure Functions

k	$d_{ij,k}$	$t_{ij,k}$	$n_{ij,k}$	$\eta_{ij,k}$	$\epsilon_{ij,k}$	$\beta_{ij,k}$	$\gamma_{ij,k}$
			Methane−Nitrogen[a]				
1	1	0.000	$-0.98038985517335\cdot10^{-2}$				
2	4	1.850	$0.42487270143005\cdot10^{-3}$				
3	1	7.850	$-0.34800214576142\cdot10^{-1}$	1.000	0.5	1.000	0.5
4	2	5.400	−0.13333813013896	1.000	0.5	1.000	0.5
5	2	0.000	$-0.11993694974627\cdot10^{-1}$	0.250	0.5	2.500	0.5
6	2	0.750	$0.69243379775168\cdot10^{-1}$	0.000	0.5	3.000	0.5
7	2	2.800	−0.31022508148249	0.000	0.5	3.000	0.5
8	2	4.450	0.24495491753226	0.000	0.5	3.000	0.5
9	3	4.250	0.22369816716981	0.000	0.5	3.000	0.5
			Methane−Carbon Dioxide[b]				
1	1	2.600	−0.10859387354942				
2	2	1.950	$0.80228576727389\cdot10^{-1}$				
3	3	0.000	$-0.93303985115717\cdot10^{-2}$				
4	1	3.950	$0.40989274005848\cdot10^{-1}$	1.000	0.5	1.000	0.5
5	2	7.950	−0.24338019772494	0.500	0.5	2.000	0.5
6	3	8.000	0.23855347281124	0.000	0.5	3.000	0.5
			Methane−Ethane[c]				
1	3	0.650	$-0.80926050298746\cdot10^{-3}$				
2	4	1.550	$-0.75381925080059\cdot10^{-3}$				
3	1	3.100	$-0.41618768891219\cdot10^{-1}$	1.000	0.5	1.000	0.5
4	2	5.900	−0.23452173681569	1.000	0.5	1.000	0.5
5	2	7.050	0.14003840584586	1.000	0.5	1.000	0.5
6	2	3.350	$0.63281744807738\cdot10^{-1}$	0.875	0.5	1.250	0.5
7	2	1.200	$-0.34660425848809\cdot10^{-1}$	0.750	0.5	1.500	0.5
8	2	5.800	−0.23918747334251	0.500	0.5	2.000	0.5
9	2	2.700	$0.19855255066891\cdot10^{-2}$	0.000	0.5	3.000	0.5
10	3	0.450	$0.61777746171555\cdot10^{1}$	0.000	0.5	3.000	0.5
11	3	0.550	$-0.69575358271105\cdot10^{1}$	0.000	0.5	3.000	0.5
12	3	1.950	$0.10630185306388\cdot10^{1}$	0.000	0.5	3.000	0.5
			Methane−Propane[d]				
1	3	1.850	$0.13746429958576\cdot10^{-1}$				
2	3	3.950	$-0.74425012129552\cdot10^{-2}$				
3	4	0.000	$-0.45516600213685\cdot10^{-2}$				
4	4	1.850	$-0.54546603350237\cdot10^{-2}$				
5	4	3.850	$0.23682016824471\cdot10^{-2}$				
6	1	5.250	0.18007763721438	0.250	0.5	0.750	0.5
7	1	3.850	−0.44773942932486	0.250	0.5	1.000	0.5
8	1	0.200	$0.19327374888200\cdot10^{-1}$	0.000	0.5	2.000	0.5
9	2	6.500	−0.30632197804624	0.000	0.5	3.000	0.5
			Nitrogen−Carbon Dioxide[e]				
1	2	1.850	0.28661625028399				
2	3	1.400	−0.10919833861247				
3	1	3.200	$-0.11374032082270\cdot10^{1}$	0.250	0.5	0.750	0.5
4	1	2.500	0.76580544237358	0.250	0.5	1.000	0.5
5	1	8.000	$0.42638000926819\cdot10^{-2}$	0.000	0.5	2.000	0.5
6	2	3.750	0.17673538204534	0.000	0.5	3.000	0.5
			Nitrogen−Ethane[f]				
1	2	0.000	−0.47376518126608				
2	2	0.050	0.48961193461001				
3	3	0.000	$-0.57011062090535\cdot10^{-2}$				
4	1	3.650	−0.19966820041320	1.000	0.5	1.000	0.5
5	2	4.900	−0.69411103101723	1.000	0.5	1.000	0.5
6	2	4.450	0.69226192739021	0.875	0.5	1.250	0.5
			Methane−Hydrogen[g]				
1	1	2.000	−0.25157134971934				
2	3	−1.000	$-0.62203841111983\cdot10^{-2}$				
3	3	1.750	$0.88850315184396\cdot10^{-1}$				
4	4	1.400	$-0.35592212573239\cdot10^{-1}$				

dx.doi.org/10.1021/je300655b | J. Chem. Eng. Data 2012, 57, 3032−3091

Table A7. continued

k	$d_{ij,k}$	$t_{ij,k}$	$n_{ij,k}$	$\eta_{ij,k}$	$\varepsilon_{ij,k}$	$\beta_{ij,k}$	$\gamma_{ij,k}$
Methane−*n*-Butane, Methane−Isobutane, Ethane−Propane, Ethane−*n*-Butane, Ethane−Isobutane, Propane−*n*-Butane, Propane−Isobutane, and *n*-Butane−Isobutane[h]							
1	1	1.000	$0.25574776844118\cdot10^{1}$				
2	1	1.550	$-0.79846357136353\cdot10^{1}$				
3	1	1.700	$0.47859131465806\cdot10^{1}$				
4	2	0.250	−0.73265392369587				
5	2	1.350	$0.13805471345312\cdot10^{1}$				
6	3	0.000	0.28349603476365				
7	3	1.250	−0.49087385940425				
8	4	0.000	−0.10291888921447				
9	4	0.700	0.11836314681968				
10	4	5.400	$0.55527385721943\cdot10^{-4}$				

[a] $K_{Pol,ij}$ = 2, $K_{Exp,ij}$ = 7. [b] $K_{Pol,ij}$ = 3, $K_{Exp,ij}$ = 3. [c] $K_{Pol,ij}$ = 2, $K_{Exp,ij}$ = 10. [d] $K_{Pol,ij}$ = 5, $K_{Exp,ij}$ = 4. [e] $K_{Pol,ij}$ = 2, $K_{Exp,ij}$ = 4. [f] $K_{Pol,ij}$ = 3, $K_{Exp,ij}$ = 3. [g] $K_{Pol,ij}$ = 4, $K_{Exp,ij}$ = 0. [h] $K_{Pol,ij}$ = 10, $K_{Exp,ij}$ = 0.

Table A8. Binary Parameters of the Reducing Functions for Density and Temperature, eqs 16 and 17

mixture $i-j$	$\beta_{v,ij}$	$\gamma_{v,ij}$	$\beta_{T,ij}$	$\gamma_{T,ij}$
CH_4-N_2	0.998721377	1.013950311	0.998098830	0.979273013
CH_4-CO_2	0.999518072	1.002806594	1.022624490	0.975665369
$CH_4-C_2H_6$	0.997547866	1.006617867	0.996336508	1.049707697
$CH_4-C_3H_8$	1.004827070	1.038470657	0.989680305	1.098655531
$CH_4-n-C_4H_{10}$	0.979105972	1.045375122	0.994174910	1.171607691
$CH_4-i-C_4H_{10}$	1.011240388	1.054319053	0.980315756	1.161117729
$CH_4-n-C_5H_{12}$	0.948330120	1.124508039	0.992127525	1.249173968
$CH_4-i-C_5H_{12}$	1.0	1.343685343	1.0	1.188899743
$CH_4-n-C_6H_{14}$	0.958015294	1.052643846	0.981844797	1.330570181
$CH_4-n-C_7H_{16}$	0.962050831	1.156655935	0.977431529	1.379850328
$CH_4-n-C_8H_{18}$	0.994740603	1.116549372	0.957473785	1.449245409
$CH_4-n-C_9H_{20}$	1.002852287	1.141895355	0.947716769	1.528532478
$CH_4-n-C_{10}H_{22}$	1.033086292	1.146089637	0.937777823	1.568231489
CH_4-H_2	1.0	1.018702573	1.0	1.352643115
CH_4-O_2	1.0	1.0	1.0	0.950000000
CH_4-CO	0.997340772	1.006102927	0.987411732	0.987473033
CH_4-H_2O	1.012783169	1.585018334	1.063333913	0.775810513
CH_4-H_2S	1.012599087	1.040161207	1.011090031	0.961155729
CH_4-He	1.0	0.881405683	1.0	3.159776855
CH_4-Ar	1.034630259	1.014678542	0.990954281	0.989843388
N_2-CO_2	0.977794634	1.047578256	1.005894529	1.107654104
$N_2-C_2H_6$	0.978880168	1.042352891	1.007671428	1.098650964
$N_2-C_3H_8$	0.974424681	1.081025408	1.002677329	1.201264026
$N_2-n-C_4H_{10}$	0.996082610	1.146949309	0.994515234	1.304886838
$N_2-i-C_4H_{10}$	0.986415830	1.100576129	0.992868130	1.284462634
$N_2-n-C_5H_{12}$	1.0	1.078877166	1.0	1.419029041
$N_2-i-C_5H_{12}$	1.0	1.154135439	1.0	1.381770770
$N_2-n-C_6H_{14}$	1.0	1.195952177	1.0	1.472607971
$N_2-n-C_7H_{16}$	1.0	1.404554090	1.0	1.520975334
$N_2-n-C_8H_{18}$	1.0	1.186067025	1.0	1.733280051
$N_2-n-C_9H_{20}$	1.0	1.100405929	0.956379450	1.749119996
$N_2-n-C_{10}H_{22}$	1.0	1.0	0.957934447	1.822157123
N_2-H_2	0.972532065	0.970115357	0.946134337	1.175696583
N_2-CO	1.0	1.008690943	1.0	0.993425388
N_2-H_2O	1.0	1.094749685	1.0	0.968808467
N_2-O_2	0.999521770	0.997082328	0.997190589	0.995157044
N_2-H_2S	0.910394249	1.256844157	1.004692366	0.960174200
N_2-He	0.969501055	0.932629867	0.692868765	1.471831580
N_2-Ar	1.004166412	1.002212182	0.999069843	0.990034831
$CO_2-C_2H_6$	1.002525718	1.032876701	1.013871147	0.900949530
$CO_2-C_3H_8$	0.996898004	1.047596298	1.033620538	0.908772477
$CO_2-n-C_4H_{10}$	1.174760923	1.222437324	1.018171004	0.911498231
$CO_2-i-C_4H_{10}$	1.076551882	1.081909003	1.023339824	0.929982936

dx.doi.org/10.1021/je300655b | J. Chem. Eng. Data 2012, 57, 3032−3091

Table A8. continued

mixture $i-j$	$\beta_{v,ij}$	$\gamma_{v,ij}$	$\beta_{T,ij}$	$\gamma_{T,ij}$
$CO_2-n\text{-}C_5H_{12}$	1.024311498	1.068406078	1.027000795	0.979217302
$CO_2-i\text{-}C_5H_{12}$	1.060793104	1.116793198	1.019180957	0.961218039
$CO_2-n\text{-}C_6H_{14}$	1.0	0.851343711	1.0	1.038675574
$CO_2-n\text{-}C_7H_{16}$	1.205469976	1.164585914	1.011806317	1.046169823
$CO_2-n\text{-}C_8H_{18}$	1.026169373	1.104043935	1.029690780	1.074455386
$CO_2-n\text{-}C_9H_{20}$	1.0	0.973386152	1.007688620	1.140671202
$CO_2-n\text{-}C_{10}H_{22}$	1.000151132	1.183394668	1.020028790	1.145512213
CO_2-H_2	0.904142159	1.152792550	0.942320195	1.782924792
CO_2-O_2	1.0	1.0	1.0	1.0
CO_2-CO	1.0	1.0	1.0	1.0
CO_2-H_2O	0.949055959	1.542328793	0.997372205	0.775453996
CO_2-H_2S	0.906630564	1.024085837	1.016034583	0.926018880
CO_2-He	0.846647561	0.864141549	0.768377630	3.207456948
CO_2-Ar	1.008392428	1.029205465	0.996512863	1.050971635
$C_2H_6-C_3H_8$	0.997607277	1.003034720	0.996199694	1.014730190
$C_2H_6-n\text{-}C_4H_{10}$	0.999157205	1.006179146	0.999130554	1.034832749
$C_2H_6-i\text{-}C_4H_{10}$	1.0	1.006616886	1.0	1.033283811
$C_2H_6-n\text{-}C_5H_{12}$	0.993851009	1.026085655	0.998688946	1.066665676
$C_2H_6-i\text{-}C_5H_{12}$[a]	1.0	1.045439935	1.0	1.021150247
$C_2H_6-n\text{-}C_6H_{14}$	1.0	1.169701102	1.0	1.092177796
$C_2H_6-n\text{-}C_7H_{16}$	1.0	1.057666085	1.0	1.134532014
$C_2H_6-n\text{-}C_8H_{18}$	1.007469726	1.071917985	0.984068272	1.168636194
$C_2H_6-n\text{-}C_9H_{20}$[a]	1.0	1.143534730	1.0	1.056033030
$C_2H_6-n\text{-}C_{10}H_{22}$	0.995676258	1.098361281	0.970918061	1.237191558
$C_2H_6-H_2$	0.925367171	1.106072040	0.932969831	1.902008495
$C_2H_6-O_2$	1.0	1.0	1.0	1.0
C_2H_6-CO	1.0	1.201417898	1.0	1.069224728
$C_2H_6-H_2O$	1.0	1.0	1.0	1.0
$C_2H_6-H_2S$	1.010817909	1.030988277	0.990197354	0.902736660
C_2H_6-He	1.0	1.0	1.0	1.0
C_2H_6-Ar	1.0	1.0	1.0	1.0
$C_3H_8-n\text{-}C_4H_{10}$	0.999795868	1.003264179	1.000310289	1.007392782
$C_3H_8-i\text{-}C_4H_{10}$	0.999243146	1.001156119	0.998012298	1.005250774
$C_3H_8-n\text{-}C_5H_{12}$	1.044919431	1.019921513	0.996484021	1.008344412
$C_3H_8-i\text{-}C_5H_{12}$	1.040459289	0.999432118	0.994364425	1.003269500
$C_3H_8-n\text{-}C_6H_{14}$	1.0	1.057872566	1.0	1.025657518
$C_3H_8-n\text{-}C_7H_{16}$	1.0	1.079648053	1.0	1.050044169
$C_3H_8-n\text{-}C_8H_{18}$	1.0	1.102764612	1.0	1.063694129
$C_3H_8-n\text{-}C_9H_{20}$	1.0	1.199769134	1.0	1.109973833
$C_3H_8-n\text{-}C_{10}H_{22}$	0.984104227	1.053040574	0.985331233	1.140905252
$C_3H_8-H_2$	1.0	1.074006110	1.0	2.308215191
$C_3H_8-O_2$	1.0	1.0	1.0	1.0
C_3H_8-CO	1.0	1.108143673	1.0	1.197564208
$C_3H_8-H_2O$	1.0	1.011759763	1.0	0.600340961
$C_3H_8-H_2S$	0.936811219	1.010593999	0.992573556	0.905829247
C_3H_8-He	1.0	1.0	1.0	1.0
C_3H_8-Ar	1.0	1.0	1.0	1.0
$n\text{-}C_4H_{10}-i\text{-}C_4H_{10}$	1.000880464	1.000414440	1.000077547	1.001432824
$n\text{-}C_4H_{10}-n\text{-}C_5H_{12}$	1.0	1.018159650	1.0	1.002143640
$n\text{-}C_4H_{10}-i\text{-}C_5H_{12}$[a]	1.0	1.002728434	1.0	1.000792201
$n\text{-}C_4H_{10}-n\text{-}C_6H_{14}$	1.0	1.034995284	1.0	1.009157060
$n\text{-}C_4H_{10}-n\text{-}C_7H_{16}$	1.0	1.019174227	1.0	1.021283378
$n\text{-}C_4H_{10}-n\text{-}C_8H_{18}$	1.0	1.046905515	1.0	1.033180106
$n\text{-}C_4H_{10}-n\text{-}C_9H_{20}$[a]	1.0	1.049219137	1.0	1.014096448
$n\text{-}C_4H_{10}-n\text{-}C_{10}H_{22}$	0.976951968	1.027845529	0.993688386	1.076466918
$n\text{-}C_4H_{10}-H_2$	1.0	1.232939523	1.0	2.509259945
$n\text{-}C_4H_{10}-O_2$	1.0	1.0	1.0	1.0
$n\text{-}C_4H_{10}-CO$[a]	1.0	1.084740904	1.0	1.173916162
$n\text{-}C_4H_{10}-H_2O$	1.0	1.223638763	1.0	0.615512682
$n\text{-}C_4H_{10}-H_2S$	0.908113163	1.033366041	0.985962886	0.926156602
$n\text{-}C_4H_{10}-He$	1.0	1.0	1.0	1.0

dx.doi.org/10.1021/je300655b | J. Chem. Eng. Data 2012, 57, 3032−3091

Table A8. continued

mixture $i-j$	$\beta_{v,ij}$	$\gamma_{v,ij}$	$\beta_{T,ij}$	$\gamma_{T,ij}$
n-C_4H_{10}−Ar	1.0	1.214638734	1.0	1.245039498
i-C_4H_{10}−n-C_5H_{12}[a]	1.0	1.002779804	1.0	1.002495889
i-C_4H_{10}−i-C_5H_{12}[a]	1.0	1.002284353	1.0	1.001835788
i-C_4H_{10}−n-C_6H_{14}[a]	1.0	1.010493989	1.0	1.006018054
i-C_4H_{10}−n-C_7H_{16}[a]	1.0	1.021668316	1.0	1.009885760
i-C_4H_{10}−n-C_8H_{18}[a]	1.0	1.032807063	1.0	1.013945424
i-C_4H_{10}−n-C_9H_{20}[a]	1.0	1.047298475	1.0	1.017817492
i-C_4H_{10}−n-$C_{10}H_{22}$[a]	1.0	1.060243344	1.0	1.021624748
i-C_4H_{10}−H_2[a]	1.0	1.147595688	1.0	1.895305393
i-C_4H_{10}−O_2	1.0	1.0	1.0	1.0
i-C_4H_{10}−CO[a]	1.0	1.087272232	1.0	1.161390082
i-C_4H_{10}−H_2O	1.0	1.0	1.0	1.0
i-C_4H_{10}−H_2S	1.012994431	0.988591117	0.974550548	0.937130844
i-C_4H_{10}−He	1.0	1.0	1.0	1.0
i-C_4H_{10}−Ar	1.0	1.0	1.0	1.0
n-C_5H_{12}−i-C_5H_{12}[a]	1.0	1.000024335	1.0	1.000050537
n-C_5H_{12}−n-C_6H_{14}[a]	1.0	1.002480637	1.0	1.000761237
n-C_5H_{12}−n-C_7H_{16}[a]	1.0	1.008972412	1.0	1.002441051
n-C_5H_{12}−n-C_8H_{18}	1.0	1.069223964	1.0	1.016422347
n-C_5H_{12}−n-C_9H_{20}	1.0	1.034910633	1.0	1.103421755
n-C_5H_{12}−n-$C_{10}H_{22}$	1.0	1.016370338	1.0	1.049035838
n-C_5H_{12}−H_2[a]	1.0	1.188334783	1.0	2.013859174
n-C_5H_{12}−O_2	1.0	1.0	1.0	1.0
n-C_5H_{12}−CO[a]	1.0	1.119954454	1.0	1.206043295
n-C_5H_{12}−H_2O	1.0	0.956677310	1.0	0.447666011
n-C_5H_{12}−H_2S	0.984613203	1.076539234	0.962006651	0.959065662
n-C_5H_{12}−He	1.0	1.0	1.0	1.0
n-C_5H_{12}−Ar	1.0	1.0	1.0	1.0
i-C_5H_{12}−n-C_6H_{14}[a]	1.0	1.002995876	1.0	1.001204174
i-C_5H_{12}−n-C_7H_{16}[a]	1.0	1.009928206	1.0	1.003194615
i-C_5H_{12}−n-C_8H_{18}[a]	1.0	1.017880545	1.0	1.005647480
i-C_5H_{12}−n-C_9H_{20}[a]	1.0	1.028994325	1.0	1.008191499
i-C_5H_{12}−n-$C_{10}H_{22}$[a]	1.0	1.039372957	1.0	1.010825138
i-C_5H_{12}−H_2[a]	1.0	1.184340443	1.0	1.996386669
i-C_5H_{12}−O_2	1.0	1.0	1.0	1.0
i-C_5H_{12}−CO[a]	1.0	1.116694577	1.0	1.199326059
i-C_5H_{12}−H_2O	1.0	1.0	1.0	1.0
i-C_5H_{12}−H_2S	1.0	0.835763343	1.0	0.982651529
i-C_5H_{12}−He	1.0	1.0	1.0	1.0
i-C_5H_{12}−Ar	1.0	1.0	1.0	1.0
n-C_6H_{14}−n-C_7H_{16}	1.0	1.001508227	1.0	0.999762786
n-C_6H_{14}−n-C_8H_{18}[a]	1.0	1.006268954	1.0	1.001633952
n-C_6H_{14}−n-C_9H_{20}	1.0	1.020761680	1.0	1.055369591
n-C_6H_{14}−n-$C_{10}H_{22}$	1.001516371	1.013511439	0.997641010	1.028939539
n-C_6H_{14}−H_2	1.0	1.243461678	1.0	3.021197546
n-C_6H_{14}−O_2	1.0	1.0	1.0	1.0
n-C_6H_{14}−CO[a]	1.0	1.155145836	1.0	1.233272781
n-C_6H_{14}−H_2O	1.0	1.170217596	1.0	0.569681333
n-C_6H_{14}−H_2S	0.754473958	1.339283552	0.985891113	0.956075596
n-C_6H_{14}−He	1.0	1.0	1.0	1.0
n-C_6H_{14}−Ar	1.0	1.0	1.0	1.0
n-C_7H_{16}−n-C_8H_{18}	1.0	1.006767176	1.0	0.998793111
n-C_7H_{16}−n-C_9H_{20}	1.0	1.001370076	1.0	1.001150096
n-C_7H_{16}−n-$C_{10}H_{22}$	1.0	1.002972346	1.0	1.002229938
n-C_7H_{16}−H_2	1.0	1.159131722	1.0	3.169143057
n-C_7H_{16}−O_2	1.0	1.0	1.0	1.0
n-C_7H_{16}−CO[a]	1.0	1.190354273	1.0	1.256123503
n-C_7H_{16}−H_2O	1.0	1.0	1.0	1.0
n-C_7H_{16}−H_2S	0.828967164	1.087956749	0.988937417	1.013453092
n-C_7H_{16}−He	1.0	1.0	1.0	1.0
n-C_7H_{16}−Ar	1.0	1.0	1.0	1.0

dx.doi.org/10.1021/je300655b | J. Chem. Eng. Data 2012, 57, 3032−3091

Table A8. continued

mixture $i-j$	$\beta_{v,ij}$	$\gamma_{v,ij}$	$\beta_{T,ij}$	$\gamma_{T,ij}$
n-C_8H_{18}−n-C_9H_{20}[a]	1.0	1.001357085	1.0	1.000235044
n-C_8H_{18}−n-$C_{10}H_{22}$	1.0	1.002553544	1.0	1.007186267
n-C_8H_{18}−H_2[a]	1.0	1.305249405	1.0	2.191555216
n-C_8H_{18}−O_2	1.0	1.0	1.0	1.0
n-C_8H_{18}−CO[a]	1.0	1.219206702	1.0	1.276565536
n-C_8H_{18}−H_2O	1.0	0.599484191	1.0	0.662072469
n-C_8H_{18}−H_2S	1.0	1.0	1.0	1.0
n-C_8H_{18}−He	1.0	1.0	1.0	1.0
n-C_8H_{18}−Ar	1.0	1.0	1.0	1.0
n-C_9H_{20}−n-$C_{10}H_{22}$[a]	1.0	1.000810520	1.0	1.000182392
n-C_9H_{20}−H_2[a]	1.0	1.342647661	1.0	2.234354040
n-C_9H_{20}−O_2	1.0	1.0	1.0	1.0
n-C_9H_{20}−CO[a]	1.0	1.252151449	1.0	1.294070556
n-C_9H_{20}−H_2O	1.0	1.0	1.0	1.0
n-C_9H_{20}−H_2S	1.0	1.082905109	1.0	1.086557826
n-C_9H_{20}−He	1.0	1.0	1.0	1.0
n-C_9H_{20}−Ar	1.0	1.0	1.0	1.0
n-$C_{10}H_{22}$−H_2	1.695358382	1.120233729	1.064818089	3.786003724
n-$C_{10}H_{22}$−O_2	1.0	1.0	1.0	1.0
n-$C_{10}H_{22}$−CO	1.0	0.870184960	1.049594632	1.803567587
n-$C_{10}H_{22}$−H_2O	1.0	0.551405318	0.897162268	0.740416402
n-$C_{10}H_{22}$−H_2S	0.975187766	1.171714677	0.973091413	1.103693489
n-$C_{10}H_{22}$−He	1.0	1.0	1.0	1.0
n-$C_{10}H_{22}$−Ar	1.0	1.0	1.0	1.0
H_2−O_2	1.0	1.0	1.0	1.0
H_2−CO	1.0	1.121416201	1.0	1.377504607
H_2−H_2O	1.0	1.0	1.0	1.0
H_2−H_2S	1.0	1.0	1.0	1.0
H_2−He	1.0	1.0	1.0	1.0
H_2−Ar	1.0	1.0	1.0	1.0
O_2−CO	1.0	1.0	1.0	1.0
O_2−H_2O	1.0	1.143174289	1.0	0.964767932
O_2−H_2S	1.0	1.0	1.0	1.0
O_2−He	1.0	1.0	1.0	1.0
O_2−Ar	0.999746847	0.993907223	1.000023103	0.990430423
CO−H_2O	1.0	1.0	1.0	1.0
CO−H_2S	0.795660392	1.101731308	1.025536736	1.022749748
CO−He	1.0	1.0	1.0	1.0
CO−Ar	1.0	1.159720623	1.0	0.954215746
H_2O−H_2S	1.0	1.014832832	1.0	0.940587083
H_2O−He	1.0	1.0	1.0	1.0
H_2O−Ar	1.0	1.038993495	1.0	1.070941866
H_2S−He	1.0	1.0	1.0	1.0
H_2S−Ar	1.0	1.0	1.0	1.0
He−Ar	1.0	1.0	1.0	1.0

[a]The values for the binary parameters $\gamma_{v,ij}$ and $\gamma_{T,ij}$ were calculated from eq 39.

- binary mixtures of the air components, i.e., nitrogen−oxygen, nitrogen−argon, and oxygen−argon;
- binary mixtures of carbon dioxide with the hydrocarbons ethane, propane, *n*-butane, etc.;
- binary hydrocarbon mixtures consisting of or containing the heavier hydrocarbons from *n*-pentane to *n*-octane (or even *n*-decane);
- binary mixtures containing helium (e.g., nitrogen−helium, carbon dioxide−helium, and helium−argon) or hydrogen with other components;
- binary mixtures of water with nitrogen, argon, and carbon dioxide.

The developed mixture model already yields a fairly accurate description of the thermal and caloric properties of (dry) air (see also Kunz et al.[1]). For example, for air, the uncertainty in gas-phase and gas-like supercritical densities is (0.1 to 0.2) % for temperatures up to 900 K and pressures to 90 MPa. The uncertainty in liquid-phase and liquid-like supercritical densities amounts to (0.2 to 0.5) % for temperatures down to 60 K. For the sound speed, similar uncertainties are estimated. The uncertainty in isobaric and isochoric heat capacity is estimated to be (1 to 2) % in the homogeneous gas, liquid, and supercritical regions. However, investigations have shown that a very accurate description of densities and sound speeds similar to that achieved for natural gases can be obtained by developing a short

dx.doi.org/10.1021/je300655b | J. Chem. Eng. Data 2012, 57, 3032−3091

Table B1. Definitions of Common Thermodynamic Properties and Their Relation to the Reduced Helmholtz Free Energy α for GERG-2008, eq 8

property and definition	relation to α and its derivatives[a,b]
pressure $p(T, \rho, \bar{x}) = -(\partial a/\partial v)_{T,\bar{x}}$	$\frac{p(\delta, \tau, \bar{x})}{\rho RT} = 1 + \delta\alpha_\delta^r$
compression factor $Z(T, \rho, \bar{x}) = p/(\rho RT)$	$Z(\delta, \tau, \bar{x}) = 1 + \delta\alpha_\delta^r$
entropy $s(T, \rho, \bar{x}) = -(\partial a/\partial T)_{v,\bar{x}}$	$\frac{s(\delta, \tau, \bar{x})}{R} = \tau(\alpha_\tau^o + \alpha_\tau^r) - \alpha^o - \alpha^r$
internal energy $u(T, \rho, \bar{x}) = a + Ts$	$\frac{u(\delta, \tau, \bar{x})}{RT} = \tau(\alpha_\tau^o + \alpha_\tau^r)$
isochoric heat capacity $c_v(T, \rho, \bar{x}) = (\partial u/\partial T)_{v,\bar{x}}$	$\frac{c_v(\delta, \tau, \bar{x})}{R} = -\tau^2(\alpha_{\tau\tau}^o + \alpha_{\tau\tau}^r)$
enthalpy $h(T, p, \bar{x}) = u + pv$	$\frac{h(\delta, \tau, \bar{x})}{RT} = 1 + \tau(\alpha_\tau^o + \alpha_\tau^r) + \delta\alpha_\delta^r$
isobaric heat capacity $c_p(T, p, \bar{x}) = (\partial h/\partial T)_{p,\bar{x}}$	$\frac{c_p(\delta, \tau, \bar{x})}{R} = -\tau^2(\alpha_{\tau\tau}^o + \alpha_{\tau\tau}^r) + \frac{(1 + \delta\alpha_\delta^r - \delta\tau\alpha_{\delta\tau}^r)^2}{1 + 2\delta\alpha_\delta^r + \delta^2\alpha_{\delta\delta}^r}$
Gibbs free energy $g(T, p, \bar{x}) = h - Ts$	$\frac{g(\delta, \tau, \bar{x})}{RT} = 1 + \alpha^o + \alpha^r + \delta\alpha_\delta^r$
speed of sound $w(T, p, \bar{x}) = \sqrt{(1/M)(\partial p/\partial \rho)_{s,\bar{x}}}$	$\frac{w^2(\delta, \tau, \bar{x})M}{RT} = 1 + 2\delta\alpha_\delta^r + \delta^2\alpha_{\delta\delta}^r - \frac{(1 + \delta\alpha_\delta^r - \delta\tau\alpha_{\delta\tau}^r)^2}{\tau^2(\alpha_{\tau\tau}^o + \alpha_{\tau\tau}^r)}$
Joule–Thomson coefficient $\mu_{JT}(T, p, \bar{x}) = (\partial T/\partial p)_{h,\bar{x}}$	$\mu_{JT}R\rho = \frac{-(\delta\alpha_\delta^r + \delta^2\alpha_{\delta\delta}^r + \delta\tau\alpha_{\delta\tau}^r)}{(1 + \delta\alpha_\delta^r - \delta\tau\alpha_{\delta\tau}^r)^2 - \tau^2(\alpha_{\tau\tau}^o + \alpha_{\tau\tau}^r)(1 + 2\delta\alpha_\delta^r + \delta^2\alpha_{\delta\delta}^r)}$
isothermal throttling coefficient $\delta_T(T, p, \bar{x}) = (\partial h/\partial p)_{T,\bar{x}}$	$\delta_T\rho = 1 - \frac{1 + \delta\alpha_\delta^r - \delta\tau\alpha_{\delta\tau}^r}{1 + 2\delta\alpha_\delta^r + \delta^2\alpha_{\delta\delta}^r}$
isentropic exponent $\kappa(T, p, \bar{x}) = -(v/p)(\partial p/\partial v)_{s,\bar{x}}$	$\kappa = \frac{1 + 2\delta\alpha_\delta^r + \delta^2\alpha_{\delta\delta}^r}{1 + \delta\alpha_\delta^r} \cdot \left[1 - \frac{(1 + \delta\alpha_\delta^r - \delta\tau\alpha_{\delta\tau}^r)^2}{\tau^2(\alpha_{\tau\tau}^o + \alpha_{\tau\tau}^r)(1 + 2\delta\alpha_\delta^r + \delta^2\alpha_{\delta\delta}^r)}\right]$
second thermal virial coefficient $B(T, \bar{x}) = \lim_{\rho\to 0}(\partial Z/\partial\rho)_{T,\bar{x}}$	$B(\tau)\rho_r = \lim_{\delta\to 0}\alpha_\delta^r$
third thermal virial coefficient $C(T, \bar{x}) = \frac{1}{2}\lim_{\rho\to 0}(\partial^2 Z/\partial\rho^2)_{T,\bar{x}}$	$C(\tau)\rho_r^2 = \lim_{\delta\to 0}\alpha_{\delta\delta}^r$

[a] See eq 11 for the definition of δ and τ and eq 16 for ρ_r. [b] See Table B5 for the derivatives of α^o and α^r with respect to δ and τ.

generalized departure function for the binary mixtures of the main air constituents nitrogen, oxygen, and argon. Such a development would offer the opportunity to calculate the thermal and caloric properties of natural gases and air in the homogeneous gas, liquid, and supercritical regions and also for vapor–liquid equilibrium states very accurately from a single and consistent mixture model.

As mentioned in Section 5.2.1.6, potential further improvements might be achievable for the description of the $p\rho T$ relation of rich natural gases containing large carbon dioxide mole fractions of 0.14 or more. The developed mixture model achieves a very accurate description for the $p\rho T$ relation of natural gases rich in carbon dioxide and of synthetic natural gas mixtures containing high fractions of nitrogen, carbon dioxide, and ethane. Therefore, the higher deviations mentioned in Section 5.2.1.6 (partly also in Section 5.2.1.5) are most likely due to the relatively large amounts of propane, *n*-butane, *n*-pentane, and *n*-hexane found in rich natural gases. The development of a generalized departure function for binary mixtures of carbon dioxide with these hydrocarbons seems to be worthwhile. This might also apply for the binary mixtures of water with nitrogen, argon, and carbon dioxide with regard to the calculation of the properties of flue-gas mixtures.

In general, data for binary hydrocarbon mixtures consisting of or containing heavier hydrocarbons are lacking. However, for certain binary hydrocarbon mixtures, a number of recently published and comparatively accurate measurements are available, which cover a fairly wide range of mixture conditions. The accuracy in the description of the thermodynamic properties of binary hydrocarbon mixtures for which only limited experimental information is available can possibly be improved by the development of a generalized departure function for hydrocarbon mixtures containing the heavier hydrocarbons from *n*-pentane to *n*-octane (or even *n*-decane), or by the extension of the existing generalized departure function for secondary alkanes to these mixtures.

7. SUMMARY

A new equation of state for the thermodynamic properties of natural gases, similar gases, and other mixtures, the GERG-2008 equation of state, is presented in this work. This equation is an expanded version of the previously developed GERG-2004 wide-range equation of state for natural gases and other mixtures of Kunz et al.[1] It is explicit in the Helmholtz free energy as a function of density, temperature, and composition.

Table B2. Derivatives of Pressure, Density, Total Volume, and Temperature, and Their Relation to the Reduced Helmholtz Free Energy α, eq 8

derivatives of pressure p with respect to temperature T, density ρ, and total volume V in relation to α and its derivatives[a,b]
$\left(\frac{\partial p}{\partial T}\right)_{V,\bar{n}} = \left(\frac{\partial p}{\partial T}\right)_{\rho,\bar{x}} = \rho R(1 + \delta\alpha_\delta^r - \delta\tau\alpha_{\delta\tau}^r)$
$\left(\frac{\partial p}{\partial \rho}\right)_{T,\bar{n}} = \left(\frac{\partial p}{\partial \rho}\right)_{T,\bar{x}} = RT(1 + 2\delta\alpha_\delta^r + \delta^2\alpha_{\delta\delta}^r)$
$n\left(\frac{\partial p}{\partial V}\right)_{T,\bar{n}} = -\rho^2 RT(1 + 2\delta\alpha_\delta^r + \delta^2\alpha_{\delta\delta}^r)$
derivative of pressure p with respect to the mole number n_i of component i[c]
$n\left(\frac{\partial p}{\partial n_i}\right)_{T,V,n_j} = \rho RT\left[1 + \delta\alpha_\delta^r\left[2 - \frac{1}{\rho_r}\cdot n\left(\frac{\partial \rho_r}{\partial n_i}\right)_{n_j}\right] + \delta\cdot n\left(\frac{\partial \alpha_\delta^r}{\partial n_i}\right)_{T,V,n_j}\right]$
relations resulting from pressure derivatives
Derivative of V with respect to T and vice versa: $\frac{1}{n}\left(\frac{\partial V}{\partial T}\right)_{p,\bar{n}} = \frac{-(\partial p/\partial T)_{V,\bar{n}}}{n(\partial p/\partial V)_{T,\bar{n}}} = \frac{1}{n(\partial T/\partial V)_{p,\bar{n}}}$
Derivative of ρ with respect to T and vice versa: $\left(\frac{\partial \rho}{\partial T}\right)_{p,\bar{x}} = \frac{-(\partial p/\partial T)_{\rho,\bar{x}}}{(\partial p/\partial \rho)_{T,\bar{x}}} = \frac{1}{(\partial T/\partial \rho)_{p,\bar{x}}}$
Derivative of V with respect to n_i: $\left(\frac{\partial V}{\partial n_i}\right)_{T,p,n_j} = \hat{v}_i = \frac{-(\partial p/\partial n_i)_{T,V,n_j}}{(\partial p/\partial V)_{T,\bar{n}}}$
Derivative of T with respect to n_i: $n\left(\frac{\partial T}{\partial n_i}\right)_{p,V,n_j} = \frac{-n(\partial p/\partial n_i)_{T,V,n_j}}{(\partial p/\partial T)_{V,\bar{n}}}$

[a] See eq 11 for the definition of δ and τ and eq 16 for ρ_r. [b] See Table B5 for the derivatives of α^o and α^r with respect to δ and τ. [c] See Table B4 and Kunz et al.[1] for the derivatives of ρ_r and α_δ^r with respect to n_i.

Table B3. Definitions of the Chemical Potential, the Fugacity Coefficient, and the Fugacity of Component *i*, and Their Relation to the Reduced Helmholtz Free Energy α, eq 8

property and definition	relation to α and its derivatives[a]
Chemical Potential of Component i: $\mu_i(T, V, \bar{n}) = \left(\frac{\partial A}{\partial n_i}\right)_{T,V,n_j}$	$\frac{\mu_i}{RT} = \left(\frac{\partial n\alpha^o}{\partial n_i}\right)_{T,V,n_j} + \left(\frac{\partial n\alpha^r}{\partial n_i}\right)_{T,V,n_j}$
Fugacity Coefficient of Component i: $\ln \varphi_i(T, p, \bar{n}) = \int_0^p \left(\frac{\hat{v}_i}{RT} - \frac{1}{p}\right) dp_{T,\bar{n}}$	$\ln \varphi_i = \left(\frac{\partial n\alpha^r}{\partial n_i}\right)_{T,V,n_j} - \ln(1 + \delta\alpha_\delta^r)$
Fugacity of Component i: $f_i(T, p, \bar{n}) = x_i\, p\varphi_i(T, p, \bar{n})$	$f_i = x_i\rho RT \exp\left(\frac{\partial n\alpha^r}{\partial n_i}\right)_{T,V,n_j}$

[a] See Table B4 for the derivatives of $n\alpha^o$ and $n\alpha^r$ with respect to n_i and Table B5 for the derivative of α^r with respect to δ, i.e., α_δ^r; see eq 11 for the definition of δ.

The expanded equation covers the 21 natural gas components methane, nitrogen, carbon dioxide, ethane, propane, *n*-butane, isobutane, *n*-pentane, isopentane, *n*-hexane, *n*-heptane, *n*-octane, *n*-nonane, *n*-decane, hydrogen, oxygen, carbon monoxide, water, hydrogen sulfide, helium, and argon. The equation is valid over wide ranges of temperature, pressure, and composition and covers the gas phase, liquid phase, supercritical region, and vapor−liquid equilibrium states for natural gases and other mixtures consisting of the 21 components.

The basis for the development of this fully consistent mixture model and its evaluation is the continuously updated database composed of more than 125 000 experimental data for multiple thermodynamic properties in different fluid regions. About 76 % of the collected data accounts for binary mixtures, and the remaining 24 % accounts for multi-component mixtures, including various types of natural gases, hydrocarbon mixtures, and other mixtures.

As a multi-fluid correlation, the GERG-2008 mixture model uses accurate equations of state in the form of fundamental equations for each mixture component along with several functions developed for the binary mixtures of the components to take into account the residual mixture behavior. This allows for an accurate description of the properties of multi-component mixtures over a wide range of compositions. The different binary correlation equations were developed using a linear structure-optimization method and nonlinear multiproperty fitting techniques in an iterative procedure. For most of the 210 binary systems that result from the 21 components studied in this work, adjusted reducing functions for density and temperature

Table B4. First Derivatives of the Helmholtz Free Energy α and the Reducing Functions for Mixture Density ρ_r and Temperature T_r with Respect to the Mole Numbers n_i[a]

derivatives of $n\alpha^o$ and $n\alpha^r$ with respect to the mole number n_i of component i[b]

$$\left(\frac{\partial n\alpha^o}{\partial n_i}\right)_{T,V,n_j} = \alpha^o_{oi}(\rho, T) + 1 + \ln x_i$$

$$\left(\frac{\partial n\alpha^r}{\partial n_i}\right)_{T,V,n_j} = \alpha^r + n\left(\frac{\partial \alpha^r}{\partial n_i}\right)_{T,V,n_j}$$

derivatives of α^r and α^r_δ with respect to the mole number n_i of component i[c]

$$n\left(\frac{\partial \alpha^r}{\partial n_i}\right)_{T,V,n_j} = \delta\alpha^r_\delta\left[1 - \frac{1}{\rho_r}\cdot n\left(\frac{\partial \rho_r}{\partial n_i}\right)_{n_j}\right] + \tau\alpha^r_\tau\frac{1}{T_r}\cdot n\left(\frac{\partial T_r}{\partial n_i}\right)_{n_j} + \alpha^r_{x_i} - \sum_{k=1}^{N} x_k\alpha^r_{x_k}$$

$$n\left(\frac{\partial \alpha^r_\delta}{\partial n_i}\right)_{T,V,n_j} = \delta\alpha^r_{\delta\delta}\left[1 - \frac{1}{\rho_r}\cdot n\left(\frac{\partial \rho_r}{\partial n_i}\right)_{n_j}\right] + \tau\alpha^r_{\delta\tau}\frac{1}{T_r}\cdot n\left(\frac{\partial T_r}{\partial n_i}\right)_{n_j} + \alpha^r_{\delta x_i} - \sum_{k=1}^{N} x_k\alpha^r_{\delta x_k}$$

derivatives of $\rho_r = \rho_r(\bar{x})$ and $T_r = T_r(\bar{x})$ with respect to the mole number n_i of component i[d]

$$n\left(\frac{\partial \rho_r}{\partial n_i}\right)_{n_j} = \left(\frac{\partial \rho_r}{\partial x_i}\right)_{x_j} - \sum_{k=1}^{N} x_k\left(\frac{\partial \rho_r}{\partial x_k}\right)_{x_j} \quad \text{with} \quad \left(\frac{\partial \rho_r}{\partial x_i}\right)_{x_j} = -\rho_r^2\left(\frac{\partial(1/\rho_r)}{\partial x_i}\right)_{x_j}$$

$$n\left(\frac{\partial T_r}{\partial n_i}\right)_{n_j} = \left(\frac{\partial T_r}{\partial x_i}\right)_{x_j} - \sum_{k=1}^{N} x_k\left(\frac{\partial T_r}{\partial x_k}\right)_{x_j}$$

[a] See Kunz et al.[1] for further and second derivatives of α, ρ_r, and T_r with respect to n_i. [b] See eq 12 for α^o_{oi} and eq 10 for α^r. [c] See Table B5 for the derivatives of α^r with respect to δ and τ, eq 11. [d] See Table B9 for the derivatives of $1/\rho_r(\bar{x})$ and $T_r(\bar{x})$, eqs 16 and 17, with respect to x_i.

Table B5. The Parts $\alpha^o(\rho,T,\bar{x})$ and $\alpha^r(\delta,\tau,\bar{x})$ of the Dimensionless Helmholtz Free Energy α, and Their Derivatives with Respect to the Reduced Mixture Variables δ and τ, and Mole Fractions x_i[a]

first and second derivatives of α^o with respect to δ and τ[b,c]

$\alpha^o(\rho, T, \bar{x})$	$\alpha^o = \sum_{i=1}^{N} x_i[\alpha^o_{oi}(\rho, T) + \ln x_i]$
$\left(\frac{\partial \alpha^o}{\partial \delta}\right)_{\tau,\bar{x}}$	$\alpha^o_\delta = \sum_{i=1}^{N} x_i\frac{\rho_r}{\rho_{c,i}}\left(\frac{\partial \alpha^o_{oi}}{\partial(\rho/\rho_{c,i})}\right)_T$
$\left(\frac{\partial^2 \alpha^o}{\partial \delta^2}\right)_{\tau,\bar{x}}$	$\alpha^o_{\delta\delta} = \sum_{i=1}^{N} x_i\left(\frac{\rho_r}{\rho_{c,i}}\right)^2\left(\frac{\partial^2 \alpha^o_{oi}}{\partial(\rho/\rho_{c,i})^2}\right)_T$
$\left(\frac{\partial^2 \alpha^o}{\partial \delta\partial \tau}\right)_{\bar{x}}$	$\alpha^o_{\delta\tau} = \sum_{i=1}^{N} x_i\frac{\rho_r}{\rho_{c,i}}\frac{T_{c,i}}{T_r}\left(\frac{\partial^2 \alpha^o_{oi}}{\partial(\rho/\rho_{c,i})\partial(T_{c,i}/T)}\right)$
$\left(\frac{\partial \alpha^o}{\partial \tau}\right)_{\delta,\bar{x}}$	$\alpha^o_\tau = \sum_{i=1}^{N} x_i\frac{T_{c,i}}{T_r}\left(\frac{\partial \alpha^o_{oi}}{\partial(T_{c,i}/T)}\right)_\rho$
$\left(\frac{\partial^2 \alpha^o}{\partial \tau^2}\right)_{\delta,\bar{x}}$	$\alpha^o_{\tau\tau} = \sum_{i=1}^{N} x_i\left(\frac{T_{c,i}}{T_r}\right)^2\left(\frac{\partial^2 \alpha^o_{oi}}{\partial(T_{c,i}/T)^2}\right)_\rho$

first and second derivatives of α^r with respect to δ, τ, and x_i[d]

$\alpha^r(\delta, \tau, \bar{x})$	$\alpha^r = \sum_{i=1}^{N} x_i\alpha^r_{oi}(\delta, \tau) + \sum_{i=1}^{N-1}\sum_{j=i+1}^{N} x_ix_jF_{ij}\alpha^r_{ij}(\delta, \tau)$
$\left(\frac{\partial \alpha^r}{\partial \delta}\right)_{\tau,\bar{x}}$	$\alpha^r_\delta = \sum_{i=1}^{N} x_i\left(\frac{\partial \alpha^r_{oi}}{\partial \delta}\right)_\tau + \sum_{i=1}^{N-1}\sum_{j=i+1}^{N} x_ix_jF_{ij}\left(\frac{\partial \alpha^r_{ij}}{\partial \delta}\right)_\tau$
$\left(\frac{\partial^2 \alpha^r}{\partial \delta^2}\right)_{\tau,\bar{x}}$	$\alpha^r_{\delta\delta} = \sum_{i=1}^{N} x_i\left(\frac{\partial^2 \alpha^r_{oi}}{\partial \delta^2}\right)_\tau + \sum_{i=1}^{N-1}\sum_{j=i+1}^{N} x_ix_jF_{ij}\left(\frac{\partial^2 \alpha^r_{ij}}{\partial \delta^2}\right)_\tau$
$\left(\frac{\partial^2 \alpha^r}{\partial \delta\partial \tau}\right)_{\bar{x}}$	$\alpha^r_{\delta\tau} = \sum_{i=1}^{N} x_i\left(\frac{\partial^2 \alpha^r_{oi}}{\partial \delta\partial \tau}\right) + \sum_{i=1}^{N-1}\sum_{j=i+1}^{N} x_ix_jF_{ij}\left(\frac{\partial^2 \alpha^r_{ij}}{\partial \delta\partial \tau}\right)$
$\left(\frac{\partial \alpha^r}{\partial \tau}\right)_{\delta,\bar{x}}$	$\alpha^r_\tau = \sum_{i=1}^{N} x_i\left(\frac{\partial \alpha^r_{oi}}{\partial \tau}\right)_\delta + \sum_{i=1}^{N-1}\sum_{j=i+1}^{N} x_ix_jF_{ij}\left(\frac{\partial \alpha^r_{ij}}{\partial \tau}\right)_\delta$
$\left(\frac{\partial^2 \alpha^r}{\partial \tau^2}\right)_{\delta,\bar{x}}$	$\alpha^r_{\tau\tau} = \sum_{i=1}^{N} x_i\left(\frac{\partial^2 \alpha^r_{oi}}{\partial \tau^2}\right)_\delta + \sum_{i=1}^{N-1}\sum_{j=i+1}^{N} x_ix_jF_{ij}\left(\frac{\partial^2 \alpha^r_{ij}}{\partial \tau^2}\right)_\delta$
$\left(\frac{\partial \alpha^r}{\partial x_i}\right)_{\delta,\tau,x_j}$	$\alpha^r_{x_i} = \alpha^r_{oi} + \sum_{\substack{k=1\\k\neq i}}^{N} x_kF_{ik}\alpha^r_{ik}$
$\left(\frac{\partial^2 \alpha^r}{\partial x_i^2}\right)_{\delta,\tau,x_j}$	$\alpha^r_{x_ix_i} = 0$
$\left(\frac{\partial^2 \alpha^r}{\partial x_i\partial x_j}\right)_{\delta,\tau}$	$\alpha^r_{x_ix_j} = F_{ij}\alpha^r_{ij}(\delta, \tau), \quad i \neq j$
$\left(\frac{\partial^2 \alpha^r}{\partial \delta\partial x_i}\right)_{\tau,x_j}$	$\alpha^r_{\delta x_i} = \left(\frac{\partial \alpha^r_{oi}}{\partial \delta}\right)_\tau + \sum_{\substack{k=1\\k\neq i}}^{N} x_kF_{ik}\left(\frac{\partial \alpha^r_{ik}}{\partial \delta}\right)_\tau$
$\left(\frac{\partial^2 \alpha^r}{\partial \tau\partial x_i}\right)_{\delta,x_j}$	$\alpha^r_{\tau x_i} = \left(\frac{\partial \alpha^r_{oi}}{\partial \tau}\right)_\delta + \sum_{\substack{k=1\\k\neq i}}^{N} x_kF_{ik}\left(\frac{\partial \alpha^r_{ik}}{\partial \tau}\right)_\delta$

[a] See eq 11 for the definition of δ and τ. [b] See Table B6 for the equation of α^o_{oi} and its derivatives with respect to $\rho/\rho_{c,i}$ and $T_{c,i}/T$. [c] See eqs 16 and 17 for the reducing functions $\rho_r = \rho_r(\bar{x})$ and $T_r = T_r(\bar{x})$; $\rho_{c,i}$ and $T_{c,i}$ are the critical parameters of component i. [d] See Tables B7 and B8 for the equations of α^r_{oi} and α^r_{ij} and their derivatives with respect to δ and τ.

dx.doi.org/10.1021/je300655b | J. Chem. Eng. Data 2012, 57, 3032−3091

Table B6. Dimensionless Helmholtz Free Energy in the Ideal-Gas State of Component i, $\alpha^{o}_{oi}(\rho,T)$, and Its Derivatives with Respect to $\rho/\rho_{c,i}$ and $T_{c,i}/T$

$$\alpha^{o}_{oi}(\rho, T) = \ln\left(\frac{\rho}{\rho_{c,i}}\right) + \frac{R^*}{R}\left[n^{o}_{oi,1} + n^{o}_{oi,2}\frac{T_{c,i}}{T} + n^{o}_{oi,3}\ln\left(\frac{T_{c,i}}{T}\right) + \sum_{k=4,6} n^{o}_{oi,k}\ln\left(\left|\sinh\left(\vartheta^{o}_{oi,k}\frac{T_{c,i}}{T}\right)\right|\right) - \sum_{k=5,7} n^{o}_{oi,k}\ln\left(\cosh\left(\vartheta^{o}_{oi,k}\frac{T_{c,i}}{T}\right)\right)\right]$$

$$\left(\frac{\partial\alpha^{o}_{oi}}{\partial(\rho/\rho_{c,i})}\right)_T = \frac{\rho_{c,i}}{\rho}, \qquad \left(\frac{\partial^2\alpha^{o}_{oi}}{\partial(\rho/\rho_{c,i})^2}\right)_T = -\left(\frac{\rho_{c,i}}{\rho}\right)^2,$$

$$\left(\frac{\partial^2\alpha^{o}_{oi}}{\partial(\rho/\rho_{c,i})^2}\right)_T = -\left(\frac{\rho_{c,i}}{\rho}\right)^2, \qquad \left(\frac{\partial^2\alpha^{o}_{oi}}{\partial(\rho/\rho_{c,i})\partial(T_{c,i}/T)}\right) = 0$$

$$\left(\frac{\partial\alpha^{o}_{oi}}{\partial(T_{c,i}/T)}\right)_\rho = \frac{R^*}{R}\left[n^{o}_{oi,2} + n^{o}_{oi,3}\frac{T}{T_{c,i}} + \sum_{k=4,6} n^{o}_{oi,k}\frac{\vartheta^{o}_{oi,k}}{\tanh(\vartheta^{o}_{oi,k}\cdot T_{c,i}/T)} - \sum_{k=5,7} n^{o}_{oi,k}\vartheta^{o}_{oi,k}\tanh\left(\vartheta^{o}_{oi,k}\frac{T_{c,i}}{T}\right)\right]$$

$$\left(\frac{\partial^2\alpha^{o}_{oi}}{\partial(T_{c,i}/T)^2}\right)_\rho = \frac{R^*}{R}\left[-n^{o}_{oi,3}\left(\frac{T}{T_{c,i}}\right)^2 - \sum_{k=4,6} n^{o}_{oi,k}\frac{(\vartheta^{o}_{oi,k})^2}{(\sinh(\vartheta^{o}_{oi,k}\cdot T_{c,i}/T))^2} - \sum_{k=5,7} n^{o}_{oi,k}\frac{(\vartheta^{o}_{oi,k})^2}{(\cosh(\vartheta^{o}_{oi,k}\cdot T_{c,i}/T))^2}\right]$$

Table B7. Residual Part of the Dimensionless Helmholtz Free Energy of Component i, $\alpha^{r}_{oi}(\delta,\tau)$, and Its Derivatives with Respect to the Reduced Mixture Variables δ and τ, eq 11

$$\alpha^{r}_{oi}(\delta, \tau) = \sum_{k=1}^{K_{Pol,i}} n_{oi,k}\delta^{d_{oi,k}}\tau^{t_{oi,k}} + \sum_{k=K_{Pol,i}+1}^{K_{Pol,i}+K_{Exp,i}} n_{oi,k}\delta^{d_{oi,k}}\tau^{t_{oi,k}}\cdot\exp(-\delta^{c_{oi,k}})$$

$$\left(\frac{\partial\alpha^{r}_{oi}}{\partial\delta}\right)_\tau = \sum_{k=1}^{K_{Pol,i}} n_{oi,k}d_{oi,k}\delta^{d_{oi,k}-1}\tau^{t_{oi,k}} + \sum_{k=K_{Pol,i}+1}^{K_{Pol,i}+K_{Exp,i}} n_{oi,k}\delta^{d_{oi,k}-1}(d_{oi,k} - c_{oi,k}\delta^{c_{oi,k}})\cdot\tau^{t_{oi,k}}\cdot\exp(-\delta^{c_{oi,k}})$$

$$\left(\frac{\partial^2\alpha^{r}_{oi}}{\partial\delta^2}\right)_\tau = \sum_{k=1}^{K_{Pol,i}} n_{oi,k}d_{oi,k}(d_{oi,k} - 1)\delta^{d_{oi,k}-2}\tau^{t_{oi,k}} + \sum_{k=K_{Pol,i}+1}^{K_{Pol,i}+K_{Exp,i}} n_{oi,k}\delta^{d_{oi,k}-2}((d_{oi,k} - c_{oi,k}\delta^{c_{oi,k}})(d_{oi,k} - 1 - c_{oi,k}\delta^{c_{oi,k}}) - c^2_{oi,k}\delta^{c_{oi,k}})\tau^{t_{oi,k}}\cdot\exp(-\delta^{c_{oi,k}})$$

$$\left(\frac{\partial^2\alpha^{r}_{oi}}{\partial\delta\partial\tau}\right) = \sum_{k=1}^{K_{Pol,i}} n_{oi,k}d_{oi,k}t_{oi,k}\delta^{d_{oi,k}-1}\tau^{t_{oi,k}-1} + \sum_{k=K_{Pol,i}+1}^{K_{Pol,i}+K_{Exp,i}} n_{oi,k}t_{oi,k}\delta^{d_{oi,k}-1}(d_{oi,k} - c_{oi,k}\delta^{c_{oi,k}})\tau^{t_{oi,k}-1}\cdot\exp(-\delta^{c_{oi,k}})$$

$$\left(\frac{\partial\alpha^{r}_{oi}}{\partial\tau}\right)_\delta = \sum_{k=1}^{K_{Pol,i}} n_{oi,k}t_{oi,k}\delta^{d_{oi,k}}\tau^{t_{oi,k}-1} + \sum_{k=K_{Pol,i}+1}^{K_{Pol,i}+K_{Exp,i}} n_{oi,k}t_{oi,k}\delta^{d_{oi,k}}\tau^{t_{oi,k}-1}\cdot\exp(-\delta^{c_{oi,k}})$$

$$\left(\frac{\partial^2\alpha^{r}_{oi}}{\partial\tau^2}\right)_\delta = \sum_{k=1}^{K_{Pol,i}} n_{oi,k}t_{oi,k}(t_{oi,k} - 1)\delta^{d_{oi,k}}\tau^{t_{oi,k}-2} + \sum_{k=K_{Pol,i}+1}^{K_{Pol,i}+K_{Exp,i}} n_{oi,k}t_{oi,k}(t_{oi,k} - 1)\delta^{d_{oi,k}}\tau^{t_{oi,k}-2}\cdot\exp(-\delta^{c_{oi,k}})$$

are used. For a number of well-measured binary mixtures of important natural gas components, binary-specific or generalized departure functions were additionally developed. For binary mixtures for which only limited or poor data are available, which neither allow for the development of a departure function nor the fitting of the parameters of the reducing functions, different combining rules for the pure component critical parameters are used. This combined strategy proved to be clearly superior to the early model for mixtures of natural gas components developed by Lemmon and Jacobsen,[21] who use a single generalized departure function for all of the binary mixtures considered by the authors.

The GERG-2008 wide-range equation of state is able to represent the most accurate experimental binary and multi-component data for gas-phase and gas-like supercritical densities, sound speeds, and enthalpy differences mostly to within their low experimental uncertainties, which is not true for the AGA8-DC92 equation of state.[6] The normal range of validity covers temperatures from (90 to 450) K and pressures up to 35 MPa. The uncertainties in gas-phase density and sound speed for a broad variety of natural gases and related mixtures are 0.1 % over the temperature range from (250 to 450) K at pressures up to 35 MPa. Accurate data for isobaric enthalpy differences of binary and multi-component mixtures are reproduced to within their experimental uncertainty, which amounts to (0.2 to 0.5) %. In the liquid phase of many binary and multi-component mixtures, the uncertainty of the equation in density is generally (0.1 to 0.5) %, which is again in agreement with the experimental uncertainty of the data. The vapor−liquid equilibrium of binary and multi-component mixtures, including the dew points of natural gases, is accurately described as well. For instance, accurate vapor-pressure data for binary and ternary mixtures of the main natural gas constituents or of hydrocarbons are reproduced to within their experimental uncertainty, which is in general (1 to 3) %.

Compared to the AGA8-DC92 equation of state,[6] the new equation of state achieves important and fundamental improvements in the description of gas-phase and gas-like supercritical densities of natural gas mixtures containing, for example, high fractions of nitrogen, carbon dioxide, or ethane, or substantial amounts of ethane, propane, and heavier hydrocarbons. The GERG-2008 equation of state allows for the accurate description of natural gas−hydrogen mixtures, low-calorific natural gases, and other mixtures of uncommon composition. Moreover, the new equation is much more accurate for rich natural gases and in the description of all caloric properties and also satisfies the demands on the accuracy in the description of liquid-phase properties and vapor−liquid equilibrium states.

The wide range of validity enables the use of the GERG-2008 equation of state in both standard and advanced technical applications for natural gases, similar gases, and other mixtures. This includes, for example, pipeline transport, natural gas storage, improved and integrated processes with liquefied natural gas, the design of separation processes as encountered in the processing of rich natural gas to meet pipeline-quality specifications, acid-gas injection, the production of NGLs and liquefied petroleum gas, the production and refining of light oil, processes using mixtures of hydrocarbons as alternative refrigerants, and future applications with natural gas−hydrogen mixtures.

Table B8. Function $\alpha_{ij}^{r}(\delta,\tau)$ and Its Derivatives with Respect to the Reduced Mixture Variables δ and τ, eq 11

$$\alpha_{ij}^{r}(\delta,\tau) = \sum_{k=1}^{K_{Pol,ij}} n_{ij,k}\delta^{d_{ij,k}}\tau^{t_{ij,k}} + \sum_{k=K_{Pol,ij}+1}^{K_{Pol,ij}+K_{Exp,ij}} n_{ij,k}\delta^{d_{ij,k}}\tau^{t_{ij,k}}\cdot \exp(-\eta_{ij,k}(\delta-\varepsilon_{ij,k})^2 - \beta_{ij,k}(\delta-\gamma_{ij,k}))$$

$$\left(\frac{\partial\alpha_{ij}^{r}}{\partial\delta}\right)_{\tau} = \sum_{k=1}^{K_{Pol,ij}} n_{ij,k}d_{ij,k}\delta^{d_{ij,k}-1}\tau^{t_{ij,k}} + \sum_{k=K_{Pol,ij}+1}^{K_{Pol,ij}+K_{Exp,ij}} n_{ij,k}\delta^{d_{ij,k}}\tau^{t_{ij,k}}\cdot \exp(-\eta_{ij,k}(\delta-\varepsilon_{ij,k})^2 - \beta_{ij,k}(\delta-\gamma_{ij,k}))\cdot\left[\frac{d_{ij,k}}{\delta} - 2\eta_{ij,k}(\delta-\varepsilon_{ij,k}) - \beta_{ij,k}\right]$$

$$\left(\frac{\partial^2\alpha_{ij}^{r}}{\partial\delta^2}\right)_{\tau} = \sum_{k=1}^{K_{Pol,ij}} n_{ij,k}d_{ij,k}(d_{ij,k}-1)\delta^{d_{ij,k}-2}\tau^{t_{ij,k}} + \sum_{k=K_{Pol,ij}+1}^{K_{Pol,ij}+K_{Exp,ij}} n_{ij,k}\delta^{d_{ij,k}}\tau^{t_{ij,k}}\cdot\exp(-\eta_{ij,k}(\delta-\varepsilon_{ij,k})^2 - \beta_{ij,k}(\delta-\gamma_{ij,k}))\cdot\left[\left(\frac{d_{ij,k}}{\delta} - 2\eta_{ij,k}(\delta-\varepsilon_{ij,k}) - \beta_{ij,k}\right)^2 - \frac{d_{ij,k}}{\delta^2} - 2\eta_{ij,k}\right]$$

$$\left(\frac{\partial^2\alpha_{ij}^{r}}{\partial\delta\partial\tau}\right) = \sum_{k=1}^{K_{Pol,ij}} n_{ij,k}d_{ij,k}t_{ij,k}\delta^{d_{ij,k}-1}\tau^{t_{ij,k}-1} + \sum_{k=K_{Pol,ij}+1}^{K_{Pol,ij}+K_{Exp,ij}} n_{ij,k}t_{ij,k}\delta^{d_{ij,k}}\tau^{t_{ij,k}-1}\cdot\exp(-\eta_{ij,k}(\delta-\varepsilon_{ij,k})^2 - \beta_{ij,k}(\delta-\gamma_{ij,k}))\cdot\left[\frac{d_{ij,k}}{\delta} - 2\eta_{ij,k}(\delta-\varepsilon_{ij,k}) - \beta_{ij,k}\right]$$

$$\left(\frac{\partial\alpha_{ij}^{r}}{\partial\tau}\right)_{\delta} = \sum_{k=1}^{K_{Pol,ij}} n_{ij,k}t_{ij,k}\delta^{d_{ij,k}}\tau^{t_{ij,k}-1} + \sum_{k=K_{Pol,ij}+1}^{K_{Pol,ij}+K_{Exp,ij}} n_{ij,k}t_{ij,k}\delta^{d_{ij,k}}\tau^{t_{ij,k}-1}\cdot\exp(-\eta_{ij,k}(\delta-\varepsilon_{ij,k})^2 - \beta_{ij,k}(\delta-\gamma_{ij,k}))$$

$$\left(\frac{\partial^2\alpha_{ij}^{r}}{\partial\tau^2}\right)_{\delta} = \sum_{k=1}^{K_{Pol,ij}} n_{ij,k}t_{ij,k}(t_{ij,k}-1)\delta^{d_{ij,k}}\tau^{t_{ij,k}-2} + \sum_{k=K_{Pol,ij}+1}^{K_{Pol,ij}+K_{Exp,ij}} n_{ij,k}t_{ij,k}(t_{ij,k}-1)\delta^{d_{ij,k}}\tau^{t_{ij,k}-2}\cdot\exp(-\eta_{ij,k}(\delta-\varepsilon_{ij,k})^2 - \beta_{ij,k}(\delta-\gamma_{ij,k}))$$

Table B9. Reducing Functions for Mixture Density $1/\rho_r(\bar{x})$ and Temperature $T_r(\bar{x})$ and Their Derivatives with Respect to the Mole Fractions x_i

reducing function for density $1/\rho_r$ ($Y = v$) and temperature T_r ($Y = T$)[a]

$$Y_r = Y_r(\bar{x}) = \sum_{i=1}^{N}\sum_{j=1}^{N} x_i x_j \beta_{Y,ij}\gamma_{Y,ij}\frac{x_i+x_j}{\beta_{Y,ij}^2 x_i + x_j}Y_{c,ij} = \sum_{i=1}^{N} x_i^2 Y_{c,i} + \sum_{i=1}^{N-1}\sum_{j=i+1}^{N} c_{Y,ij}f_{Y,ij}(x_i,x_j)$$

where $c_{Y,ij} = 2\beta_{Y,ij}\gamma_{Y,ij}Y_{c,ij}$ and $f_{Y,ij}(x_i,x_j) = x_i x_j\frac{x_i+x_j}{\beta_{Y,ij}^2 x_i + x_j}$

combining rules for $Y_{c,ij}$

$$\frac{1}{\rho_{c,ij}} = \frac{1}{8}\left(\frac{1}{\rho_{c,i}^{1/3}} + \frac{1}{\rho_{c,j}^{1/3}}\right)^3 \quad \text{for } Y = v \quad \text{and} \quad T_{c,ij} = (T_{c,i}\cdot T_{c,j})^{0.5} \quad \text{for } Y = T$$

derivatives of $Y_r = Y_r(\bar{x})$ with respect to x_i

$$\left(\frac{\partial Y_r}{\partial x_i}\right)_{x_j} = 2x_i Y_{c,i} + \sum_{k=1}^{i-1} c_{Y,ki}\frac{\partial f_{Y,ki}(x_k,x_i)}{\partial x_i} + \sum_{k=i+1}^{N} c_{Y,ik}\frac{\partial f_{Y,ik}(x_i,x_k)}{\partial x_i}$$

$$\left(\frac{\partial^2 Y_r}{\partial x_i^2}\right)_{x_j} = 2Y_{c,i} + \sum_{k=1}^{i-1} c_{Y,ki}\frac{\partial^2 f_{Y,ki}(x_k,x_i)}{\partial x_i^2} + \sum_{k=i+1}^{N} c_{Y,ik}\frac{\partial^2 f_{Y,ik}(x_i,x_k)}{\partial x_i^2}$$

$$\left(\frac{\partial^2 Y_r}{\partial x_i\partial x_j}\right) = c_{Y,ij}\frac{\partial^2 f_{Y,ij}(x_i,x_j)}{\partial x_i\partial x_j} \qquad i \neq j$$

derivatives of $f_{Y,ki}(x_k,x_i)$, $f_{Y,ik}(x_i,x_k)$, and $f_{Y,ij}(x_i,x_j)$ with respect to x_i

$$\left(\frac{\partial f_{Y,ki}(x_k,x_i)}{\partial x_i}\right)_{x_k} = x_k\frac{x_k+x_i}{\beta_{Y,ki}^2 x_k + x_i} + x_k x_i\frac{1}{\beta_{Y,ki}^2 x_k + x_i}\left(1 - \frac{x_k+x_i}{\beta_{Y,ki}^2 x_k + x_i}\right)$$

$$\left(\frac{\partial f_{Y,ik}(x_i,x_k)}{\partial x_i}\right)_{x_k} = x_k\frac{x_i+x_k}{\beta_{Y,ik}^2 x_i + x_k} + x_i x_k\frac{1}{\beta_{Y,ik}^2 x_i + x_k}\left(1 - \beta_{Y,ik}^2\frac{x_i+x_k}{\beta_{Y,ik}^2 x_i + x_k}\right)$$

$$\left(\frac{\partial^2 f_{Y,ki}(x_k,x_i)}{\partial x_i^2}\right)_{x_k} = \frac{1}{\beta_{Y,ki}^2 x_k + x_i}\left(1 - \frac{x_k+x_i}{\beta_{Y,ki}^2 x_k + x_i}\right)\cdot\left(2x_k - x_k x_i\frac{2}{\beta_{Y,ki}^2 x_k + x_i}\right)$$

$$\left(\frac{\partial^2 f_{Y,ik}(x_i,x_k)}{\partial x_i^2}\right)_{x_k} = \frac{1}{\beta_{Y,ik}^2 x_i + x_k}\left(1 - \beta_{Y,ik}^2\frac{x_i+x_k}{\beta_{Y,ik}^2 x_i + x_k}\right)\cdot\left(2x_k - x_i x_k\frac{2\beta_{Y,ik}^2}{\beta_{Y,ik}^2 x_i + x_k}\right)$$

$$\left(\frac{\partial^2 f_{Y,ij}(x_i,x_j)}{\partial x_i\partial x_j}\right) = \frac{x_i+x_j}{\beta_{Y,ij}^2 x_i + x_j} + x_j\frac{1}{\beta_{Y,ij}^2 x_i + x_j}\left(1 - \frac{x_i+x_j}{\beta_{Y,ij}^2 x_i + x_j}\right) + x_i\frac{1}{\beta_{Y,ij}^2 x_i + x_j}\left(1 - \beta_{Y,ij}^2\frac{x_i+x_j}{\beta_{Y,ij}^2 x_i + x_j}\right) - x_i x_j\frac{1}{(\beta_{Y,ij}^2 x_i + x_j)^2}\left(1 + \beta_{Y,ij}^2 - 2\beta_{Y,ij}^2\frac{x_i+x_j}{\beta_{Y,ij}^2 x_i + x_j}\right)$$

[a] $\gamma_{Y,ji} = \gamma_{Y,ij}$ and $\beta_{Y,ji} = 1/\beta_{Y,ij}$.

The structure of the new mixture model was kept as simple as possible to allow for the development of computing-time saving algorithms and an easy expansion to additional components.

With the development of the GERG-2008 wide-range equation of state, the final assembly of a property database with applications for natural gases and other mixtures over the entire fluid region has been accomplished. This new equation of state will be adopted as an ISO Standard (ISO 20765-2/3) for natural gases (gas phase, liquid phase, VLE) by the end of 2012.

APPENDIX A: NUMERICAL INFORMATION ON GERG-2008

Tables A1 to A8 give complete numerical information on the equation of state GERG-2008.

APPENDIX B: THERMODYNAMIC EQUATIONS

Tables B1 to B9 cover all of the thermodynamic equations that are necessary for calculating the several thermodynamic

dx.doi.org/10.1021/je300655b | J. Chem. Eng. Data 2012, 57, 3032−3091

properties in the homogeneous gas and liquid regions and for the vapor−liquid-equilibrium as well.

AUTHOR INFORMATION

Corresponding Author

*E-mail: wagner@thermo.rub.de.

Present Address

[†]RWE Supply & Trading GmbH, Altenessener Str. 27, D-45141 Essen, Germany.

Funding

The authors are grateful to the members of the GERG Working Groups 1.34 and 1.46 for the financial support of the respective research projects and for their very helpful collaboration. In particular, we thank very much Manfred Jaeschke, the chairman of the two GERG Working Groups, for his long lasting support. Our thanks also go to the companies E.ON Ruhrgas AG, Germany, and Statoil ASA, Norway, for their financial support of the development of parts of the software packages for the GERG-2008 equation of state. We are also indebted to the Deutsche Forschungsgemeinschaft (German Research Association) for their financial support of the development of parts of the equations of state GERG-2004 and GERG-2008. We are particularly grateful to these organizations and companies for their patience because all of the parts of the total project have taken much more time than estimated at the beginning.

Notes

The authors declare no competing financial interest.

ACKNOWLEDGMENTS

We are grateful to all of the experimentalists who carried out measurements for this equation-of-state project, as well as to those who provided us with recently measured data prior to their publication or with (older) data that are not available in the open literature. Our special thanks go to Michael L. Michelsen from the Technical University of Denmark (Lyngby, Denmark) for providing his computer codes of algorithms for phase-equilibrium calculations based on cubic equations of state and for his help in understanding the sophisticated procedures. We also thank Eric W. Lemmon for carefully reading the manuscript, for a number of suggestions on improving the English style and for valuable subject-specific comments. We are also grateful to Renate Gölzenleuchter for producing the final version of the figures.

REFERENCES

(1) Kunz, O.; Klimeck, R.; Wagner, W.; Jaeschke, M. *The GERG-2004 wide-range equation of state for natural gases and other mixtures*; GERG TM15, 2007; Fortschr.-Ber. VDI, Reihe 6, Nr. 557, VDI Verlag: Düsseldorf, 2007. Also available as GERG Technical Monograph 15, 2007.

(2) Jaeschke, M.; Humphreys, A. E. *Standard GERG virial equation for field use. Simplification of the input data requirements for the GERG virial equation − an alternative means of compressibility factor calculation for natural gases and similar mixtures*; Fortschr.-Ber. VDI, Reihe 6, Nr. 266, VDI-Verlag: Düsseldorf, 1992. Also available as GERG Technical Monograph 5, 1991.

(3) Peng, D.-Y.; Robinson, D. B. A new two-constant equation of state. *Ind. Eng. Chem. Fundam.* **1976**, *15*, 59−64.

(4) McCarty, R. D. Mathematical models for the prediction of liquefied-natural-gas densities. *J. Chem. Thermodyn.* **1982**, *14*, 837−854.

(5) ISO 20765-1. *Natural gas—Calculation of thermodynamic properties—Part 1: Gas phase properties for transmission and distribution applications*; ISO Copyright Office: Geneva, 2005.

(6) Starling, K. E.; Savidge, J. L. *Compressibility factors of natural gas and other related hydrocarbon gases*; Transmission Measurement Committee Report No. 8, 2nd ed.; American Gas Association: Washington, DC, 1992.

(7) Jaeschke, M.; Schley, P. Berechnung des Realgasfaktors von Erdgasen mit der AGA8-DC92 Zustandsgleichung. II. Vergleich mit Messwerten. *GWF Gas Erdgas* **1996**, *137*, 420−425.

(8) (a) ISO 12213-2:2006. *Natural gas—Calculation of compression factor—Part 2: Calculation using molar-composition analysis*; ISO Copyright Office: Geneva, 2005. (b) Lemmon, E. W.; Ortiz-Vega, D. O.; Starling, K. E.; Hall, K. R.; Wagner, W. Deviations between the AGA-8 and GERG-2008 equations of state for natural gases. Natural Gas Sampling Technology Conference (NGSTech), New Orleans, LA, January 26, 2011.

(9) Klimeck, R.; Span, R.; Kleinrahm, R.; Wagner, W. *Fundamental equation for calorific properties. Collecting of data and test of existing equations*; Final report to GERG WG 1.3, Lehrstuhl fuer Thermodynamik; Ruhr-University Bochum: Bochum, Germany, 1996.

(10) Setzmann, U.; Wagner, W. A new equation of state and tables of thermodynamic properties for methane covering the range from the melting line to 625 K at pressures up to 1000 MPa. *J. Phys. Chem. Ref. Data* **1991**, *20*, 1061−1155.

(11) Aavatsmark, I. *Mathematische Einführung in die Thermodynamik der Gemische*; Akademie Verlag: Berlin, 1995.

(12) Tillner-Roth, R. *Die thermodynamischen Eigenschaften von R152a, R134a und ihren Gemischen—Messungen und Fundamentalgleichungen*; Forschungsberichte des Deutschen Kälte-und Klimatechnischen Vereins (DKV), Nr. 41: Stuttgart, 1993.

(13) Lemmon, E. W. A generalized model for the prediction of the thermodynamic properties of mixtures including vapor-liquid equilibrium. Ph.D. Dissertation, University of Idaho, Moscow, ID, 1996.

(14) Tillner-Roth, R.; Friend, D. G. A Helmholtz free energy formulation of the thermodynamic properties of the mixture {water + ammonia}. *J. Phys. Chem. Ref. Data* **1998**, *27*, 63−96.

(15) Lemmon, E. W.; Jacobsen, R. T; Penoncello, S. G.; Friend, D. G. Thermodynamic properties of air and mixtures of nitrogen, argon, and oxygen from 60 to 2000 K at pressures to 2000 MPa. *J. Phys. Chem. Ref. Data* **2000**, *29*, 331−385.

(16) Miyamoto, H.; Watanabe, K. Helmholtz-type equations of state for hydrocarbon refrigerant mixtures of propane/*n*-butane, propane/isobutane, *n*-butane/isobutane, and propane/*n*-butane/isobutane. *Int. J. Thermophys.* **2003**, *24*, 1007−1031.

(17) Lemmon, E. W.; Jacobsen, R. T Equations of state for mixtures of R-32, R-125, R-134a, R-143a, and R-152a. *J. Phys. Chem. Ref. Data* **2004**, *33*, 593−620.

(18) Tillner-Roth, R.; Li, J.; Yokozeki, A.; Sato, H.; Watanabe, K. *Thermodynamic properties of pure and blended hydrofluorocarbon (HFC) refrigerants*; Japan Society of Refrigerating and Air Conditioning Engineers: Tokyo, 1998.

(19) Tillner-Roth, R. *Fundamental equations of state*; Shaker Verlag: Aachen, 1998.

(20) Lemmon, E. W.; Tillner-Roth, R. A Helmholtz energy equation of state for calculating the thermodynamic properties of fluid mixtures. *Fluid Phase Equilib.* **1999**, *165*, 1−21.

(21) Lemmon, E. W.; Jacobsen, R. T. A generalized model for the thermodynamic properties of mixtures. *Int. J. Thermophys.* **1999**, *20*, 825−835.

(22) Klimeck, R. Entwicklung einer Fundamentalgleichung für Erdgase für das Gas- und Flüssigkeitsgebiet sowie das Phasengleichgewicht. Ph.D. Dissertation, Fakultät für Maschinenbau, Ruhr-Universität Bochum, Bochum, Germany, 2000.

(23) Span, R.; Wagner, W. Equations of state for technical applications. II. Results for nonpolar fluids. *Int. J. Thermophys.* **2003**, *24*, 41−109.

(24) Lemmon, E. W.; Span, R. Short fundamental equations of state for 20 industrial fluids. *J. Chem. Eng. Data* **2006**, *51*, 785−850.

(25) Jaeschke, M.; Schley, P. Ideal-gas thermodynamic properties for natural-gas applications. *Int. J. Thermophys.* **1995**, *16*, 1381−1392.

(26) Jaeschke, M.; Hinze, H.-M.; Humphreys, A. E. *Supplement to the GERG databank of high-accuracy compression factor measurements*; Fortschr.-Ber. VDI, Reihe 6, Nr. 355; VDI-Verlag: Düsseldorf, 1997. Also available as GERG Technical Monograph 7, 1996. Data partly

published in: Jaeschke, M.; Humphreys, A. E. *The GERG databank of high accuracy compressibility factor measurements*; Fortschr.-Ber. VDI, Reihe 6, Nr. 251, VDI-Verlag: Düsseldorf, 1991. Also available as GERG Technical Monograph 4, 1990.

(27) Glos, S.; Kleinrahm, R.; Wagner, W. Density measurements on the binary gas mixture (CH_4 + CO_2) at temperatures 273.15 and 290 K and pressures up to 9.5 MPa. In *Density measurements on ethane and propane in the temperature range from 340 to 520 K at pressures up to 30 MPa*; Report to GERG WG 1.34; Claus, P., Kleinrahm, R., Wagner, W., Eds.; Lehrstuhl für Thermodynamik, Ruhr-Universität Bochum: Bochum, Germany, 2001.

(28) Chamorro, C. R.; Segovia, J. J.; Martín, M. C.; Villamañán, M. A.; Estela-Uribe, J. F.; Trusler, J. P. M. Measurement of the (pressure, density, temperature) relation of two (methane + nitrogen) gas mixtures at temperatures between 240 and 400 K and pressures up to 20 MPa using an accurate single-sinker densimeter. *J. Chem. Thermodyn.* **2006**, *38*, 916−922.

(29) Costa Gomes, M. F.; Trusler, J. P. M. The speed of sound in two methane-rich gas mixtures at temperatures between 250 and 350 K and at pressures up to 20 MPa. *J. Chem. Thermodyn.* **1998**, *30*, 1121−1129.

(30) Estela-Uribe, J. F. *Equation of state for natural gas systems*. Ph.D. Thesis, Department of Chemical Engineering and Chemical Technology, Imperial College, London, 1999.

(31) Trusler, J. P. M. *Speeds of sound in the gas mixtures: {(1−x)CH_4 + xN_2} with x = 0.1 or 0.2 and {(1−x)C_2H_6 + xN_2} with x = 0.3 or 0.7*; Report to GERG WG 1.34; Department of Chemical Engineering and Chemical Technology, Imperial College: London, 2000.

(32) Hiza, M. J.; Haynes, W. M.; Parrish, W. R. Orthobaric liquid densities and excess volumes for binary mixtures of low molar-mass alkanes and nitrogen between 105 and 140 K. *J. Chem. Thermodyn.* **1977**, *30*, 873−896.

(33) Hiza, M. J.; Haynes, W. M. Orthobaric liquid densities and excess volumes for multi-component mixtures of low molar-mass alkanes and nitrogen between 105 and 125 K. *J. Chem. Thermodyn.* **1980**, *12*, 1−10.

(34) Haynes, W. M. Measurements of orthobaric-liquid densities of multi-component mixtures of LNG components (N_2, CH_4, C_2H_6, C_3H_8, $CH_3CH(CH_3)CH_3$, C_4H_{10}, $CH_3CH(CH_3)C_2H_5$, and C_5H_{12}) between 110 and 130 K. *J. Chem. Thermodyn.* **1982**, *14*, 603−612.

(35) Haynes, W. M. Orthobaric liquid densities and dielectric constants of (methane + 2-methyl-propane) and (methane + *n*-butane) at low temperatures. *J. Chem. Thermodyn.* **1983**, *15*, 903−911.

(36) Raabe, G.; Janisch, J.; Koehler, J. Experimental studies of phase equilibria in mixtures relevant for the description of natural gases. *Fluid Phase Equilib.* **2001**, *185*, 199−208.

(37) Webster, L. A.; Kidnay, A. J. Vapor-liquid equilibria for the methane−propane−carbon dioxide systems at 230 and 270 K. *J. Chem. Eng. Data* **2001**, *46*, 759−764.

(38) VonNiederhausern, D. M.; Giles, N. F. *Vapor-liquid equilibrium measurements on propane, n-butane, isobutane, ethane, n-pentane and n-hexane*; Research Report RR-179, GPA Project 012; Gas Processors Association: Tulsa, 2001.

(39) Lim, J. S.; Ho, Q. N.; Park, J.-Y.; Lee, B. G. Measurement of vapor-liquid equilibria for the binary mixture of propane (R-290) + isobutane (R-600a). *J. Chem. Eng. Data* **2004**, *49*, 192−198.

(40) McLinden, M. O. *p-ρ-T* behavior of four lean natural-gas-like mixtures from 250 to 450 K with pressures to 37 MPa. *J. Chem. Eng. Data* **2011**, *56*, 606−613.

(41) Atilhan, M.; Aparicio, S.; Ejaz, S.; Cristancho, D.; Hall, K. R. *pρT* behavior of a lean synthetic natural gas mixture using magnetic suspension densimeters and an isochoric apparatus: Part I. *J. Chem. Eng. Data* **2011**, *56*, 212−221.

(42) Atilhan, M.; Aparicio, S.; Ejaz, S.; Cristancho, D.; Mantilla, I.; Hall, K. R. *p-ρ-T* behavior of three lean synthetic natural gas mixtures using magnetic suspension densimeter and isochoric apparatus from 250 to 450 K with pressures up to 150 MPa: Part II. *J. Chem. Eng. Data* **2011**, *56*, 3766−3774.

(43) Rousseaux, P.; Richon, D.; Renon, H. A static method for determination of vapour-liquid equilibria and saturated liquid molar volumes at high pressures and temperatures using a new variable-volume cell. *Fluid Phase Equilib.* **1983**, *11*, 153−168.

(44) Schlichting, H.; Langhorst, R.; Knapp, H. Saturation of high pressure gases with low volatile solvents: experiments and correlation. *Fluid Phase Equilib.* **1993**, *84*, 143−163.

(45) Shipman, L. M.; Kohn, J. P. Heterogeneous phase and volumetric equilibrium in the methane−*n*-nonane system. *J. Chem. Eng. Data* **1966**, *11*, 176−180.

(46) Audonnet, F.; Pádua, A. A. H. Viscosity and density of mixtures of methane and *n*-decane from 298 to 393 K and up to 75 MPa. *Fluid Phase Equilib.* **2004**, *216*, 235−244.

(47) Beaudoin, J. M.; Kohn, J. P. Multiphase and volumetric equilibria of the methane−*n*-decane binary system at temperatures between −36° and 150 °C. *J. Chem. Eng. Data* **1967**, *12*, 189−191.

(48) Canet, X.; Baylaucq, A.; Boned, C. High-pressure (up to 140 MPa) dynamic viscosity of the methane + decane system. *Int. J. Thermophys.* **2002**, *23*, 1469−1486.

(49) D'Avila, S. G.; Kaul, B. K.; Prausnitz, J. M. Solubilities of heavy hydrocarbons in compressed methane and nitrogen. *J. Chem. Eng. Data* **1976**, *21*, 488−491.

(50) Koonce, K. T.; Kobayashi, R. A method for determining the solubility of gases in relatively nonvolatile liquids. Solubility of methane in *n*-decane. *J. Chem. Eng. Data* **1964**, *9*, 490−494.

(51) Lin, H.-M.; Sebastian, H. M.; Simnick, J. J.; Chao, K.-C. Gas-liquid equilibrium in binary mixtures of methane with *n*-decane, benzene, and toluene. *J. Chem. Eng. Data* **1979**, *24*, 146−149.

(52) Reamer, H. H.; Olds, R. H.; Sage, B. H.; Lacey, W. N. Phase equilibria in hydrocarbon systems. Methane−decane system. *Ind. Eng. Chem.* **1942**, *34*, 1526−1531.

(53) Rijkers, M. P. W. M.; Malais, M.; Peters, C. J.; de Swaan Arons, J. Measurements on the phase behavior of binary hydrocarbon mixtures for modelling the condensation behavior of natural gas. Part I. The system methane + decane. *Fluid Phase Equilib.* **1992**, *71*, 143−168.

(54) Sage, B. H.; Lavender, H. M.; Lacey, W. N. Phase equilibria in hydrocarbon systems. Methane−decane system. *Ind. Eng. Chem.* **1940**, *32*, 743−747.

(55) Srivastan, S.; Darwish, N. A.; Gasem, K. A. M.; Robinson, R. L., Jr. Solubility of methane in hexane, decane, and dodecane at temperatures from 311 to 423 K and pressures to 10.4 MPa. *J. Chem. Eng. Data* **1992**, *37*, 516−520.

(56) Wiese, H. C.; Reamer, H. H.; Sage, B. H. Phase equilibria in hydrocarbon systems. Phase behavior in the methane−propane−*n*-decane system. *J. Chem. Eng. Data* **1970**, *15*, 75−82.

(57) Bailey, D. M.; Liu, C. H.; Holste, J. C.; Hall, K. R.; Eubank, P. T.; Marsh, K. M. *Thermodynamic properties of pure hydrogen sulfide and mixtures containing hydrogen sulfide with methane, carbon dioxide, methylcyclohexane and toluene*; Research Report RR-107, Project 792; Gas Processors Association, Tulsa, OK, 1987.

(58) Kohn, J. P.; Kurata, F. Heterogeneous phase equilibria of the methane−hydrogen sulfide system. *AIChE J.* **1958**, *4*, 211−217.

(59) Kohn, J. P.; Kurata, F. Volumetric behavior of the methane−hydrogen sulfide system at low temperatures and high pressures. *J. Chem. Eng. Data* **1959**, *4*, 33−36.

(60) Reamer, H. H.; Sage, B. H.; Lacey, W. N. Phase equilibria in hydrocarbon systems. Volumetric and phase behavior of the methane−hydrogen sulfide system. *Ind. Eng. Chem.* **1951**, *43*, 976−981.

(61) Seelbach, M. Kalibrierung einer neuen Versuchsanlage mit Magnetschwebekupplung für die simultane Adsorptions- und Dichtemessung und Untersuchung der Koadsorptionsgleichgewichte von CH_4/H_2S Mischungen an einem Zeolith. Diploma Thesis, Lehrstuhl für Thermodynamik, Universität Gesamthochschule Siegen, Siegen, 1999.

(62) Seelbach, M. Private communication to M. Jaeschke. Institut für Fluid- und Thermodynamik, Universität Siegen, Siegen, 2001.

(63) Llave, F. M.; Chung, T. H. Vapor-liquid equilibria of nitrogen−hydrocarbon systems at elevated pressures. *J. Chem. Eng. Data* **1988**, *33*, 123−128.

(64) Silva-Oliver, G.; Eliosa-Jiménez, G.; García-Sánchez, F.; Avendaño-Gómez, J. R. High-pressure vapor-liquid equilibria in the nitrogen−*n*-nonane system. *J. Supercrit. Fluids* **2007**, *42*, 36−47.

(65) Azarnoosh, A.; McKetta, J. J. Nitrogen−*n*-decane system in the two-phase region. *J. Chem. Eng. Data* **1963**, *8*, 494−496.
(66) Pearce, D. L.; Peters, C. J.; de Swaan Arons, J. Measurement of the gas phase solubility of decane in nitrogen. *Fluid Phase Equilib.* **1993**, *89*, 335−343.
(67) Prausnitz, J. M.; Benson, P. R. Solubility of liquids in compressed hydrogen, nitrogen, and carbon dioxide. *AIChE J.* **1959**, *5*, 161−164.
(68) Tong, J.; Gao, W.; Robinson, R. L., Jr.; Gasem, K. A. M. Solubilities of nitrogen in heavy normal paraffins from 323 to 423 K at pressures to 18.0 MPa. *J. Chem. Eng. Data* **1999**, *44*, 784−787.
(69) Besserer, G. J.; Robinson, D. B. Equilibrium-phase properties of nitrogen−hydrogen sulfide system. *J. Chem. Eng. Data* **1975**, *20*, 157−161.
(70) Kalra, H.; Krishnan, T. R.; Robinson, D. B. Equilibrium-phase properties of carbon dioxide−*n*-butane and nitrogen−hydrogen sulfide systems at subambient temperatures. *J. Chem. Eng. Data* **1976**, *21*, 222−225.
(71) Robinson, D. B.; Hamaliuk, G. P.; Krishnan, T. R.; Bishnoi, P. R. Compressibility factors of nitrogen−hydrogen sulfide mixtures. *J. Chem. Eng. Data* **1975**, *20*, 153−157.
(72) Camacho-Camacho, L. E.; Galicia-Luna, L. A.; Elizalde-Solis, O.; Martínez-Ramírez, Z. New isothermal vapor-liquid equilibria for the CO_2 + *n*-nonane, and CO_2 + *n*-undecane systems. *Fluid Phase Equilib.* **2007**, *259*, 45−50.
(73) Choi, E.-J.; Yeo, S.-D. Critical properties for carbon dioxide + *n*-alkane mixtures using a variable-volume view cell. *J. Chem. Eng. Data* **1998**, *43*, 714−716.
(74) Jennings, D. W.; Schucker, R. C. Comparison of high-pressure vapor-liquid equilibria of mixtures of CO_2 or propane with nonane and C_9 alkylbenzenes. *J. Chem. Eng. Data* **1996**, *41*, 831−838.
(75) Bessières, D.; Saint-Guirons, H.; Daridon, J.-L. Volumetric behavior of decane + carbon dioxide at high pressures. Measurement and calculation. *J. Chem. Eng. Data* **2001**, *46*, 1136−1139.
(76) Chou, G. F.; Forbert, R. R.; Prausnitz, J. M. High-pressure vapor-liquid equilibria for CO_2/*n*-decane, CO_2/tetralin, and CO_2/*n*-decane/tetralin at 71.1 and 104.4 °C. *J. Chem. Eng. Data* **1990**, *35*, 26−29.
(77) Cullick, A. S.; Mathis, M. L. Densities and viscosities of mixtures of carbon dioxide and *n*-decane from 310 to 403 K and 7 to 30 MPa. *J. Chem. Eng. Data* **1984**, *29*, 393−396.
(78) Inomata, H.; Tuchiya, K.; Arai, K.; Saito, S. Measurement of vapor-liquid equilibria at elevated temperatures and pressures using a flow type apparatus. *J. Chem. Eng. Jpn.* **1986**, *19*, 386−391.
(79) Iwai, Y.; Hosotani, N.; Morotomi, T.; Koga, Y.; Arai, Y. High-pressure vapor-liquid equilibria for carbon dioxide + linalool. *J. Chem. Eng. Data* **1994**, *39*, 900−902.
(80) Jiménez-Gallegos, R.; Galicia-Luna, L. A.; Elizalde-Solis, O. Experimental vapor-liquid equilibria for the carbon dioxide + octane and carbon dioxide + decane systems. *J. Chem. Eng. Data* **2006**, *51*, 1624−1628.
(81) Nagarajan, N.; Robinson, R. L., Jr. Equilibrium phase compositions, phase densities, and interfacial tensions for CO_2 + hydrocarbon systems. 2. CO_2 + *n*-decane. *J. Chem. Eng. Data* **1986**, *31*, 168−171.
(82) Polikhronidi, N. G.; Batyrova, R. G. P-V-T measurements of *n*-decane−CO_2 binary system. *High Temperature* **1997**, *35*, 537−541.
(83) Reamer, H. H.; Sage, B. H. Phase equilibria in hydrocarbon systems. Volumetric and phase behavior of the *n*-decane−CO_2 system. *J. Chem. Eng. Data* **1963**, *8*, 508−513.
(84) Reamer, H. H.; Sage, B. H. Partial volumetric behavior in hydrocarbon systems. *n*-decane and carbon dioxide in the liquid phase of the *n*-decane−carbon dioxide system. *J. Chem. Eng. Data* **1965**, *10*, 49−57.
(85) Sebastian, H. M.; Simnick, J. J.; Lin, H.-M.; Chao, K.-C. Vapor-liquid equilibrium in binary mixtures of carbon dioxide + *n*-decane and carbon dioxide + *n*-hexadecane. *J. Chem. Eng. Data* **1980**, *25*, 138−140.
(86) Shaver, R. D.; Robinson, R. L., Jr.; Gasem, K. A. M. An automated apparatus for equilibrium phase compositions, densities, and interfacial tensions: data for carbon dioxide + decane. *Fluid Phase Equilib.* **2001**, *179*, 43−66.
(87) Tsuji, T.; Tanaka, S.; Hiaki, T.; Saito, R. Measurements of bubble point pressure for CO_2 + decane and CO_2 + lubricating oil. *Fluid Phase Equilib.* **2004**, *219*, 87−92.
(88) Zúñiga-Moreno, A.; Galicia-Luna, L. A.; Camacho-Camacho, L. E. Compressed liquid densities and excess volumes of CO_2 + decane mixtures from (313 to 363) K and pressures up to 25 MPa. *J. Chem. Eng. Data* **2005**, *50*, 1030−1037.
(89) Bierlein, J. A.; Kay, W. B. Phase-equilibrium properties of system carbon dioxide−hydrogen sulfide. *Ind. Eng. Chem.* **1953**, *45*, 618−624.
(90) Robinson, R. L., Jr.; Jacoby, R. H. Better compressibility factors. *Hydrocarbon Process. Pet. Refin.* **1965**, *44*, 141−145.
(91) Sobocinski, D. P.; Kurata, F. Heterogeneous phase equilibria of the hydrogen sulfide−carbon dioxide system. *AIChE J.* **1959**, *5*, 545−551.
(92) Stouffer, C. E.; Kellerman, S. J.; Hall, K. R.; Holste, J. C.; Gammon, B. E.; Marsh, K. N. Densities of carbon dioxide + hydrogen sulfide mixtures from 220 to 450 K at pressures up to 25 MPa. *J. Chem. Eng. Data* **2001**, *46*, 1309−1318.
(93) Bufkin, B. A.; Robinson, R. L., Jr.; Estrera, S. S.; Luks, K. D. Solubility of ethane in *n*-decane at pressures to 8.2 MPa and temperatures from 278 to 411 K. *J. Chem. Eng. Data* **1986**, *31*, 421−423.
(94) Gardeler, H.; Fischer, K.; Gmehling, J. Experimental determination of vapor-liquid equilibrium data for asymmetric systems. *Ind. Eng. Chem. Res.* **2002**, *41*, 1051−1056.
(95) Reamer, H. H.; Sage, B. H. Phase equilibria in hydrocarbon systems. Volumetric and phase behavior of the ethane−*n*-decane system. *J. Chem. Eng. Data* **1962**, *7*, 161−168.
(96) Kalra, H.; Robinson, D. B.; Krishnan, T. R. The equilibrium phase properties of the ethane−hydrogen sulfide system at subambient temperatures. *J. Chem. Eng. Data* **1977**, *22*, 85−88.
(97) Kay, W. B.; Brice, D. B. Liquid-vapor equilibrium relations in ethane−hydrogen sulfide system. *Ind. Eng. Chem.* **1953**, *45*, 615−618.
(98) Lobo, L. Q.; Ferreira, A. G. M.; Fonseca, I. M. A.; Senra, A. M. P. Vapour pressure and excess Gibbs free energy of binary mixtures of hydrogen sulphide with ethane, propane, and *n*-butane at temperature of 182.33 K. *J. Chem. Thermodyn.* **2006**, *38*, 1651−1654.
(99) Lobo, L. Q.; Ferreira, A. G. M.; Fonseca, I. M. A.; Senra, A. M. P. Corrigendum to "Vapour pressure and excess Gibbs free energy of binary mixtures of hydrogen sulphide with ethane, propane, and n-butane at temperature of 182.33 K", see ref 92. [*J. Chem. Thermodyn.* 2006, *38*, 1651−1654]. *J. Chem. Thermodyn.* **2007**, *39*, 990.
(100) Rivollet, F.; Jarne, C.; Richon, D. $p\rho T$ and VLE for ethane + hydrogen sulfide from (254.05 to 363.21) K at pressures up to 20 MPa. *J. Chem. Eng. Data* **2005**, *50*, 1883−1890.
(101) Robinson, D. B.; Kalra, H. *The equilibrium phase properties of selected binary systems at low temperature: nitrogen−hydrogen sulfide, ethane−hydrogen sulfide, n-butane−carbon dioxide*; Research Report RR-15, Project 738; Gas Processors Association: Tulsa, OK, 1975.
(102) Reamer, H. H.; Sage, B. H. Phase equilibria in hydrocarbon systems. Volumetric and phase behavior of the propane−*n*-decane system. *J. Chem. Eng. Data* **1966**, *11*, 17−24.
(103) Tiffin, D. L.; Kohn, J. P.; Luks, K. D. Three-phase solid-liquid-vapor equilibria of the binary hydrocarbon systems ethane−2-methylnaphthalene, ethane−naphthalene, propane−*n*-decane, and propane−*n*-dodecane. *J. Chem. Eng. Data* **1979**, *24*, 98−100.
(104) Brewer, J.; Rodewald, N.; Kurata, F. Phase equilibria of the propane−hydrogen sulfide system from the cricondontherm to the solid-liquid-vapor region. *AIChE J.* **1961**, *7*, 13−16.
(105) Gilliland, E. R.; Scheeline, H. W. High-pressure vapor-liquid equilibrium for the systems propylene−isobutane and propane−hydrogen sulfide. *Ind. Eng. Chem.* **1940**, *32*, 48−54.
(106) Kay, W. B.; Rambosek, G. M. Liquid-vapor equilibrium relations in binary systems. Propane−hydrogen sulfide system. *Ind. Eng. Chem.* **1953**, *5*, 221−226.
(107) Reamer, H. H.; Sage, B. H. Phase equilibria in hydrocarbon systems. Phase behavior in the *n*-butane−*n*-decane system. *J. Chem. Eng. Data* **1964**, *9*, 24−28.

(108) Reamer, H. H.; Sage, B. H.; Lacey, W. N. Phase equilibria in hydrocarbon systems. *n*-Butane−decane system in the condensed region. *Ind. Eng. Chem.* **1946**, *38*, 986−989.
(109) Leu, A.-D.; Robinson, D. B. Equilibrium phase properties of the *n*-butane−hydrogen sulfide and isobutane−hydrogen sulfide binary systems. *J. Chem. Eng. Data* **1989**, *34*, 315−319.
(110) Besserer, G. J.; Robinson, D. B. The equilibrium phase properties of the *i*-butane−hydrogen sulfide system. *J. Chem. Eng. Jpn.* **1975**, *8*, 11−15.
(111) Aucejo, A.; Burguet, M. C.; Munoz, R.; Marques, J. L. Densities, viscosities, and refractive indices of some *n*-alkane binary liquid systems at 298.15 K. *J. Chem. Eng. Data* **1995**, *40*, 141−147.
(112) Rice, P.; El-Nikheli, A. Isothermal vapour-liquid equilibrium data for the systems *n*-pentane with *n*-hexane, *n*-octane and *n*-decane. *Fluid Phase Equilib.* **1995**, *107*, 257−267.
(113) Reamer, H. H.; Sage, B. H.; Lacey, W. N. Phase equilibria in hydrocarbon systems. Volumetric and phase behavior of n-pentane−hydrogen sulfide system. *Ind. Eng. Chem.* **1953**, *45*, 1805−1809.
(114) Leu, A.-D.; Robinson, D. B. High-pressure vapor-liquid equilibrium phase properties of the isopentane−hydrogen sulfide and neopentane−hydrogen sulfide binary systems. *J. Chem. Eng. Data* **1992**, *37*, 14−17.
(115) Chevalier, J. L. E.; Petrino, P. J.; Gaston-Bonhomme, Y. H. Viscosity and density of some aliphatic, cyclic, and aromatic hydrocarbons binary liquid mixtures. *J. Chem. Eng. Data* **1990**, *35*, 206−212.
(116) Goates, J. R.; Ott, J. B.; Grigg, R. B. Excess volumes of *n*-hexane + *n*-heptane, + *n*-octane, + *n*-nonane, and + *n*-decane at 283.15, 298.15, and 313.15 K. *J. Chem. Thermodyn.* **1981**, *13*, 907−913.
(117) Cooper, E. F.; Asfour, A.-F. A. Densities and kinematic viscosities of some C_6−C_{16} *n*-alkane binary liquid systems at 293.15 K. *J. Chem. Eng. Data* **1991**, *36*, 285−288.
(118) Marsh, K. N.; Ott, J. B.; Costigan, M. J. Excess enthalpies, excess volumes, and excess Gibbs free energies for (*n*-hexane + *n*-decane) at 298.15 and 308.15 K. *J. Chem. Thermodyn.* **1980**, *12*, 343−348.
(119) Takagi, T.; Teranishi, H. Ultrasonic speeds and thermodynamics for binary solutions of n-alkanes under high pressures. *Fluid Phase Equilib.* **1985**, *20*, 315−320.
(120) Tripathi, N. Densities, viscosities, and refractive indices of mixtures of hexane with cyclohexane, decane, hexadecane, and squalane at 298.15 K. *Int. J. Thermophys.* **2005**, *26*, 693−703.
(121) Laugier, S.; Richon, D. Vapor-liquid equilibria for hydrogen sulfide + hexane, + cyclohexane, + benzene, + pentadecane, and + (hexane + pentadecane). *J. Chem. Eng. Data* **1995**, *40*, 153−159.
(122) Ng, H.-J.; Kalra, H.; Robinson, D. B.; Kubota, H. Equilibrium phase properties of the toluene−hydrogen sulfide and *n*-heptane−hydrogen sulfide binary systems. *J. Chem. Eng. Data* **1980**, *25*, 51−55.
(123) Théveneau, P.; Coquelet, C.; Richon, D. Vapour-liquid equilibrium data for the hydrogen sulphide + *n*-heptane system at temperatures from 293.25 to 373.22 K and pressures up to about 6.9 MPa. *Fluid Phase Equilib.* **2006**, *249*, 179−186.
(124) Dejoz, A.; González-Alfaro, V.; Miguel, P. J.; Vázquez, M. I. Isobaric vapor-liquid equilibria for binary systems composed of octane, decane, and dodecane at 20 kPa. *J. Chem. Eng. Data* **1996**, *41*, 93−96.
(125) Eakin, B. E.; DeVaney, W. E. Vapor-liquid equilibria in hydrogen−hydrogen sulfide−C9 hydrocarbon systems. *AIChE Symp. Ser.* **1974**, *70* (140), 80−90.
(126) Park, J.; Robinson, R. L., Jr.; Gasem, K. A. M. Solubilities of hydrogen in heavy normal paraffins at temperatures from 323.2 to 423.2 K and pressures to 17.4 MPa. *J. Chem. Eng. Data* **1995**, *40*, 241−244.
(127) Sebastian, H. M.; Simnick, J. J.; Lin, H.-M.; Chao, K.-C. Gas-liquid equilibrium in the hydrogen + *n*-decane system at elevated temperatures and pressures. *J. Chem. Eng. Data* **1980**, *25*, 68−70.
(128) Srivatsan, S.; Yi, X.; Robinson, R. L., Jr.; Gasem, K. A. M. Solubilities of carbon monoxide in heavy normal paraffins at temperatures from 311 to 423 K and pressures to 10.2 MPa. *J. Chem. Eng. Data* **1995**, *40*, 237−240.
(129) Widdoes, L. C.; Katz, D. L. Vapor-liquid equilibrium constants for carbon monoxide. *Ind. Eng. Chem.* **1948**, *40*, 1742−1746.
(130) Wang, Q.; Chao, K.-C. Vapor-liquid and liquid-liquid equilibria and critical states of water + *n*-decane mixtures. *Fluid Phase Equilib.* **1990**, *59*, 207−215.
(131) Reamer, H. H.; Selleck, F. T.; Sage, B. H.; Lacey, W. N. Phase equilibria in hydrocarbon systems. Volumetric and phase behavior of decane−hydrogen sulfide system. *Ind. Eng. Chem.* **1953**, *45*, 1810−1812.
(132) Fredenslund, A.; Mollerup, J. Gas-liquid equilibrium of hydrogen sulphide + carbon monoxide. *J. Chem. Thermodyn.* **1975**, *7*, 677−682.
(133) Burgess, M. P.; Germann, R. P. Physical properties of hydrogen sulfide−water mixtures. *AIChE J.* **1969**, *15*, 272−275.
(134) Gillespie, P. C.; Wilson, G. M. *Vapor-liquid equilibrium data on water-substitute gas components: N_2−H_2O, H_2−H_2O, CO−H_2O, H_2−CO−H_2O, and H_2S−H_2O*; Research Report RR-41, Project 758-B-79; Gas Processors Association: Tulsa, OK, 1980.
(135) Gillespie, P. C.; Wilson, G. M. *Vapor-liquid and liquid-liquid equilibria: water−methane, water−carbon dioxide, water−hydrogen sulfide, water−n-pentane, and water−methane−n-pentane*; Research Report RR-48, Project 758-B-77; Gas Processors Association: Tulsa, OK, 1982.
(136) Selleck, F. T.; Carmichael, L. T.; Sage, B. H. Phase behavior in the hydrogen sulfide−water system. *Ind. Eng. Chem.* **1952**, *44*, 2219−2226.
(137) Wieser, M. E. Atomic weights of the elements 2005 (IUPAC Technical Report). *Pure Appl. Chem.* **2006**, *78*, 2051−2066.
(138) Mohr, P. J.; Taylor, B. N.; Newell, D. B. CODATA recommended values of the fundamental physical constants: 2006. *J. Phys. Chem. Ref. Data* **2008**, *37*, 1187−1284.
(139) Michelsen, M. L. The isothermal flash problem. Part I. Stability. Phase-split calculation. *Fluid Phase Equilib.* **1982**, *9*, 1−19.
(140) Heidemann, R. A. Computation of high pressure phase equilibria. *Fluid Phase Equilib.* **1983**, *14*, 55−78.
(141) Michelsen, M. L.; Mollerup, J. M. *Thermodynamic Models: Fundamentals & Computational Aspects*; Tie-Line Publications: Holte, 2004.
(142) Michelsen, M. L. Calculation of phase envelopes and critical points for multi-component mixtures. *Fluid Phase Equilib.* **1980**, *4*, 1−10.
(143) Michelsen, M. L. The isothermal flash problem. Part II. Phase-split calculation. *Fluid Phase Equilib.* **1982**, *9*, 21−40.
(144) Michelsen, M. L. State function based flash specifications. *Fluid Phase Equilib.* **1999**, *158−160*, 617−626.
(145) Span, R.; Wagner, W. A new equation of state for carbon dioxide covering the fluid region from the triple-point temperature to 1100 K at pressures up to 800 MPa. *J. Phys. Chem. Ref. Data* **1996**, *25*, 1509−1596.
(146) Wagner, W.; Pruß, A. The IAPWS Formulation 1995 for the thermodynamic properties of ordinary water substance for general and scientific use. *J. Phys. Chem. Ref. Data* **2002**, *31*, 387−535.
(147) Span, R.; Wagner, W. Equations of state for technical applications. I. Simultaneously optimized functional forms for nonpolar and polar fluids. *Int. J. Thermophys.* **2003**, *24*, 1−39.
(148) Mathias, P. M.; Klotz, H. C.; Prausnitz, J. M. Equation-of-state mixing rules for multi-component mixtures: the problem of invariance. *Fluid Phase Equilib.* **1991**, *67*, 31−44.
(149) Michelsen, M. L.; Kistenmacher, H. On composition-dependent interaction coefficients. *Fluid Phase Equilib.* **1990**, *58*, 229−230.
(150) Avlonitis, D.; Danesh, A.; Todd, A. C. Prediction of VL and VLL equilibra of mixtures containing petroleum reservoir fluids and methanol with cubic eos. *Fluid Phase Equilib.* **1994**, *94*, 181−216.
(151) Setzmann, U.; Wagner, W. A new method for optimizing the structure of thermodynamic correlation equations. *Int. J. Thermophys.* **1989**, *10*, 1103−1126.
(152) Knapp, H.; Döring, R.; Oellrich, L.; Plöcker, U.; Prausnitz, J. M. *Vapor-liquid equilibria for mixtures of low boiling substances*; DECHEMA Chemistry Data Series, Vol. *VI*; DECHEMA: Frankfurt/Main, 1982.
(153) Jaeschke, M.; Hinze, M. *Ermittlung des Realgasverhaltens von Methan und Stickstoff und deren Gemische im Temperaturbereich von 270 K bis 353 K und Drücken bis 30 MPa*; Fortschr.-Ber. VDI, Reihe 3, Nr. 262; VDI-Verlag: Düsseldorf, 1991.

(154) Haynes, W. M.; McCarty, R. D. Low-density isochoric (p, V, T) measurements on (nitrogen + methane). *J. Chem. Thermodyn.* **1983**, *15*, 815−819.
(155) Straty, G. C.; Diller, D. E. (p, V, T) of compressed and liquefied (nitrogen + methane). *J. Chem. Thermodyn.* **1980**, *12*, 937−953.
(156) Rodosevich, J. B.; Miller, R. C. Experimental liquid mixture densities for testing and improving correlations for liquefied natural gas. *AIChE J.* **1973**, *19*, 729−735.
(157) Haynes, W. M.; McCarty, R. D.; Eaton, B. E.; Holste, J. C. Isochoric (p, V_m, x, T) measurements on (methane + ethane) from 100 to 320 K at pressures to 35 MPa. *J. Chem. Thermodyn.* **1985**, *17*, 209−232.
(158) Ruhrgas, 1990: See Jaeschke et al.[26]
(159) Ruhrgas. Private communication by Jaeschke, M.; Schley, P. (Ruhrgas AG, Essen) to Klimeck, R., 1999.
(160) Reamer, H. H.; Sage, B. H.; Lacey, W. N. Phase equilibria in hydrocarbon systems. Volumetric and phase behavior of the methane−propane system. *Ind. Eng. Chem.* **1950**, *42*, 534−539.
(161) Reamer, H. H.; Korpi, K. J.; Sage, B. H.; Lacey, W. N. Phase equilibria in hydrocarbon systems. Volumetric behavior of methane−*n*-butane system at higher pressures. *Ind. Eng. Chem.* **1947**, *39*, 206−209.
(162) Reamer, H. H.; Olds, R. H.; Sage, B. H.; Lacey, W. N. Phase equilibria in hydrocarbon systems. Methane−carbon dioxide system in the gaseous region. *Ind. Eng. Chem.* **1944**, *36*, 88−90.
(163) Reamer, H. H.; Selleck, F. T.; Sage, B. H.; Lacey, W. N. Phase equilibria in hydrocarbon systems. Volumetric behavior of the nitrogen−ethane system. *Ind. Eng. Chem.* **1952**, *44*, 198−201.
(164) Reamer, H. H.; Olds, R. H.; Sage, B. H.; Lacey, W. N. Phase equilibria in hydrocarbon systems. Volumetric behavior of ethane−carbon dioxide system. *Ind. Eng. Chem.* **1945**, *37*, 688−691.
(165) Reamer, H. H.; Sage, B. H.; Lacey, W. N. Phase equilibria in hydrocarbon systems. Volumetric and phase behavior of the propane−carbon dioxide system. *Ind. Eng. Chem.* **1951**, *43*, 2515−2520.
(166) Seitz, J. C.; Blencoe, J. G.; Bodnar, R. J. Volumetric properties for $\{(1-x)CO_2 + xCH_4\}$, $\{(1-x)CO_2 + xN_2\}$, and $\{(1-x)CH_4 + xN_2\}$ at the pressures (9.94, 19.94, 29.94, 39.94, 59.93, 79.93, and 99.93) MPa and temperatures (323.15, 373.15, 473.15, and 573.15) K. *J. Chem. Thermodyn.* **1996**, *28*, 521−538.
(167) Seitz, J. C.; Blencoe, J. G. Volumetric properties for $\{(1-x)CO_2 + xCH_4\}$, $\{(1-x)CO_2 + xN_2\}$, and $\{(1-x)CH_4 + xN_2\}$ at the pressures (19.94, 29.94, 39.94, 59.93, 79.93, and 99.93) MPa and the temperature 673.15 K. *J. Chem. Thermodyn.* **1996**, *28*, 1207−1213.
(168) Estela-Uribe, J. F.; Trusler, J. P. M.; Chamorro, C. R.; Segovia, J. J.; Martín, M. C.; Villamañán, M. A. Speeds of sound in $\{(1-x)CH_4 + xN_2\}$ with x = (0.10001, 0.19999, and 0.5422) at temperatures between 170 and 400 K and pressures up to 30 MPa. *J. Chem. Thermodyn.* **2006**, *38*, 929−937.
(169) Younglove, B. A.; Frederick, N. V.; McCarty, R. D. *Speed of sound data and related models for mixtures of natural gas constituents*; Monograph 178; NIST: Boulder, CO, 1993.
(170) Trusler, J. P. M. The speed of sound in $(0.8\ CH_4 + 0.2\ C_2H_6)$(g) at temperatures between 200 and 375 K and amount-of-substance densities up to 5 mol·dm^{-3}. *J. Chem. Thermodyn.* **1994**, *26*, 751−763.
(171) Parrish, W. R.; Hiza, M. J. *Liquid-vapor equilibria in the nitrogen−methane system between 95 and 120 K.* Cryogenic Engineering Conference, August 8−10, Atlanta, Georgia, Paper K-9, 1973.
(172) Stryjek, R.; Chappelear, P. S.; Kobayashi, R. Low-temperature vapor-liquid equilibria of nitrogen−methane system. *J. Chem. Eng. Data* **1974**, *19*, 334−339.
(173) McClure, D. W.; Lewis, K. L.; Miller, R. C.; Staveley, L. A. K. Excess enthalpies and Gibbs free energies for nitrogen + methane at temperatures below the critical point of nitrogen. *J. Chem. Thermodyn.* **1976**, *8*, 785−792.
(174) Cines, M. R.; Roach, J. T.; Hogan, R. J.; Roland, C. H. Nitrogen−methane vapor-liquid equilibria. *Chem. Eng. Prog. Symp. Ser.* **1953**, *49*, 1−10.
(175) Fontaine, J. M. Das Phasengleichgewicht Helium−Methan und die Beschreibung mit einer neuen Gemischzustandsgleichung. Ph.D. Dissertation, Fakultät für Maschinenbau und Elektrotechnik, Technische Universität Carolo-Wilhelmina zu Braunschweig, 1989.
(176) Janisch, J. Vapor-liquid phase equilibria including saturated densities for systems containing nitrogen, methane, and ethane from 130 to 270 K and pressures up to 10 MPa. Final report to GERG WG 1.34, Institut für Thermodynamik, Technische Universität Braunschweig, 2000.
(177) Magee, J. W.; Haynes, W. M.; Hiza, M. J. Isochoric (p, ρ, T) measurements for five natural gas mixtures from T = (225 to 350) K at pressures to 35 MPa. *J. Chem. Thermodyn.* **1997**, *29*, 1439−1454.
(178) Hwang, C.-A.; Simon, P. P.; Hou, H.; Hall, K. R.; Holste, J. C.; Marsh, K. N. Burnett and pycnometric (p, V_m, T) measurements for natural gas mixtures. *J. Chem. Thermodyn.* **1997**, *29*, 1455−1472.
(179) Ruhrgas (1993): See Jaeschke et al.[26]
(180) Ruhrgas (1994): See Jaeschke et al.[26]
(181) Jaeschke, M.; Schley, P. *Compression factor measurements on rich natural gases*; Final report, Contract No. 5095-260-3557; Gas Research Institute: Chicago, 1998.
(182) Watson, J. T. R.; Millington, B. The density of rich natural gas mixtures. A joint industrial project. NEL, Project No. DRG001, Report No. 110/97, 1998.
(183) Owren, G.; Grini, P. G.; Maehlum, H. S.; Jorstad, O. Enthalpy measurements on natural gas. Report to GERG WG 1.3, 1996.
(184) Trappehl, G. Experimentelle Untersuchung der Dampf-Flüssigkeits-Phasengleichgewichte und kalorischen Eigenschaften bei tiefen Temperaturen und hohen Drücken an Stoffgemischen bestehend aus N_2, CH_4, C_2H_6, C_3H_8 und CO_2. Ph.D. Dissertation, Technische Universität Berlin, 1987.
(185) Haynes, W. M.; McCarty, R. D.; Hiza, M. J. Liquefied natural gas densities: Summary of research program at the National Bureau of Standards. *Natl. Bur. Stand.*, Monograph 172, **1983**.
(186) Avila, S.; Blanco, S. T.; Velasco, I.; Rauzy, E.; Otín, S. Thermodynamic properties of synthetic natural gases. 1. Dew-point curves of synthetic natural gases and their mixtures with water and methanol. Measurement and correlation. *Ind. Eng. Chem. Res.* **2002**, *41*, 3714−3721.
(187) Avila, S.; Blanco, S. T.; Velasco, I.; Rauzy, E.; Otín, S. Thermodynamic properties of synthetic natural gases. 2. Dew point curves of synthetic natural gases and their mixtures with water and methanol. Measurement and correlation. *Energy Fuels* **2002**, *16*, 928−934.
(188) Avila, S.; Blanco, S. T.; Velasco, I.; Rauzy, E.; Otín, S. Thermodynamic properties of synthetic natural gases. Part 4. Dew point curves of synthetic natural gases and their mixtures with water: Measurement and correlation. *Fluid Phase Equilib.* **2002**, *202*, 399−412.
(189) Avila, S.; Blanco, S. T.; Velasco, I.; Rauzy, E.; Otín, S. Thermodynamic properties of synthetic natural gases. Part 3. Dew point curves of synthetic natural gases and their mixtures with water. Measurement and correlation. *Energy Fuels* **2003**, *17*, 338−343.
(190) Jarne, C.; Avila, S.; Blanco, S. T.; Rauzy, E.; Otín, S.; Velasco, I. Thermodynamic properties of synthetic natural gases. 5. Dew point curves of synthetic natural gases and their mixtures with water and with water and methanol: Measurement and correlation. *Ind. Eng. Chem. Res.* **2004**, *43*, 209−217.
(191) Jarne, C.; Blanco, S. T.; Gallardo, M. A.; Rauzy, E.; Otín, S.; Velasco, I. Dew points of ternary methane (or ethane) + carbon dioxide + water mixtures: Measurement and correlation. *Energy Fuels* **2004**, *18*, 396−404.
(192) Mørch, Ø.; Nasrifar, K.; Bolland, O.; Solbraa, E.; Fredheim, A. O.; Gjertsen, L. H. Measurement and modeling of hydrocarbon dew points for five synthetic natural gas mixtures. *Fluid Phase Equilib.* **2006**, *239*, 138−145.
(193) Lemmon, E. W.; Huber, M. L. Thermodynamic properties of *n*-dodecane. *Energy Fuels* **2004**, *18*, 960−967.
(194) Span, R. *Multiparameter equations of state. An accurate source of thermodynamic property data*; Springer: Berlin, 2000.
(195) Span, R.; Collmann, H.-J.; Wagner, W. Simultaneous optimization as a method to establish generalized functional forms for empirical equations of state. *Int. J. Thermophys.* **1998**, *19*, 491−500.

(196) Richter, M.; Kleinrahm, R.; Span, R.; Schley, P. A new apparatus for the accurate measurement of LNG densities. *GWF Int.* **2010**, *1*, 66–69.
(197) Richter, M. Modifikation eines Normdichtemessgerätes für Erdgase und Entwicklung einer Präzisions-Dichtemessanlage für verflüssigte Erdgase (LNG). Ph.D. Thesis, Fakultät für Maschinenbau, Ruhr-Universität Bochum, Bochum, Germany, 2011.